1-1-2012

Reliability and effect of partially restrained wood shear walls

John Joseph Gruber
Wayne State University, ap2056@wayne.edu

RELIABILITY AND EFFECT OF PARTIALLY RESTRAINED WOOD SHEAR WALLS

by

JOHN J. GRUBER

DISSERTATION

Submitted to the Graduate School

of Wayne State University,

Detroit, Michigan

in partial fulfillment of the requirements

for the degree of

DOCTOR OF PHILOSOPHY

2012

MAJOR: CIVIL ENGINEERING

Approved by:

_____

Advisor Date

_____

_____

_____

_____

DEDICATION

I dedicate this dissertation to my beloved wife, Jennifer.

ACKNOWLEDGMENTS

I would like to thank Dr. Christopher Eamon**,** Dr. Wen Li and Dr. Hwai Chung Wu for agreeing to serve on my dissertation committee.

I would like to thank my advisor, Dr. Gongkang Fu, for all the guidance, direction and support he has given me throughout my Doctorate program and especially for encouraging me to pursue this degree. I would also like to thank the faculty and staff of the Department of Civil and Environmental Engineering at Wayne State University for all the support and encouragement they have given me. A special thanks to the graduate school for the Graduate Professional Scholarship I received for school years 2010/2011 and 2011/2012.

I would like to also thank others who have offered direction, advice, support, and reviewing including Dr. Upul Attanayake, Dr. Dinesh Devaraj, Mr. Alexander Lamb, Mrs. Renee Ryan, P.E., and my work partners Mr. Richard Hamann, P.E. and Mr. Craig Anderson, P.E.

I would like to thank and recognize the Structural Building Components Research Institute for the use of their test facility and support. This thesis would not have been possible without their support. I would like to especially thank the lab technicians, Mr. Keith Hershey and Mr. Michael Oftedahl, for their hard work and patience; Mr. Dan Hawk for help with data management; and Mr. Kirk Grundahl, P.E., the executive director of the Structural Building Components Association, for the initiative for this project, encouragement, and support.

Additional thanks and recognition go to Testing Engineers and Consultants and Simpson Strong Tie. Testing Engineers and Consultants provided the lab for the specific gravity tests. Simpson Strong Tie provided the mechanical hold down devices.

Finally, I would like to thank my family; my parents (posthumously), Jack and Carol; my brother, Greg, and sisters, Sheila, Sharon, and Anne; my two sons, Jonathon and Alexander, and my wife, Jennifer, for their encouragement, faith, support, and patience throughout all of my studies. They have sacrificed a great deal for my education and this research. I certainly could not have completed this without them.

TABLE OF CONTENTS

LIST OF FIGURES

LIST OF GRAPHS

LIST OF TABLES

CHAPTER 1

INTRODUCTION

The purpose of this research is to examine the reliability levels of the prescriptive wall bracing requirements of the *2009 International Residential Code* (IRC) and the engineered shear wall requirements of the *2009 International Building Code* (IBC) along with the *2005 Special Design Provisions for Wind and Seismic* (AF&PA SDPWS). This research encompasses structures constructed in 90 m.p.h. wind areas with exposure B.

In order to understand the focus of the proposed research, it is necessary to understand the history of housing, housing construction practices, and wall bracing. Based upon the ASCE 7 wind speed map shown in Figure 1, this research affects the majority of the housing in the continental United States since it applies to structures in low wind speed and low seismic areas. Currently, a prescriptive design method is dominant for the design of lateral bracing for single family houses. When the limits of the prescriptive design are exceeded, then an engineered alternative is necessary. Based on the information available today, the reliability levels of these two design methods are not equivalent. It is desirable to understand the reliability levels of these two systems and compare them.

The reliability analysis is useful for several reasons. First, it provides a comparison of the two design philosophies in a way that is independent of the design methods by using the second-moment reliability index β. This "provides a relative

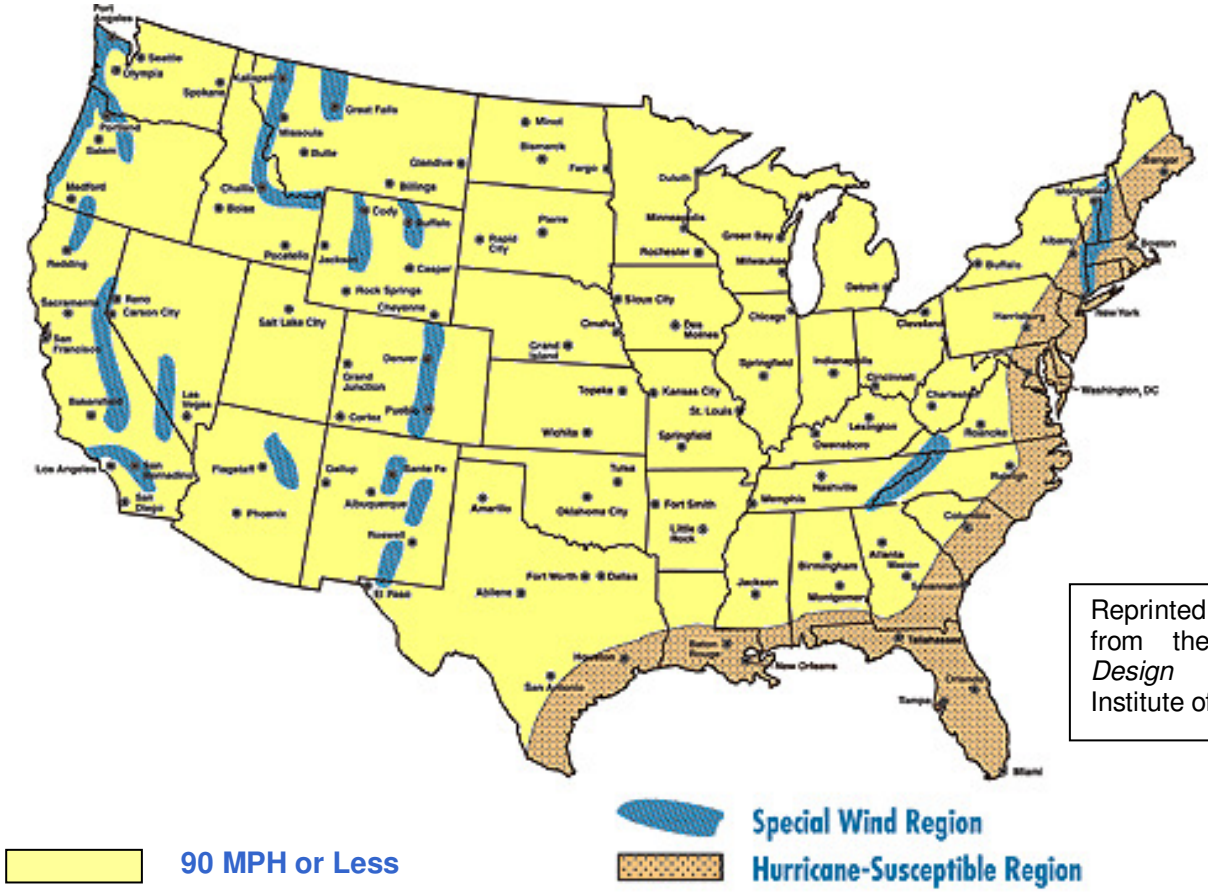

Reprinted with permission from the *Whole Building Design Guide* National Institute of Builidng Sciences.

Figure 1: Continental US Shaded Wind Speed Map (WBDG 2010)

measure of the safety of a structural component or system and serves as the cornerstone of code calibration studies" (van de Lindt and Rosowsky 2005). Second, the study is useful to calibrate resistance factors to unify the two design methods with respect to structural safety. This is beneficial for alternate building materials and systems that could provide economic, energy or sustainability benefits.

This research provides the following items:

1. The reliability index of the unit shear capacity for $^{15}/_{32}$" Wood Structural Panels (WSP) in SDPWS (2005)
2. The appropriateness of ASTM E72 for walls anchored with mechanical hold downs and partially restrained IRC (2009) prescriptive walls.
3. Verification for the resistance factor used by the SDPWS.
4. Recommended codified nominal unit shear design values for wind load for unrestrained shear walls constructed in accordance with the 2009 IRC using $^{15}/_{32}$" WSP.
5. Recommended codified nominal unit shear design values for wind load for fully restrained shear walls constructed in accordance with the 2009 IRC using $^{15}/_{32}$" WSP.
6. Proposed requirement for unrestrained shear wall tests for WSP manufacturers in the *Voluntary Product Standard* PS 2-04 titled *Performance Standards for Wood-Based Structural-Use Panels* (NIST 2004) for WSP.

7. Recommended IRC utilization of the unrestrained shear wall nominal unit shear design values or definition of some minimum restraining force to be known present.

The above results will create an equitable design methodology between the IRC prescriptive method and the SDPWS. When implemented and utilized in the IRC, alternate products and engineered alternatives can be provided without the appearance of over-conservatism.

1.1 History

1.1.1 Historic House Data

The total load resistance of wall bracing in houses is not only dependent upon the material, but also the spacing of brace wall lines and aspect ratios of brace walls. The spacing of the brace wall lines obviously affects the tributary wind area of each brace wall line. The aspect ratios typically affect the strength and certainly affect the stiffness of the brace walls. Therefore, the number of openings in a wall as well as the height of a wall can affect the load resistance of the lateral load resisting system. These geometric features have been changing during the past century, creating a greater demand on lateral bracing systems.

Beyond the structural history of brace walls, the economic value of homes is also of concern. As the value of homes increase, the financial risk due to wind damage also increases.

Table 1 shows a comparison of house construction over the 20th century. The average size of houses more than doubled in this period of time, while the number of bedrooms remained about the same. Today's homes include more large open spaces than homes built in the early 1900s. Over the same time period, housing costs have increased by a factor of 100. The inflation-adjusted housing cost in the early 1900s was about $35.00/sq. ft. The cost in 2000 was about $100.00/sq. ft.

Table 1: Historic House Data (HUD 2001)

	Early 1900's	**Mid 1900's**	**Late 1900's**
Population	76 Million (40% urban, 60% rural)	150 Million (64 % urban, 36% rural)	270 Million (76% urban, 24% rural)
Median Family Income	$490	$3,319	$45,000
New Home Price	Average Unknown[1]	$11,000	$200,000
Type of Purchase	Typically Cash	FHA Mortgage, 4.25% (few options)	8% (many options)
Ownership Rate	46 %	55%	67%
Total Housing Units	16 Million	43 Million	107 Million (approx. 50% single-family)
Number of annual housing starts	189,000 (65% single-family)	1.95 Million (85% single-family)	1.54 Million (approx. 50% single family)
Average Size (starts)	< 1,000 sq. ft.	1,000 sq. ft.	2,000 sq. ft. or more
Stories	1 to 2	1 (86%); 2 or more (14%)	1 (48%); 1½ or 2 (49%)
Bedrooms	2 to 3	2 (66%); 3 (33%)	2 or less (12%); 3 (54%); 4 or more (34%)
Bathrooms	0 or 1	1½ or less (96%)	1½ or less (7%); 2 (40%); 2½ + (53%)
Garage		1 car (41%); 0 (53%)	2 car (65%)

Table 1 also indicates that there has been a large movement to urban settings from rural. The shift from rural to urban settings indicates that wind exposure is decreasing as the exposure category is B for urban locations and typically C for rural locations (ASCE 7-05).

[1] Based on "*Housing at the Millennium: Facts, Figures, and Trends*," the average new home cost was less than $5,000. However, this estimate is potentially skewed in that many people could not afford a "house" of the nature considered in the study. Based on Sears, Roebuck, and Co. catalogue prices at the turn of the century, a typical house may have ranged from $1,000 to $2,000, including land.

Construction methods for housing have also changed throughout the 20th century. A summary of the current construction methods for 2001 is presented in Table 2. Of interest for this research are the foundation type, wall sheathing and wall framing. The dominant foundation type is a slab on grade system. This system includes perimeter footings, typically to frost depth; interior footings at interior-bearing locations; and a floor slab constructed on grade. The dominant wall sheathing is oriented strand board (OSB) with foam panels used in 24% of the construction. The foam panels are typically non-structural sheathing. The dominant wall framing is 2x4 studs at 16" o.c. This research considers slab on grade construction, OSB intermittent sheathing, and 2x4 stud wall framing at 16" o.c.

Table 2: Current Construction Methods (HUD 2001)

Foundation Type	Basement (34%); Crawlspace (11%); Slab (54%)
Floor Framing	Type: Lumber (62%); Wood Trusses (9%); Wood I-joists (28%) Size of Lumber: 2x8 (8%); 2x10 (70%); 2x12 (21%) Type of Lumber: SYP (39%); DF (23%); other (37%)
Floor Sheathing	Plywood (37%); OSB (30%); Board (6%)
Wall Framing	2x4 @ 16" (73%); 2x4 @ 24" (17%); 2x6 @ 16" (17%); 2x6 @ 24" (3%)
Wall Sheathing	Plywood (11.2%); OSB (44.2%); Foam Panels (24%); Other (20.6%)
Ceiling Height	8' (54%); 9' (29%); 10' (8%)
Wall Openings	2.3 Ext. Doors; 1.2 Patio Doors; 14.5 Windows; 1.2 Fireplaces (13-15% of wall area on average)
Roof Sheathing	Plywood (27.6%); OSB (71%)
Roof Framing	Rafters (6%); I-joists (29%); Wood Trusses (65%)
Roof Pitch	4/12 or less (7%); 5/12 to 6/12 (63%); 7/12 or greater (30%)
Roof Shape	Gable (63%); Hip (36%)

Note: Percentages for floor, wall, and roof sheathing and framing are based on total aggregated floor and wall area for housing starts. Other values are given as a percentage of housing starts.

1.1.2 Historic Wall Bracing

Wall bracing in houses to provide lateral stability has evolved over the past century as framing methods changed from balloon to platform framing and as materials other than sawn boards and plaster became available. Bracing methods in the early 1900s consisted of no bracing, 1x4 let-in bracing, or horizontal or diagonal wood

sheathing (HUD 2001). The method of no bracing apparently relied on the interior wood lath and plaster for the bracing system.

As early as 1929 the Forest Products Laboratory began comparison testing of various bracing methods (HUD 2001). The walls tested were 9' x 14' and 7'-4" x 12' with enough vertical restraint to prevent over-turning. These walls were either solid, had one window opening, or had one window and one door opening. The results of the tests are presented in (HUD 2001).

1.1.3 Prescriptive Code History

Plywood was introduced in the mid 1900s. This renewed the interest in bracing methods. Plywood is typically manufactured in 4' x 8' sheets and is installed either continuously over the exterior walls or intermittently. Until the early 2000s, with the introduction of the International Codes (a combination of the BOCA, UBC, and SBC), the primary bracing methods in the late 1900s were metal T-bracing, wood structural panels (plywood or OSB), or gypsum.

Table 1 shows that houses are larger, but don't have more rooms, therefore houses have larger rooms today than they did a century ago. This, coupled with larger window and door openings, has led to less lateral resistance in houses. Although typically discounted, interior partitions provide additional strength and stiffness to the lateral resisting system of houses. The percentage of interior partitions in comparison to floor area has decreased with the increased house size and especially with the large open spaces enjoyed in the later part of the 1900s. Table 3 summarizes the change in the amount of interior walls from early last century to late last century. Note that there is

a 1.1% and 1.7% reduction in interior walls, as a percent of floor area, for the second and first floor of two-story houses respectively.

Table 3: Interior Wall Amounts (HUD 2001)
(Lineal feet as a percent of floor area of story)

OLDER HOMES (early 1900s)[1]		MODERN HOMES (late 1900s)[2]	
1 Story	9% ± 1%	1st Floor of 1 to 2 Story	4.3% ± 1%
1st Floor of 2 Story	6% ± 1%	2nd Floor of 2 Story	7.9% ± 1%
2nd Floor of 2 Story	9% ± 1.5%		

Notes:
[1]Values based on a small sample of traditional house plans in Sears Catalogues (1910-1926) including affordable and more expensive construction of 1 and 2 stories.
[2]Values based on a small sample of representative modern home plans (1990s) including economy and move-up construction (no luxury homes).

By the late 1900s, Hurricane Andrew and the Northridge Earthquake had highlighted the importance of lateral bracing in houses. This timing, along with the development of the International Codes, changed the bracing methods used in prescriptive design. Much research of wood shear walls and bracing methods focused on seismic design and cyclic testing. As a result, the codes began prescribing more lateral bracing.

The current IRC (IRC 2009) uses more of a rational design method to prescribe wall bracing to resist wind loads than previous editions but varies greatly from the typical rational (engineered) design method using the ASCE 7-05 and the SDPWS. The current IRC (IRC 2009) has also made an attempt to utilize both partial wall restraint and a whole house effect. It is the goal of this research to compare the reliability of the prescriptive design with the rational design using SDPWS.

1.2 Reliability Analysis

1.2.1 Testing

As part of this research, (25) 4' x 8' brace walls were monotonically load tested. These walls varied from full restraint (a mechanical hold down device) to unrestrained (only a single anchor bolt). The testing was performed at the Structural Building Components Research Institute located in Madison, WI. The goal of the testing was to understand the load-deflection behavior and ultimate strength of the varying restraint conditions and the variability of the ultimate strength.

1.2.2 Verification of Empirical Partial Restraint Factor

The test data was used to verify the empirical partial restraint factor previously developed by Ni and Karacabeyli (2000). This factor is intended to predict the capacity of an unrestrained or partially restrained shear wall using the nominal unit shear strength of a fully restrained wall. Differences between the IRC prescriptive sole plate anchorage and the anchorage used to develop the empirical partial restraint factor necessitate a verification of this factor for the IRC wall.

1.2.3 Reliability Model

Using the test results from the 25 tests, ultimate strengths and variability were used in a first order second moment reliability model (FOSM) and Monte Carlo Simulation (MCS) to determine the reliability index, β, for the current SDPWS nominal unit shear strength and the nominal unit shear strength used in the 2009 IRC. The tests results were also used to identify the random variables used in the reliability model.

The reliability analysis used both numerical analysis and Monte Carlo simulation to evaluate the model.

Once the model was constructed for the varying wall restraint conditions, two items were varied to provide a target value for β (3.25) for each of these conditions which is similar to the current reliability index of 3.27 for the SDPWS nominal values. These items included the resistance factor, ϕ, and the nominal tabulated unit shear values for the varying cases.

1.3 Recommendations for Code Revisions

The conclusions of this research include recommendations for code revisions for unrestrained, partially restrained, and fully restrained shear walls constructed with WSP with 8d common nails and recommendations for finite element models. These are based on a 4'x8' WSP shear wall. The following is a list of these conclusions.

1. The reliability index of the SDPWS nominal unit shear value for $^{15}/_{32}$" WSP was determined using the allowable stress design (ASD) reduction factor and resistance factor, ϕ, and APA Research Report 154 (APA 2004).
2. The use of ASTM E72 is inappropriate to determine nominal unit shear design values.
3. Present nominal unit shear values published in SDPWS cannot be achieved with a mechanical hold down at the base of the wall.
4. Using reliability analysis for calibration, partial restraint modification factors are determined for both mechanical hold downs and a dead load restraining force. These modification factors will be used to modify the nominal unit

shear capacity values in SDPWS. These modification factors are presented for both allowable stress design (ASD) and load and resistance factored design (LRFD) methods.

5. For equitable designs providing the same level of safety, the IRC 2009 should publish the required dead load restraining force to achieve the unit shear design value used. This restraining force should be clearly stated as a design requirement for the use of the prescriptive method.
6. Finite element models should always include the effect of the boundary conditions, restraining force, and the connection behavior of the studs-to-top/sole-plate connections.

1.4 Organization of Thesis

Chapter 2 provides a literature review of codes and standards applicable to this thesis; previous research regarding partially restrained wood shear walls; finite element modeling; and reliability studies. The background of the prescriptive wall bracing methods, design philosophy, and engineered alternate design methods are reviewed to provide the reader with a basis for this thesis. Finite element modeling methods, nail strength and load deformation modeling, as well as the nail yield limit theory are reviewed. A reliability analysis of wood shear walls with wind loads conducted by van de Lindt is also presented.

In Chapter 3 a summary of the wood shear wall testing conducted is presented. This includes a brief overview of both ASTM E72 and E564. Summary of data obtained from the test program that is used for both the finite element modeling and the reliability study is presented here.

In Chapter 4 a finite element model is presented. This model includes a non-linear finite element model created to simulate the behavior of partially restrained wood shear walls and shear walls restrained with a mechanical hold down. This model utilizes nonlinear orthogonal spring pairs using data obtained from the tests conducted. Results from the finite element model are presented at the end of CHAPTER 4.

In Chapter 5, a systematic reliability analysis is presented. This analysis concludes with a Monte Carlo simulation including four random variables: wind load, dead load, wall unit shear capacity, and specific gravity. A partial restraint factor was developed by calibrating the bias factor with the M-C simulation so that a constant reliability index of 3.25 is obtained for all restraint conditions for the 4'x 8' wood shear wall.

A discussion regarding the intent and use of both ASTM E72 and E564 is presented in Chapter 6. This describes the limitations of ASTM E72 and the appropriateness of its use for determining design values.

Conclusions of this thesis are presented in Chapter 7. A brief summary of this thesis is included here as well as suggestions for future research. The calibrated partial restraint factors for both allowable stress design (ASD) and load and resistance factored design (LRFD) are summarized.

CHAPTER 2

LITERATURE REVIEW

In this chapter a general introduction is given to the current design requirements for intermittent brace walls in residential construction, a review of previous reliability studies, a review of previous finite element modeling methods, and a review of recent IRC wall testing. Specifically, the prescriptive requirements of the *2009 International Residential Code* (IRC) is discussed as well as requirements for an alternate engineered design utilizing the *2009 International Building Code* (IBC); *Minimum Design Loads for Buildings and Other Structures* (ASCE 7-05); and the *2005 Special Design Provisions for and Seismic (SDPWS)* (AF&PA SDPWS).

2.2 2009 IRC Requirements

2.2.1 Development of the 2009 IRC Requirements

The 2009 IRC is the result of years of empirical methods. "The art and science behind accurately understanding conventional wall bracing is still considered to be in its infancy and subject to disparate interpretations, even though it has been studied at various times since the early 1900s and especially in recent years," (Crandell 2007).

The development of the 2009 IRC wind load provisions occurred under the direction of an Ad Hoc Committee-Wall Bracing (AHC-WB). The AHC-WB was created by the International Code Council (ICC). The AHC-WB committee had the support of a second group led by Dan Dolan, PhD, which was supported by The Building Seismic Safety Council (BSSC) (Crandell and Martin 2009).

The 2009 IRC wind bracing provisions attempt to equate historic construction methods and performance with an engineered design. The historic construction method dictated that the brace panels do not require mechanical hold downs in addition to the prescribed connections. Therefore, the committee agreed to develop a net brace wall capacity based on a fully restrained wall capacity using the following equation (Crandell and Martin 2009).

$$BWC = FRSWC \times NAF$$

Where,

BWC = Braced wall capacity
FRSWC = Fully-restrained wall capacity
NAF = Net adjustment factor

The net adjustment factor contained a factor for the partially restrained shear walls' (PRSW) capacity as well as a whole house effect. This was justified by realizing that PRSW have some capacity. PRSW have been studied by several researchers (Ni and Karacabeyli 2000, Salenikovich 2000, Dolan and Heine 1997). Reduction in shear capacity of an unrestrained shear wall can be as great as 67% (Ni and Karacabeyli). This reduction will be discussed later in the unrestrained shear wall discussion.

For a PRSW the dead load of the structure and building finishes can provide the restraint. The magnitude of this restraint is impossible to determine for a code application that can be used in any residential structure. The AHC-WB committee, in fact, could not agree upon the value for this partial restraint (Crandell and Martin 2009).

The whole house factor is a factor that recognizes the additional strength of a residential structure due to redundancies, bracing that is either ignored or does not meet the prescribed brace wall requirements, or even building finishes that wouldn't be

considered in an engineering analysis. Some may refer to this as a "system effect" factor. According to Crandell and Martin 2009, five whole house tests were reviewed to determine the value of this factor when compared to the IRC bracing method. Three of these tests are described (Crandell and Martin 2009). They are the BRANZ, CSIRO, and CUREe/FEMA. The ratio of tested values (failure) to the predicted (ultimate) values ranged from 1.5 (discounting interior partitions) to 3.1. The Dolan-AHC-WB committee could not reach a consensus on either of the two factors, but did agree to one factor, 1.2, which includes both factors (Crandell and Martin 2009). Crandell reported the factors discussed by the committee and they are shown here in Table 4.

Table 4: Nominal Shear Strength Adjustment Factors for Conventional Wall Bracing

Walls Supporting:	Partial-Restraint Factor	Whole Building Factor	Net Adjustment Factor
Roof Only	0.8	1.5	1.2
Roof + One Story	0.9	1.33	1.2
Roof + Two Stories	1.0	1.2	1.2

1. These factors are limited to residential construction in accordance with the 2009 IRC and bracing methods that have a nominal shear strength "capped" at about 700 plf.

Therefore, a PRSW has a 20% advantage to a fully restrained shear wall that does not include the whole building factor. The committee placed a further limit on the brace wall requirements. This limit is that the net uplift at the top of the brace wall shall not exceed 100 plf. If this is exceeded, then an additional connection at the base of the wall is required.

2.2.2 2009 IRC Requirements

The IRC has several options for providing lateral bracing to a residential structure. The lateral forces on the structure are resisted by braced wall panels. The

braced wall panels can be constructed with either continuous sheathing methods or intermittent bracing methods. Intermittent braced wall panels can include diagonal let-in bracing, diagonal sheathing, horizontal siding, or portals. The option which is the focus of this thesis is intermittent braced wall panel construction, as shown in Figure 2, utilizing the Wood Structural Panel (WSP) bracing option. The WSP option can be thought of as a shear wall but is constructed differently than traditional engineered wood shear walls, i.e. they may not have a special hold down connector.

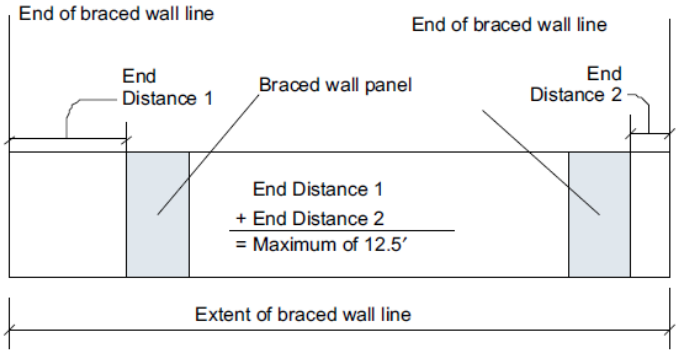

Braced wall panel shall be permitted to be located away from the end of a braced wall line, provided the total end distance from each end to the nearest braced wall panel does not exceed 12.5′. If braced wall panel is located at the end of the braced wall line, then end distance is 0′.

Figure 602.10.1.4(2)
Excerpted from the *2009 International Residential Code*, Copyright 2009.
Washington, D.C.: International Code Council.
Reproduced with permission. All rights reserved. www.ICCSAFE.org

Figure 2: IRC Braced Wall Panel Location (IRC)

The IRC provides a prescriptive method of lateral bracing for residential structures. The bracing requirements are dependent upon both wind loads and seismic loads. For each lateral load condition, the IRC tabulates the total length of braced wall panels per braced wall line as well as braced wall line spacing. A braced wall line is a wall selected by the designer to contain braced wall panels. The designer then selects the braced wall panel type. The braced wall panels must then be located within the

braced wall lines as specified in the IRC. For WSP, the minimum panel width for the intermittent brace panel method is 48" and the minimum panel thickness is $^3/_8$". This thesis will be limited to wind loading and not seismic loading.

Wind Speed = 90 mph → 9' Braced Panel Length Required
Exposure B, 1 Story, 8 ft walls → Multiply x1
Roof Eave-to-Ridge Height <6' → Multiply by 0.7 and 0.9
No gypsum on interior → Multiply by 1.4

Required Braced Panel Length including all factors:

$$L' = 9 \times 1.0 \times 0.7 \times 0.9 \times 1.4 = 7.94' \quad \leftarrow \text{Say } 8'$$

From IRC Section R602.10.1.2 and Table R602.10.1.2(1)

Figure 3: IRC Braced Wall Panel Length

The IRC tabulates the braced wall panels by basic wind speed varying from 85 m.p.h. to 110 m.p.h. A series of adjustment factors are then applied to the tabulated length of brace wall panels. These factors include: exposure and building height adjustment; roof to eave height adjustment; number of braced wall line adjustment (to account for increased shear on braced wall lines from continuous diaphragms, see discussion below); and an adjustment factor if gypsum or equivalent is not installed on the interior face of the wall panel. An example of a required length of a braced wall line is given in Figure 3.

The IRC also specifies all of the connections required for the braced wall panels as well as the connections of the structure to the wall panels. This includes the sheathing fastening to the studs, the studs to the plates, the sole plate to the floor or

foundation, and the roof or floor to the wall top plate. The sheathing fastening is typical for a braced wall panel and ordinary sheathing.

The IRC bracing method distributes the lateral loads equally amongst brace wall panels. This is because it is assumed that the braced wall lines have the minimum lengths of brace wall panels and therefore are of equal stiffness. Whole building tests have shown that roof systems behave more like rigid diaphragms than flexible diaphragms (Crandell and Kochkin 2003). Therefore, the IRC includes an adjustment factor to increase the length of the braced wall when two or more brace wall lines exist. This factor is 1.3 for 3 braced wall lines, 1.45 for 4 braced wall lines, and 1.6 for 5 or more braced wall lines.

Aside from the combined partial restraint and whole building factor of 1.2 discussed earlier, the IRC uses a rational approach. For WSP, the nominal brace wall capacity used is 700 plf which includes 200 plf capacity for ½" gypsum applied to the interior face (Crandell and Martin 2009). Using allowable stress design (ASD), a factor of safety of 2 was applied to the nominal value. This is in accordance with the *2005 Special Design Provisions for and Seismic* (AF&PA SDPWS).

2.3 Differences between Prescriptive and Engineered Solutions

The major difference between the prescriptive design of the 2009 IRC and a rational design using SDPWS is that the IRC applies a combined partial restraint and whole building factor of 1.2 discussed earlier. An engineered design typically neglects any applied dead load to the wall and requires a special hold down connector. This is illustrated in Figure 4.

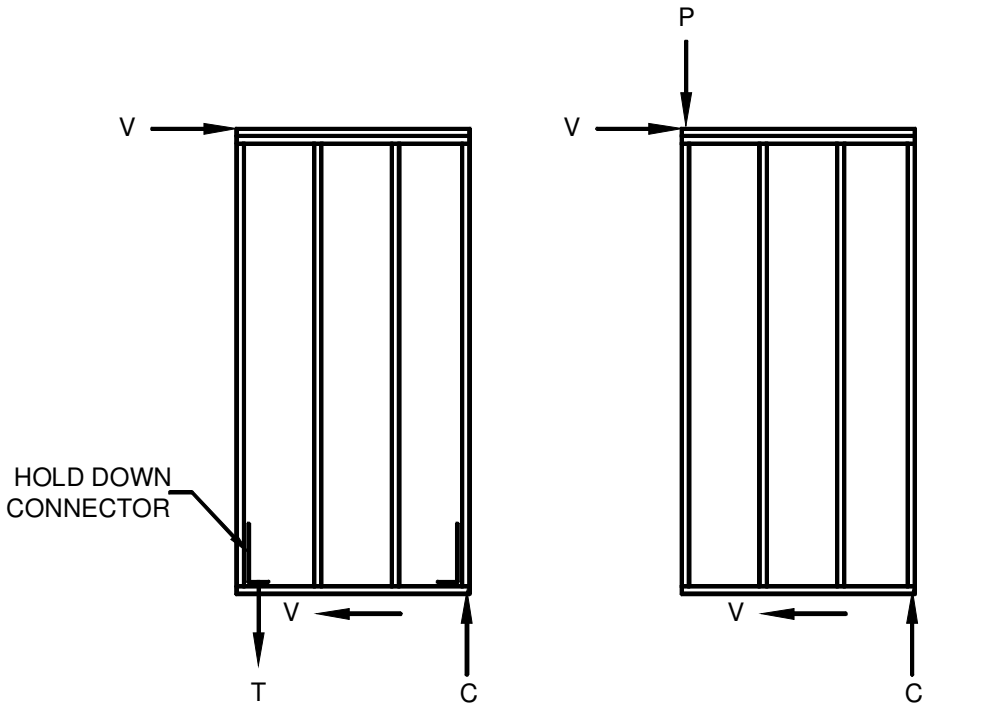

Figure 4: Engineered Shear Wall Restraint Methods

In order to resist the uplift force in a WSP shear wall, one of three methods must be present for equilibrium. These are a special hold down connector, a dead load force applied at the tension chord, or some other dead load applied along the wall. It is common engineering practice to provide a special hold down connector neglecting any dead loads. This assures that there is a proper load path to resist the overturning of the wall. If a dead load occurs directly over the tension chord, this could be used to restrain or partially restrain the wall, but it has a major limitation for an engineered approach. This limitation is the load combination that requires using only 60% of the dead load to resist wind overturning forces (ASCE 7). This 40% reduction can have a huge impact on the uplift resistance. For the last option, special fastening of the wall sheathing is required. From a mechanics analysis of the wall, the sheathing resists the

shear and therefore the sheathing must be resisted from overturning. Therefore, it is necessary to transmit, for example, a uniform dead load applied to the top of the wall from the wall studs to the sheathing. This may require closer fastener spacing along the studs near the end of the wall than would otherwise be specified if a mechanical restraint was applied directly to the tension chord.

These differences in design approaches make a huge difference when trying to add a braced wall line or a complete bracing design based on SDPWS to a residential structure that doesn't meet the criteria to use the prescriptive method. Although the whole building factor may be different for a building that meets the prescriptive criteria than for a building that may have larger wall openings or otherwise doesn't meet the prescriptive criteria, there should be some whole building factor that applies to a design based on SDPWS as well. Also, what effect does the 40% reduction in dead load to resist overturning per the code imposed load combinations have on the reliability of the prescriptive system without hold downs?

2.4 Actual Wind Load on a Shear Wall

There are several factors that determine the actual wind load on a shear wall. The first main factor is on the load side of the design equation. There are several variables to consider in determining the wind load using ASCE 7. The second main factor is the load path. A simple analysis may consider flexible diaphragms, while a more complex analysis may consider a rigid diaphragm.

To determine the wind load on a structure, the location must be known as well as site conditions. ASCE 7 provides a wind speed map for the United States for the building designer to determine the nominal 3 second wind gust at a height of 33 feet

above the ground for an exposure C terrain category with a 2% probability of occurrence. ASCE 7 provides two methods to calculate the design wind pressure, the simplified procedure and the analytical procedure. Either procedure relies upon the following factors to adjust wind for specific site conditions:

- Exposure Adjustment
- Wind Directionality
- Topographic Adjustment

Building specific adjustments are also required. These include:

- Height Adjustment
- Importance Factor
- Pressure Coefficient
- Gust Factor

Of the adjustments noted, only the exposure, topographic, and height would vary from building to building for a residential structure. Of course, the wind speed can vary as well depending upon the location. However, more than 90 percent of conventional building stock is located in an Exposure B category based on experimentally controlled building assessments (Crandell and Kochkin 2003). Additionally, high wind regions typically require additional bracing and detailing to prevent cladding breaches. Therefore, the limit of this thesis will be for a nominal wind speed of 90 mph and an Exposure B category.

ASCE 7 further adds a requirement to design wind pressures, that the minimum wind pressure shall be 10 psf acting normal to the projected area of the structure in the direction of the wind, as an additional load case. According to the spreadsheet calculations available to support the 2009 IRC code change (RB148), the required 10 psf minimum wind load was not used for the prescriptive method in the IRC (FSC).

This can make an appreciable difference in the total wind load for this type of structure with this exposure category.

Residential structures typically don't have ideally constructed diaphragms (Crandell and Kochkin 2003) nor are they simple rectangular diaphragms. For more contemporary homes, it is not uncommon to have a break in the diaphragm such as at a bridge or two story room. For these reasons, actual wall shear forces may vary considerably for an actual structure compared to the idealized structures of the IRC prescriptive design. Therefore, there may be appreciable differences in the actual load on a braced wall panel when a structure-specific engineering analysis is performed then the simplified analysis used for the prescriptive method of the IRC.

2.5 Partially and Unrestrained Shear Walls

A great deal of shear wall testing has been performed since as early as 1929 (Crandell and Kochkin 2003). So much testing and studying has occurred since 1983 that John van de Lindt, PhD prepared a paper titled *Evolution of Wood Shear Wall Testing, Modeling, and Reliability Analysis: Bibliography* (van de Lindt 2004) This document tabulates much of the research that was performed, but is not intended to be inclusive of all work.

The beginning of the acceptance of an unrestrained shear wall in the United States seems to stem from the perforated shear wall (PSW) method that the American Forest & Paper Association/American Wood Council (AF&PA/AWC) discovered from Japan (Crandell 2007). Although the PSW method did require hold downs at each end, the method allowed for full height openings within the shear wall. Previous to this

method, the shear wall was considered a series of shorter shear walls, called a segmented wall, with each segment requiring hold downs.

The PSW method still didn't correlate with conventional construction practices of not providing hold downs. Thus research began to develop a design method to construct shear walls without hold downs (Crandell 2007). This included using corners as restraint (Dolan and Heine 1997) and PRSW (Ni and Karacabeyli 2000). Walls with IRC prescribed anchorage compared to full restraint (mechanical hold down) and partial restraint by an applied load was conducted to compare the difference between monotonic and cyclic loading (Seaders 2004). The PRSW method (Ni and Karacabeyli 2000) is of interest since it presents both a mechanics-based method and an empirical method to determine the capacity of the wall under partial restraint. Also of interest is the IRC prescribed anchorage monotonic and cyclic comparison study.

Many factors can affect the shear capacity of a PRSW (Crandell and Martin 2009). These conditions include:

- Length of wall extending beyond either end of the bracing element
- Wall components or opening conditions adjacent to a bracing element
- Support conditions (framing assembly stiffness and dead load above the bracing element)
- Strength of bracing method relative to strength of conventional framing and connections providing restraint to a given brace panel at its boundaries.
- Contribution of non-structural components and non-compliant bracing elements in a whole house test.

The mechanics-based method derived in Ni and Karacabeyli (2000) assumes that some of the boundary fasteners in the sole plate are used only for the uplift resistance while the remaining fasteners resist the shear. The result is the reduction

factor, α, which is multiplied by the fully restrained shear capacity of a wood shear wall.

Eq. 1 is presented in Graph 1. Note that the relationship is nearly linear:

$$\alpha = \sqrt{1 + 2\phi\gamma + \gamma^2} - \gamma \qquad \text{Eq. 1}$$

Where,

$$\gamma = \frac{H}{L}$$

$$\phi = \frac{P}{MC_N}$$

H = height of the shear wall
L = length of the shear wall
P = uplift restraint force on end stud of a shear wall segment
M = total number of nails along the end stud
C_N = lateral load capacity of a single nailed joint

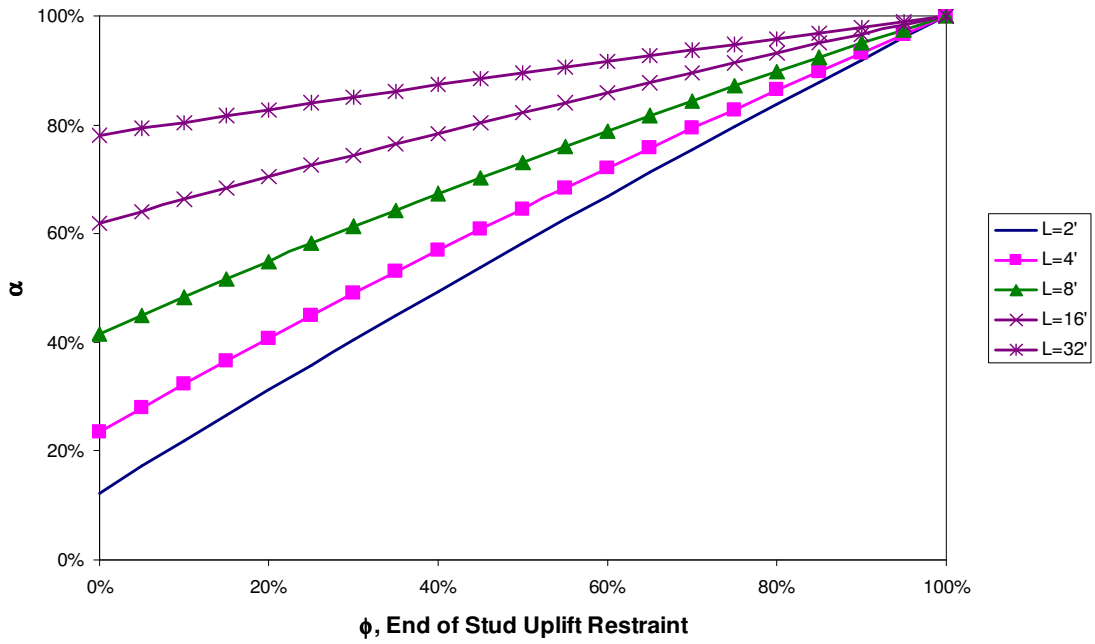

Graph 1: Effect of Uplift Restraint on the Lateral Load Capacity of a Shear Wall Based on Mechanics-Based Approach (Ni and Karacabeyli 2000)

Using the results of both monotonic and cyclic testing, the ratio of the lateral load capacity of a wall with no restraint to a wall with full restraint, α, the following empirical relationship was determined (Ni and Karacabeyli 2000).

$$\alpha = \frac{1}{1+\gamma(1-\phi)^3} \qquad \textbf{Eq. 2}$$

This equation is presented graphically in Graph 2.

Although Graph 2 seems to indicate that there is no uplift restraint, i.e. ϕ=0, the test method used to develop Eq. 2 used ½" diameter anchor bolts at 16" o.c. with the first bolt 8" from the end of the wall, providing some uplift resistance.

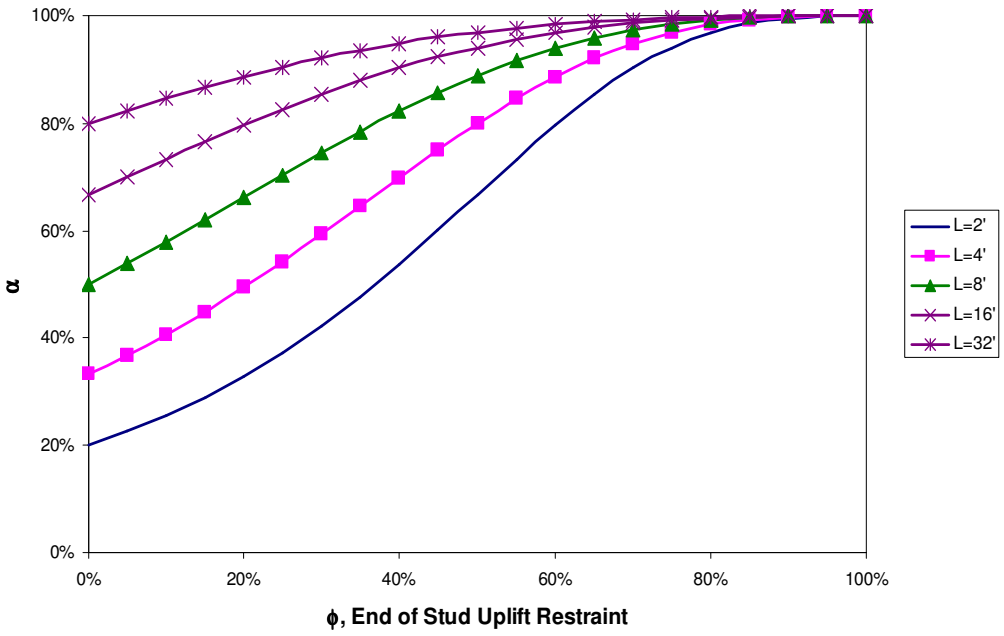

Graph 2: Effect of Uplift Restraint on the Lateral Load Capacity of a Shear Wall Based on Empirical Approach (Ni and Karacabeyli 2000)

The *SDPWS* also provides a method for designing PSW, but still requires hold downs at the very ends of the wall. This method allows for unrestrained segments within the length of the wall.

Seaders (2004) specifically studied walls constructed in accordance with the IRC prescriptive requirements. All of the walls tested were 8' x 8' with $^{7}/_{16}$" OSB sheathing fastened with 8d Common nails at 6" o.c. at the perimeter edges and 12" o.c. along intermediate members. The walls also had a layer of ½" gypsum on the opposite face to resemble a typical residential wall. The gypsum was fastened with #6 x $1^{5}/_{8}$" bugle head screws at 12" o.c. at the perimeter edges and along intermediate members. This study was of seven unstrained shear walls monotonically loaded; eight unrestrained shear walls cyclically loaded; one Partially Restrained Shear Wall (PRSW) with a 2.41 K load concentrically placed; one Partially Restrained Shear Wall with a 4.00 K load concentrically placed; two Fully Restrained Shear Walls (FRSW) monotonically loaded; and two Fully Restrained Shear Walls cyclically loaded. The restraining forces were applied at the quarter points of the wall on a steel spreader bar. The results of the monotonic tests are presented in Table 5.

Table 5: Summary of Test Data (Seaders 2004)

		Monotonic				
# of Tests Anchorage		N=7 Unrestrained		N=1 PRSW	N=1 PRSW	N=2 FRSW
Load	Units	Average	COV			
P_{DL}	lb			2405	4002	
P_{Peak}	lb	2169	14.9%	3062	4071	5472
P_{Peak}	plf	271		383	509	684

There are three notable differences between Seaders' (2004) research and Ni and Karacabeyli's (2000). First, Seaders (2004) anchored the wall in accordance with the IRC. The anchorage consisted of one ½" diameter anchor 12" from each end. This is the maximum distance from the end of the wall allowed by the IRC and results in bolt

spacing of 6', the maximum spacing allowed by the IRC. Second, Seaders (2004) used gypsum on the opposite face of the wall than the WSP. The intent was to apply the dead load of the gypsum rather than add additional stiffness from the gypsum. It is important to note that the fastener spacing in the gypsum was 12" o.c. throughout compared with 7" o.c. specified in the IRC. Third, Seaders (2004) compared the variability of monotonic testing with the variability of cyclic testing while Ni and Karacabeyli (2000) proposed a method of determining the capacity of an unrestrained wall.

It is very important to point out that both Seaders (2004) and Ni and Karacabeyli's (2000) work considered the full restraint capacity as the capacity of the shear wall with a mechanical hold down at the base of the wall. Therefore, Ni and Karacabeyli's (2000) partial restraint factor, Eq. 2, is derived from the capacity of the wall when a mechanical hold down is used at the base of the wall.

2.6 Special Design Provisions for Wind and Seismic (2005)

The SDPWS (2005) provides design methodologies for wood diaphragms and shear walls and contains nominal ultimate unit shear capacities for shear walls constructed with WSPs. These capacities are tabulated for various thickness sheathing and fastener spacing for both wind and seismic. The values in these tables are 2.8 times the values given in APA Research Report 154 (2004), the source of the capacities. APA Research Report 154 (2004) will be discussed later. SDPWS (2005) is also the source of the semi-rational design values for the 2009 IRC.

Of interest to this research is the capacity of the $^{15}/_{32}$" WSP fastened with 8d Common nails at 6" o.c. along the edges and 12" o.c. at the intermediate members.

Also, for comparison purposes of previous testing (Seaders 2004, SBCRI 2010) the capacity of $^{7}/_{16}$" WSPs fastened with 8d Common nails at 6" o.c. along the edges and 12" o.c. at the intermediate members is also of interest, as well as $^{3}/_{8}$" panel thickness. The SDPWS values for these three panels are tabulated in Table 6.

The values tabulated in Table 6 are required to be modified by either a factor of safety, Ω, for allowable stress design (ASD) or multiplied by a resistance factor, ϕ, for load and resistance factored design (LRFD). These values are given in SDPWS as:

$$\Omega=2.0 \text{ and } \phi=0.80$$

Table 6: Nominal Unit Shear Capacities for Wood-Frame Shear Walls (SDPWS 2005)

Sheathing Material	Minimum Nominal Panel Thickness (in)	Fastener Type & Size	Wind
			Panel Edge Fastener Spacing (in)
			6
		Nail (common or galvanized box)	v_w[2]
			(plf)
Wood Structural Panels - Sheathing	$^{3}/_{8}$"	6d	560
	$^{7}/_{16}$"[1]	8d	670
	$^{15}/_{32}$"	8d	730

[1]Shears are permitted to be increased to values shown for 15/32" sheathing with same nailing provided (a) studs are spaced a maximum of 16" o.c. or (b) panels are applied with long dimension across studs.

[2]For framing grades other that Douglas Fir-Larch or Southern Pine, reduced nominal unit shear capacities shall be determined by multiplying the tabulated nominal unit shear capacity by the Specific Gravity Adjustment Factor = [1-(0.5-G)], where G=Specific Gravity of the framing lumber from the *NDS*. The Specific Gravity Adjustment Factor shall not be greater than 1.

Of further interest in SDPWS is the discussion of the resistance factor. The commentary states that the "LRFD resistance factors have been determined by a ASTM consensus standard committee" (SDPWS 2005). This statement is referring to the *Standard Specification for Computing Reference Resistance of Wood-Based Materials and Structural Connections for Load and Resistance Factor Design, ASTM D 5457*

(ASTM D 5457). The resistance factors were reportedly "derived to achieve a target reliability index, β, of 2.4 for a reference design condition" (SDPWS 2005).

SDPWS also has a method for determining the capacity of intermittent bracing known as the Perforated Shear Wall (PSW) as mentioned earlier. The 2009 IRC used the PSW method to approximate the partial restraint factor. The PSW method in the SDPWS differs from Ni and Karacabeyli's (2000) method to determine the capacity of a PRSW.

SDPWS uses a shear capacity adjustment factor, C_o, to modify the nominal shear capacities of the full height sheathed wall segment which is a function of the wall openings and the length of the wall. For intermittent shear walls, C_o is determined assuming that all openings are full height. It is tabulated in SDPWS as a function of the percent of full-height sheathing. The tabulated values of C_o are calculated as shown in Eq. 3.

$$C_0 = \frac{\mathrm{F}}{\%\,\mathrm{FH}} \qquad \textbf{Eq. 3}$$

where,

$\%\,\mathrm{FH} = \%$ of Full-Height Sheathing

$L =$ total length of shear wall

$\sum \mathrm{L_i} =$ sum of the width of full-height sheathing

$$F = \frac{r}{3 - 2r}$$

$$r = \frac{1}{\left(1 + {A_o}/{h\sum L_i}\right)}$$

$r =$ sheathing area ratio

$A_o =$ total area of openings

$h =$ wall height

The IRC originally used a modified version of Eq. 3 to estimate the partial restraint factors indicated in Table 4. The modified version used F=r/(2-r) deemed to be more accurate and less conservative (Crandell 2007). The lowest value of C_o tabulated in SDPWS is for 10% full-height sheathing and is equal to 0.36, which for 4' shear walls equates to a 5% restraining force using Ni and Karacabeyli's (2000) method. For C_o to equal 0.8 as used in the IRC, 88% of the brace wall line would have to be sheathed at full height.

The PSW requires restraints at the very ends of the walls, as does a fully restrained wall. These restraints can be mechanical hold downs or dead load. Additionally, the sole plate of each full height segment must be anchored to the foundation for a uniform uplift force equal to the unit shear (SDPWS). This is not a requirement of the 2009 IRC.

2.7 Voluntary Product Standard

The National Institute of Standards and Technology (NIST) publishes the Voluntary Product Standard PS 2-04 titled *Performance Standards for Wood-Based Structural-Use Panels* (NIST 2004). This voluntary standard specifies minimum ultimate unit shear capacities that panel manufacturers must meet. The standard utilizes the ASTM E-72 test procedure. The minimum unit shear strengths listed in this document are 2.8 times the nominal values published in APA Research Report 154 (2004). This is the source of the 2.8 value used in the SDPWS.

For a WSP to comply with the standard, two tests are required. Both tests must pass the minimum specified strength of the standard. Furthermore, both test results must be within 10% of each other. If both tests pass the strength but are not within 10%

of each other, then a third test may be performed. The lowest two of the three tests must then exceed the strength requirement and must be within 10% of each other. The standard does not have values for all nail spacings used in the SDPWS.

2.8 APA Research Report 154

APA-The Engineered Wood Association publishes APA Research Report 154 titled *Wood Structural Panel Shear Walls* (APA 2004). The source for the SDPWS tabulated nominal ultimate unit shear values is from the base values in the APA Research Report 154 (2004). The APA Research Report 154 (2004) values match the tabulated nominal ultimate unit seismic shear values in the SDPWS. The wind values tabulated in the SDPWS are 40% greater than APA Research Report 154 (2004) values.

The nominal unit shear values tabulated in APA Research Report 154 (2004) are historic values from the 1958 to 1964 Uniform Building Codes. APA Research Report 154 (2004) provides a comparison of the nominal unit shear values to previous tests and is shown here in Table 7. The target design shear is the nominal unit shear values tabulated in APA Research Report 154 (2004) or 1/2.8 the tabulated nominal ultimate unit shear values for wind tabulated in SDPWS and the nominal minimum ultimate unit shear values tabulated in PS-2 (2004).

The comparison in Table 7, noted as the load factor, is between the average test results and the target design shear and ranges from 2.1 to 4.1. Table 7 also indicates the number of tests used for the comparison as well as the minimum, maximum, and average ultimate load. Of interest is the $^{15}/_{32}$" rated sheathing with 8d nails spaced at 6" o.c. The table provides the results of seven tests with an average ultimate strength

of 913 plf; a minimum strength of 689 plf; and a maximum strength of 1033 plf. Note also that the target design shear for this wall is 260 plf which results in a load factor of 3.5. The target design shear is equal to the 730 plf tabulated in SDPWS (rounded up from 728 plf) divided by 2.8 as discussed previously, or 260 plf.

Table 7: APA Test Comparisons (APA 2004)

SUMMARY OF APA SHEAR WALL TESTS, NAILS (Common, Short, Duplex or Galvanized Box)

Fastener Size	Fastener Spacing (in.)	Panel Thickness[a] (in.)	No. of Tests	Ultimate Loads (plf) Min.	Ultimate Loads (plf) Max.	Ultimate Loads (plf) Avg.	Target Design Shear (plf)	Load Factor[b]
STRUCTURAL I								
6d	6	5/16	9	635	1168	821	200	4.1
8d	6	15/32	2	973	981	977	280	3.5
	4	15/32	1			1539	430	3.6
	3	3/8	7	1136	1513	1362	460	3.0
		7/16	7	1409	1645	1497	505	3.1
		3/8	1			1844	550[c]	3.4
	2	3/8	1			1727	610	2.8
		3/8	2	1650	2109	1880	730[c]	2.6
10d	6	15/32	1			1256	340	3.7
	4	15/32	1			1701	510	3.3
	3	15/32	30	1496	2280	1963	665	3.0
RATED SHEATHING								
6d	6	1/4	18	511	850	695	180	3.9
		3/8	5	535	1076	737	200	3.7
	4	1/4	2	771	790	781	270	2.9
		3/8	2	701	828	764	300	2.5
	3	1/4	12	955	1276	1084	350	3.0
		3/8	7	816	1390	1143	390	2.9
8d	6	3/8	2	600	764	682	220	3.1
		15/32	7	689	1033	913	260	3.5
	4	3/8	1			964	320	3.0
		15/32	2	1155	1155	1155	380	3.0
	3	3/8	17	1156	1680	1392	410	3.4
		7/16	17	1295	1860	1507	450	3.3
		3/8	25	1296	1850	1520	490[c]	3.1
	2	3/8	4	938	1363	1156	530	2.2
		3/8	3	1328	1688	1524	640[c]	2.4
10d	6	15/32	3	780	1048	929	310	3.0
		19/32	1			1134	340	3.3
	4	15/32	3	1277	1881	1526	460	3.3
	3	15/32	31	1200	1964	1651	600	2.8
		19/32	18	1396	2165	1858	665	2.8
		15/32	1			1586	770	2.1

(a) Minimum panel thickness for design shear, some walls sheathed with thicker panels.
(b) The load factor is determined by dividing the average ultimate load by the target design shear.
(c) Design shear increased for "over-thick" panel, studs 16" o.c. or panel placed with length perpendicular to framing.

Reprinted with permission from APA Research Report 154, *Wood Structural Panel Shear Walls*, Form No. Q260C by APA-*The Engineered Wood Association*.

2.9 Shear Wall Strength and Computer Modeling

Shear wall strength can be either calculated (mechanistic) or determined from testing (hysteresis). A mechanistic model is provided in APA Research Report 154 (2004) for determining the capacity of a fully restrained shear wall. This model is based on the nail capacities in the NDS (2005). The mechanistic model simply resolves the applied shear along the sole plate and the uplift force into the tension stud through the fasteners in a unidirectional shear in the direction of the sole plate and tension chord respectively. Cyclic testing is used to determine the nonlinear load-deformation response of a shear wall. From this testing the hysteresis curves are produced. The backbone curve, also referred to as the envelope curve, is formed from the peaks of the hysteresis curves. The backbone curve, shown in Figure 5, closely approximates the nonlinear load deformation curve produced from a monotonic test (van de Lindt 2003).

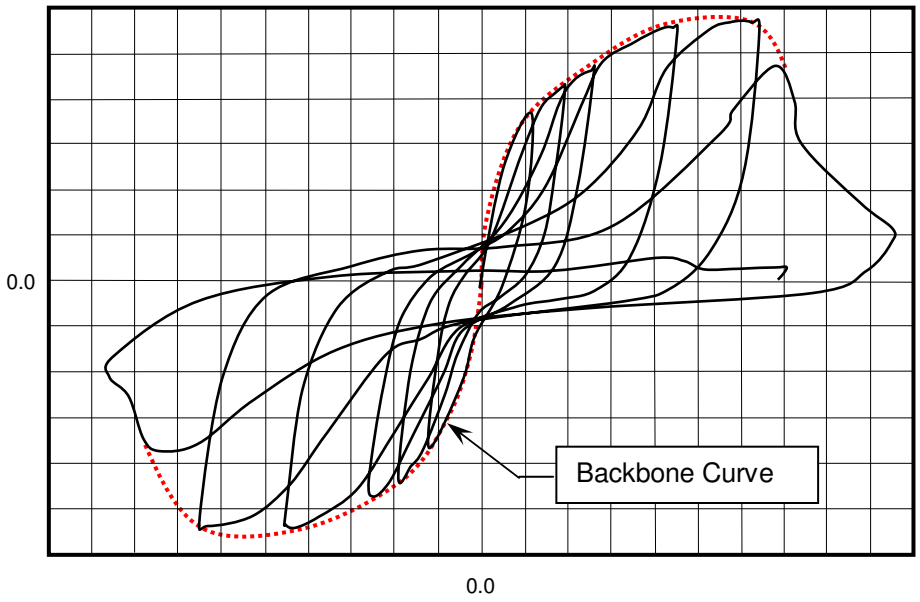

Figure 5: Hysteresis Curve Example

The *CASHEW* program was developed by CUREE (California Universities for Earthquake Engineering) to predict the load-displacement response for cyclic and monotonic loading (Folz and Filiatrault 2001). The program uses 10-parameter nail data to define the hysteresis loop as shown in Figure 6. Nail data is used from other research to define the 10 parameters (van de Lindt and Walz 2003).

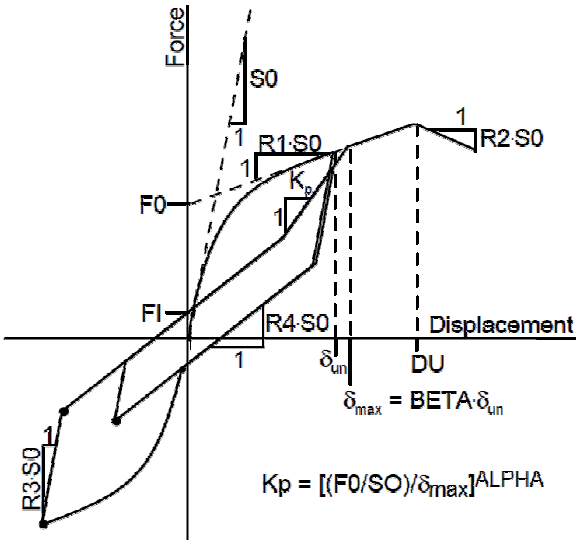

Folz and Filiatrault 2000

Figure 6: Hysteretic Response of a Sheathing-to-Framing Connector

This program and model has been used in several seismic studies for shear wall modeling. The program was altered to add pinching effects in a reliability model by van de Lindt and Walz (2003).

It is also noted that the *CASHEW* User's Manual provides an example comparing it to tests performed by Durham. The *CASHEW* results for the monotonic loading were 26% greater the actual shear wall test result (Folz and Filiatrault 2000).

2.9.1 Finite Element Modeling

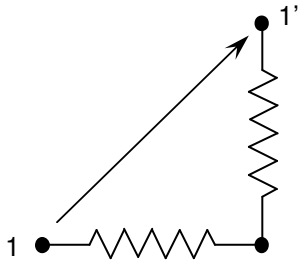

Figure 7: Spring Pair

Several studies have been done using finite element modeling (FEM) of wood shear walls. These studies have evolved over the years and can be rather simplistic models or more complex models that account for every connection in the wall. The programs used for the finite element include commercial programs such as *ABAQUS* and *ANSYS.* Others have developed programs as well, such as *SHWALL* and *CASHEW*.

This work is best summarized by Cassidy (2002) and Judd (2005). The most common models include beam elements for framing members, four and eight node plane stress elements for sheathing, and two orthogonal nonlinear springs (or spring pair), Figure 7, to model the connections from the sheathing to the framing members (e.g. Dolan and Foschi 1991; Folz and Filiatrault 2001; Cassidy 2002; Judd 2005).

Of the referenced examples, Judd, using *ABAQUS*, created an oriented spring pair as a user element. Judd recognized that for nonlinear springs, the bilinear spring isn't equivalent to a single one dimensional spring. For monotonic loading, the peak load and displacement can be accurately calculated with a bilinear spring element. However, the total energy absorbed by the system is not accurate with the bilinear spring, since the load deformation curve does not completely represent the behavior of the actual wall (Cassidy 2002). The increased resultant stiffness overestimates the total energy absorbed.

The most common method of modeling the framing connections is with pinned joints (e.g. Judd 2005, *CASHEW*). The results of these models reasonably match the

test walls that they were developed for, but this type of model doesn't accurately capture the actual behavior of the wall. Cassidy (2002) used another spring pair to model the behavior of the stud to plate connection. The spring pair had differing stiffness for the load direction.

Using a typical stud-to-plate connection of two 16d Common nails, Cassidy (2002) used a lateral stiffness of 12,000 lb/in which corresponds to results published by Dolan *et. al.* (1995). Cassidy (2002) found that this parameter had "very little effect on the overall load-displacement response of the wall." Cassidy (2002) used a nonlinear vertical stiffness. For compression, a vertical stiffness of 41,000 lb/in was used which corresponds to his reported test results for the crushing of the wood sole plate. Cassidy then used a tension stiffness of 100 lb/in. This was an assumption by Cassidy. The vertical tension stiffness of course relates to nails installed in the end grain of the stud loaded in withdrawal. According to the NDS Commentary (AF&PA 2005), there can be up to a 50% reduction in nail withdrawal strength into end grain, and coupling this with seasoning, the values are deemed too unreliable and are prohibited. However, there is definitely some resistance and stiffness in this connection; although not reported to the author's knowledge.

2.9.2 Sheathing Nail Modeling

Sheathing nail modeling is considered in two ways. The first is considering the yield limit equations from the NDS (AF&PA 2005). The second is considering the load deformation relationship of the fasteners. The latter is of interest for finite element modeling while the former is helpful in the understanding of allowable nail capacities published in the NDS.

2.9.2.1 NDS Yield Limit Equations

The yield limit equations in the NDS (AF&PA 2005) provide a method to calculate nail connection strength based on limit states or modes of failure. The yield limit equations are a mechanics based method. *Technical Report 12* (AF&PA 1999) expands on the yield limit equations used in the NDS (AF&PA 2005). The modes of failure of a dowel-type connection are "uniform bearing under the fastener, rotation of the fastener in the joint without bending, and development of one or more plastic hinges in the fastener." (AF&PA 1991). *Technical Report 12* (AF&PA 1999) provides the basis for calculating the ultimate nail capacity for each mode of failure by considering the specific gravity of the material, the thickness of each member, any gap that may exist between the members, and the yield strength of the fastener. This is not the failure load, but is rather the ultimate load. The failure load occurs after the ultimate load is reached.

For single shear, there are four modes of failure to consider, Figure 8. These modes are briefly described and explained here. They are based on no gap between the members. Additionally, *Technical Report 12* (AF&PA 1999) provides methods for calculating the failure load at the proportional limit, the 5% offset limit, and the ultimate limit. Only the ultimate limit is presented here.

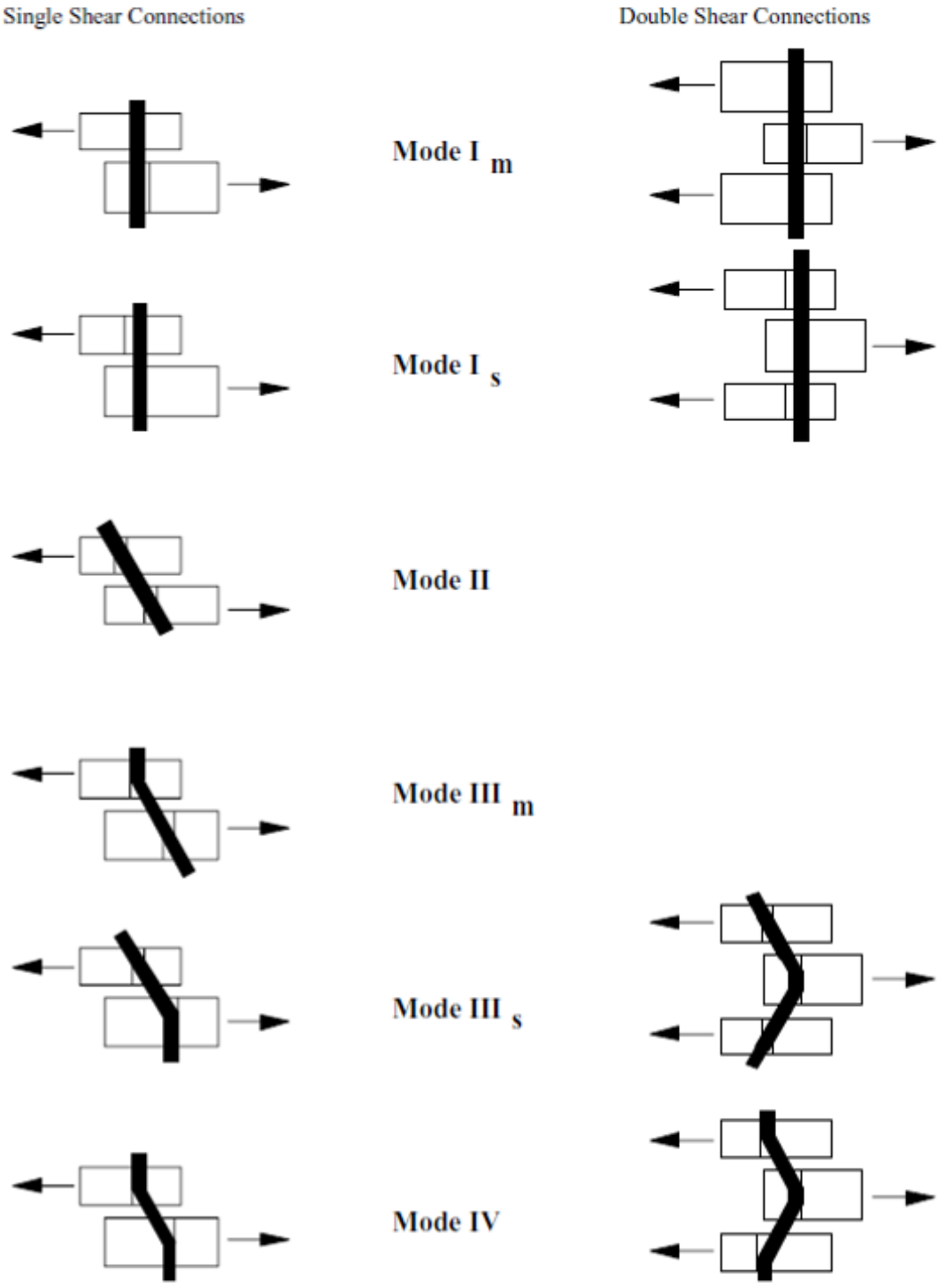

Reprinted with permission from Technical Report 12, *General Dowel Equations for Calculating Lateral Connections* by the American Wood Council, Leesburg, VA

Figure 8: Connection Yield Modes

2.9.2.1.1 Mode I_m and I_s

The limit state for failure mode I is either wood bearing in the main member (I_m) or wood bearing in the side member (I_s) with no rotation or yielding of the fastener. Mode I strength is:

I_m $\quad P = q_m l_m$ **Eq. 4**

I_s $\quad P = q_s l_s$ **Eq. 5**

2.9.2.1.2 Mode II

The limit state for failure mode II is side and main member wood bearing with rigid rotation of the fastener, but no yielding of the fastener. Mode II strength is:

$$\text{II} \qquad P = \frac{-B + \sqrt{B^2 - 4AC}}{2A} \qquad \textbf{Eq. 6}$$

where,

$$A = \frac{1}{4q_s} + \frac{1}{4q_m} \qquad B = \frac{l_s}{2} + \frac{l_m}{2} \qquad C = -\frac{q_s l_s^{\,2}}{4} - \frac{q_m l_m^{\,2}}{4}$$

2.9.2.1.3 Mode III_m and III_s

The limit state for failure mode III is either main member bearing and yielding of the fastener in the side member (III_m) or side member bearing and yielding of the fastener in the main member (III_s). Mode III_m and III_s strength is defined by Eq. 6 where,

III_m $\quad A = \frac{1}{2q_s} + \frac{1}{4q_m} \qquad B = \frac{l_m}{2} \qquad C = -M_s - \frac{q_m l_m^{\,2}}{4}$

III_s $\quad A = \frac{1}{4q_s} + \frac{1}{2q_m} \qquad B = \frac{l_s}{2} \qquad C = -\frac{q_s l_s^{\,2}}{4} - M_m$

2.9.2.1.4 Mode IV

The limit state for failure mode IV is yielding of the fastener in both the side and the main member. Mode IV strength is defined by Eq. 6 where,

$$\text{IV} \qquad A = \frac{1}{2q_s} + \frac{1}{2q_m} \qquad B = 0 \qquad C = -M_s - M_m$$

For all modes, the following definitions are used,

P = nominal lateral connection value, lb
l_s = side member dowel bearing length, in
l_m = main member dowel bearing length, in
q_s = side member dowel bearing resistance = $F_{es}D$, lb/in
q_m = side member dowel bearing resistance = $F_{em}D$, lb/in
F_{es} = side member dowel bearing strength, psi
F_{em} = main member dowel bearing strength, psi
D = dowel shank diameter, in
F_b = dowel bending strength, psi
D_s = dowel diameter at max. stress in side member, in
D_m = dowel diameter at max. stress in main member, in
M_s = side member dowel moment resistance = $F_b(D_s^3/6)$
M_m = main member dowel moment resistance = $F_b(D_m^3/6)$
F_e = 0.8 x $11735G^{1.07}/D^{0.17}$, psi (parallel to grain)
G = specific gravity
$F_b = F_{b,\,ult}$, psi

All of the limit states must be checked to determine the failure load of the fastener. The failure load is then the least of modes I_m, I_s, II, III_m, III_s, and IV.

2.9.2.2 Load Deformation of Nails

Several methods for modeling the load deformation have been developed over the years. According to Judd (2005), these range from power curve (Mack 1977; APA), logarithmic curve (McClain 1975), and exponential curve (Mack 1966; Easley et. al.

1982; Foschi 1977). The most commonly used model is the exponential curve (Cassidy 2002; Judd 2005). Only the exponential curve model will be discussed.

The exponential curve was first introduced by Foschi (1974; 1977) and is shown in Eq. 7.

$$P = (P_0 + K_2\delta)\left[1 - e^{\frac{-K_1\delta}{P_0}}\right] \qquad \textbf{Eq. 7}$$

According to Judd (2005),

> K_1 is the initial stiffness, K_2 is the secondary stiffness, and P_0 is the secondary stiffness y-axis intercept (not shown is a softening branch past the limiting point, where K_3 is the tertiary stiffness). Note that K_1, K_2, and K_3, are physically identifiable parameters. By defining it as a "physically identifiable parameter" it is intended to signify a parameter inherent (fundamental) to behavior (such as stiffness) that is not specific to any particular equation, in contrast to a parameter that is only a modifier of the equation, and thus indirectly related to behavior.

This equation was modified by Dolan (1989) to include a softening branch beyond the point of failure. Further modifications were made by Folz and Filiatrault (2001) by defining a failure displacement, δ_{fail}, terminating the softening branch. The final resulting equation is shown in Eq. 8 and graphically in Graph 3.

$$P = \begin{cases} (P_0 + K_2\delta)\left[1 - exp\left(\dfrac{-K_1\delta}{P_0}\right)\right], \text{if } \delta \le \delta_{ult} \\ (P_{ult} + K_3)(\delta - \delta_{ult}), \text{if } \delta_{ult} < \delta \le \delta_{fail} \\ 0, \text{if } \delta > \delta_{fail} \end{cases} \qquad \textbf{Eq. 8}$$

Graph 3: Nail Deformation Model

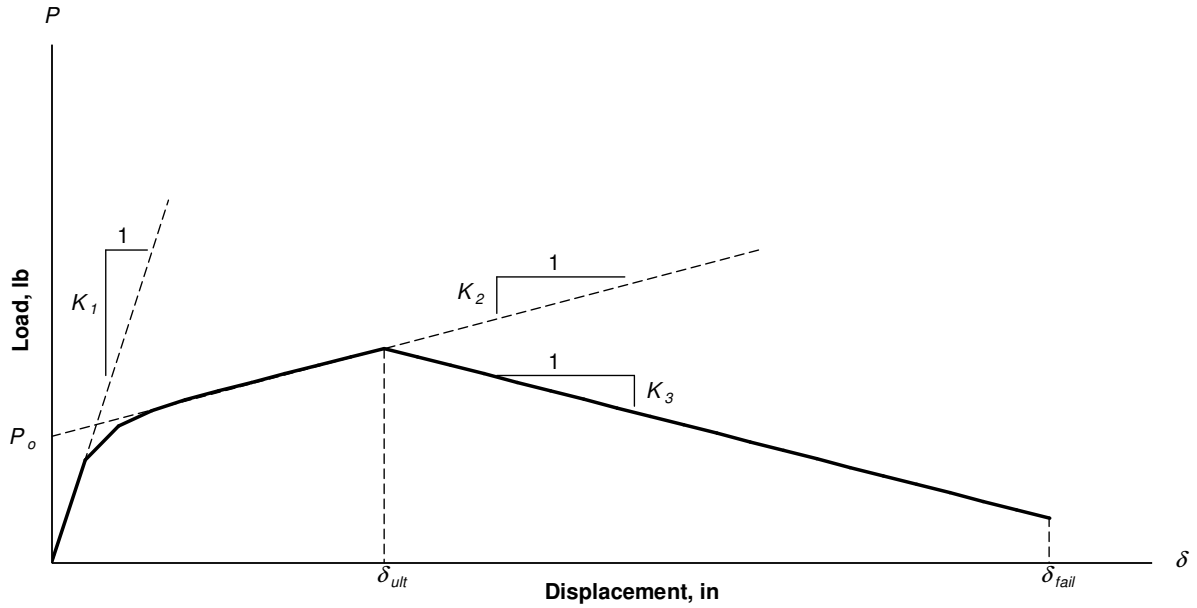

2.10 Reliability Studies

Reliability studies have been conducted of wood shear walls for both seismic (van de Lindt 2004) and wind loads (van de Lindt and Rosowsky 2005). Of interest to this research is the wind load reliability.

The reliability analysis by (van de Lindt and Rosowsky 2005) used shear wall construction methods specified in the *"Standard for Load and Resistance Factor Design (LRFD) for Engineered Wood Construction"* AF&PA/ASCE 16-95 and used a static-pushover analysis using the computer program *CASHEW* (Folz and Filiatrault 2001) to determine the monotonic load-deflection behavior (van de Lindt and Rosowsky 2005). The reliability index, β, was found to range from 3.0 to 3.5 with a mean of 3.17 and a COV = 0.05 (van de Lindt 2005).

Wind velocity is modeled as a Gumbel distribution or Type I (Ellingwood et al, 1980). This distribution is an extreme value distribution which is asymptotic with a Cumulative Distribution Function (CDF) given as the double exponential function shown in Eq. 9 (Ang and Tang 1975):

$$F_X(x) = exp[-exp(-\alpha(x-u))] \qquad -\infty < x < \infty \qquad \textbf{Eq. 9}$$

Although the wind velocity has a Type I distribution, this doesn't necessarily mean that the wind load has a Type I distribution since the wind load is a function of the velocity squared. However, this relationship was studied considering the other random variables (pressure coefficients, exposure factor and gust factor) that influence the wind load and it was determined that the probability distribution of wind load is also a Type I distribution (Ellingwood et al, 1980)

Van de Lindt used the model suggested by Ellingwood (1999). For this model, the 50-year maximum wind load is modeled as a Type I random variable, shown in Graph 4. The bias factor (mean-to-nominal value), including directionality effects, is given by:

$$\frac{\overline{W}}{W_N} = 0.8 \qquad \textbf{Eq. 10}$$

where, $\overline{W}$ = mean wind load
W_N = nominal (code-specified) wind load

The coefficient of variation is 0.35 (van de Lindt and Rosowsky 2005). Van de Lindt's model considered the capacity of the shear wall given in SDPWS multiplied by the strength reduction factor, ϕ, (the load with a Type I distribution) as the random variable. This was the only random variable used, since the resistance, computed as the ultimate

wall strength from *CASHEW*, was assumed to be deterministic as shown as the vertical line in Graph 5.

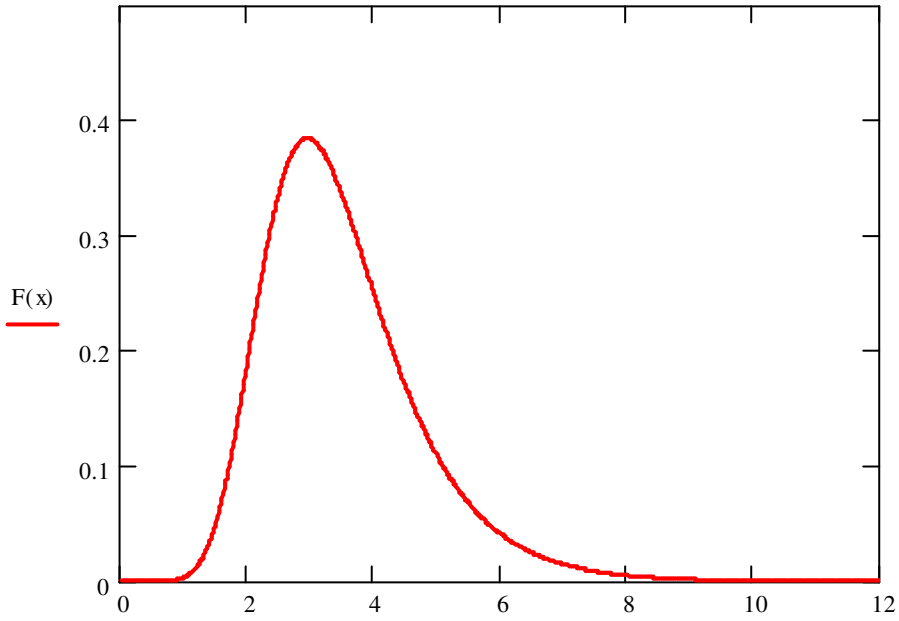

Graph 4: Probability Density Function of Shear Wall Load

Van de Lindt used the limit state in its simplest form to calculate the second-moment reliability index, β. This limit state is shown here as:

$$g(x) = R\text{-}S \qquad \textbf{Eq. 11}$$

where $g(x)$ is the limit state function, R is the structural resistance, and S is the load effect. R could be a random variable and S could be a random variable, or they could be a function of several random variables. As noted earlier, van de Lindt chose to only use S as a random variable and R as a constant (van de Lindt and Rosowsky 2005).

For the limit state shown above, failure occurs when $g(x) < 0$. As shown in the shaded portion of Graph 5**,** probability of failure, p_f, is the probability that $g(x) < 0$.

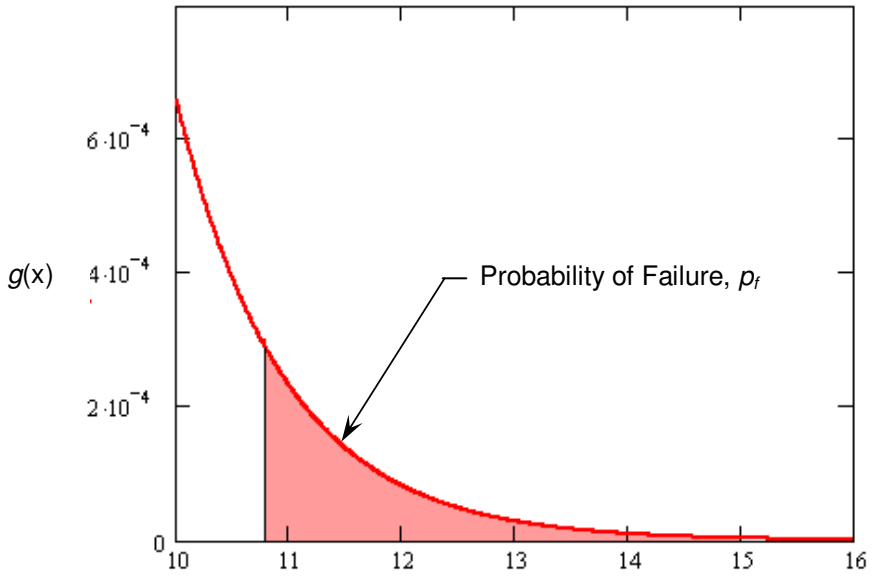

Graph 5: Failure Region of PDF of Shear Wall Load

The reliability index, β, is the inverse of the standard normal distribution function and is determined by:

$$\beta = \Phi^{-1}(1 - p_f) \qquad \textbf{Eq. 12}$$

β, shown graphically on the standard normal distribution in Graph 6 is a scale of the standard deviation, σ, to the probability of failure. This allows a measure of structural safety for any limit state, material, or load.

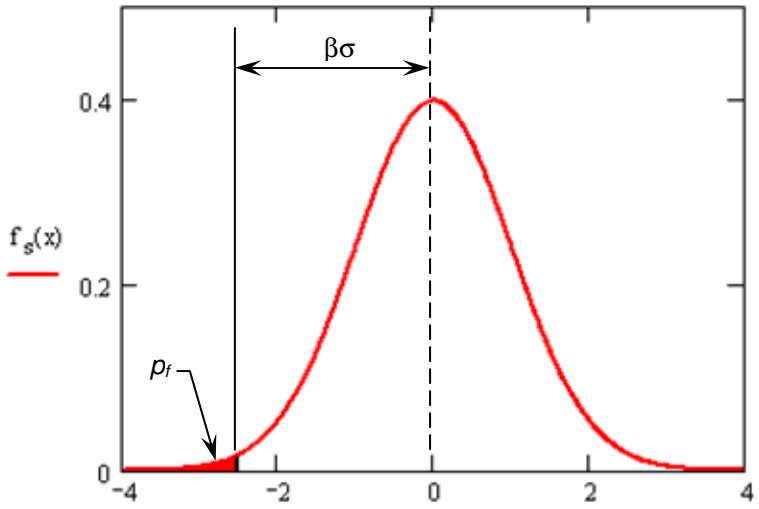

Graph 6: Reliability Index, β, on the Standard Normal Distribution

2.11 IRC Brace wall Testing - SBC Research Institute

The SBC Research Institute tested a 12' x 30' structure, Figure 9 and Figure 10, with IRC prescriptive intermittent walls in early 2010. The test results are currently available in the SBCRI Tech Note titled *2009 International Residential Code (IRC) Braced Wall Panel Design Value Comparative Equivalency Testing – Braced Wall Panel Design Values* (TN-IRC WSP 2010).

A portion of the test results are summarized in Table 8**.** There are several items of interest from this data. First, for the $^{3}/_{8}$" WSP, the average ultimate unit shear strength is 27% less than the IRC full restraint value and 8% less than the IRC value assuming the 80% PR factor. Second, the location of the $^{7}/_{16}$" WSP did not have much of an effect on the strength of the wall. It was expected that the corners would have more restraint and thus would have a greater capacity. Third, the average ultimate unit shear of the $^{7}/_{16}$" WSP with partial restraint is 18% less than the IRC full restraint value

and 3% greater than the IRC value assuming the 80% PR factor, but 39% less than the SDPWS fully restrained value.

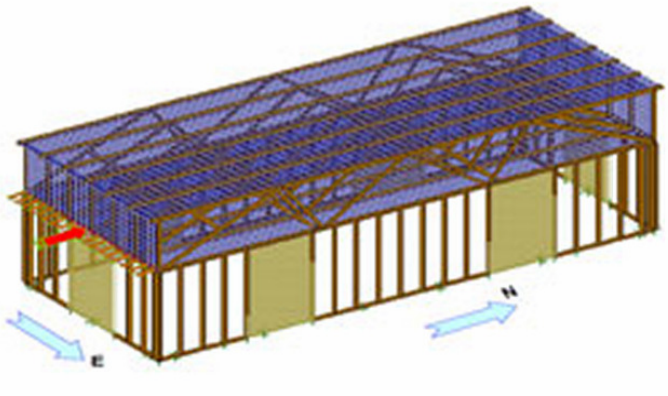

Figure 9: SBC Research Institute Test Building (SBCRI)

Figure 10: SBCA Research Institute Wall Failure (SBCARI T-IRC)

Table 8: Summary of SBCRI Tests

Wall	Sheathing Location	Restraint	Average Ultimate Unit Shear (plf)	IRC Full Restraint (plf)	IRC with 80% PR Factor (plf)
IRC $^3/_8$" WSP 6d nails at 6/12	6' From Corner	Partial – Building Dead Load and IRC Anchors	367	500	400
IRC $^7/_{16}$" WSP 8d nails at 6/12	6' From Corner	Partial – Building Dead Load and IRC Anchors	412	500	400
IRC $^7/_{16}$" WSP 8d nails at 6/12	At Corner	Partial – Building Dead Load and IRC Anchors	426	500	400
IRC $^7/_{16}$" WSP 8d nails at 6/12 with hold downs	6' From Corner	Fully Restrained	626	672[1]	N.A.

[1]SDPWS value utilizing $^{15}/_{32}$" and modified for G=0.42.

2.11.1 SBCRI Test Results

A comparison can be made between Seaders, SBCRI, and SDPWS modified by Ni and Karacabeyli's partial restraint factor, α. Recall that SBCRI test values are shown in Table 8 while Seaders' test results are shown in Table 5. Since Seaders' test used Douglas Fir-Larch, G=0.50, and the SBCRI used Spruce-Pine-Fir, G=0.42, the Seaders' values are expected to be 8% greater. Also, Seaders added gypsum to the face of the wall opposite the WSP with nominal fastening that added some additional strength.

Therefore, the comparison shown in Table 9 provides a quick view of the differences without accounting for the construction differences.

The SDPWS values shown in Table 9 are modified by the partial restraint factor, α, using Eq. 2. There is a 19% error for the unrestrained (actually greater if the gypsum strength and Douglas Fir-Larch framing are considered) and a 23% error for the partially restrained. A further comparison of Seaders' results with the SDPWS modified by the partial restraint factor, α, is shown in Table 10.

As shown in Table 10, the results of the fully restrained wall were not much different than the SDPWS, 6.3% error. However, there is a large difference in the Unrestrained (UR) and Partially Restrained (PR) values, 25.8% for UR and up to 36.2% for PR. Therefore, it appears that the partial restraint factor, α, using Eq. 2 is not accurate for IRC walls.

Table 9: Comparison of SBCRI, Seaders, SDPWS

	FR	UR	PR
SBCRI			412
Seaders		271	
SDPWS	672	336	538
% of FR	100%	40%	61%
Expected % of FR[1]	100%	50%	80%
% Error	N.A.	19.3%	23.4%

[1]IRC uses 0.8 for one story structure with 500 plf.

Table 10: Comparison of Seaders to SDPWS

			PR	
	FR	UR	40%	49%
Seaders	684	271	383	509
SDPWS	730	365	600	649
% Error	6.3%	25.8%	36.2%	21.6%

The inaccuracy of the partial restraint factor, α, is most likely due to the anchor bolt locations. Recall that the IRC wall is anchored with ½" diameter anchor bolts a maximum of 12" from the end and 6' o.c. while Ni and Karacabeyli's wall tests utilized ½" diameter anchor bolts at 16" o.c. and 8" from the ends. Therefore, some modification of Eq. 2 is necessary for IRC anchored walls.

The capacity of an unrestrained $^3/_8$" WSP shear wall constructed and anchored according to the IRC is unknown at this time. If there is a correlation between the $^7/_{16}$" and the $^3/_8$" WSP unrestrained, then the unrestrained value of the $^3/_8$" WSP would be 40% of the SDPWS value or one half of the assumed 80% value that the IRC uses. Therefore, for a lightly loaded wall, the reliability would be much less for the IRC brace wall than the SDPWS fully restrained wall.

CHAPTER 3

TESTING OF SHEAR WALLS

This chapter summarizes the test procedure, test results and numerical data from the testing of 25 wood shear walls. The 25 shear walls were divided into five groups of five walls each. The restraint of the shear walls was set differently for all five sets to understand the effect of partial restraint and full restraint on the shear wall unit shear capacity.

3.1 Current ASTM Test Procedures

Two ASTM standards exist for shear wall testing. The first is the *"Standard Test Methods of Conducting Strength Tests of Panels for Building Construction"* (ASTM E72-10). The second is the *"Standard Practice for Static Load Test for Shear Resistance of Framed Walls for Buildings"* (ASTM E564-00).

The purpose of ASTM E72 is to evaluate different types of sheathing on a standard wood frame. Since the standard wood frame is the same for all sheathing materials, the relative difference in performance of the sheathing materials is the test objective (ASTM E72). Three tests are required by this standard. ASTM E72 employs an 8' x 8' panel (two sheets of WSPs). The frame is constructed with 2x4 studs spaced at 16" on center with a single 2x4 sole plate and a double 2x4 top plate. Spaced corner posts are used at each end with fastening to the outside post only. All framing material is No. 1 Douglas Fir or Southern Pine. Fastening of the WSPs shall follow the manufacturer's recommendations. The standard emphasizes the importance of placing the fasteners exactly in the required location maintaining the correct edge distance and

angle (typically perpendicular to the WSP). Figure 11 shows the frame required by ASTM E72.

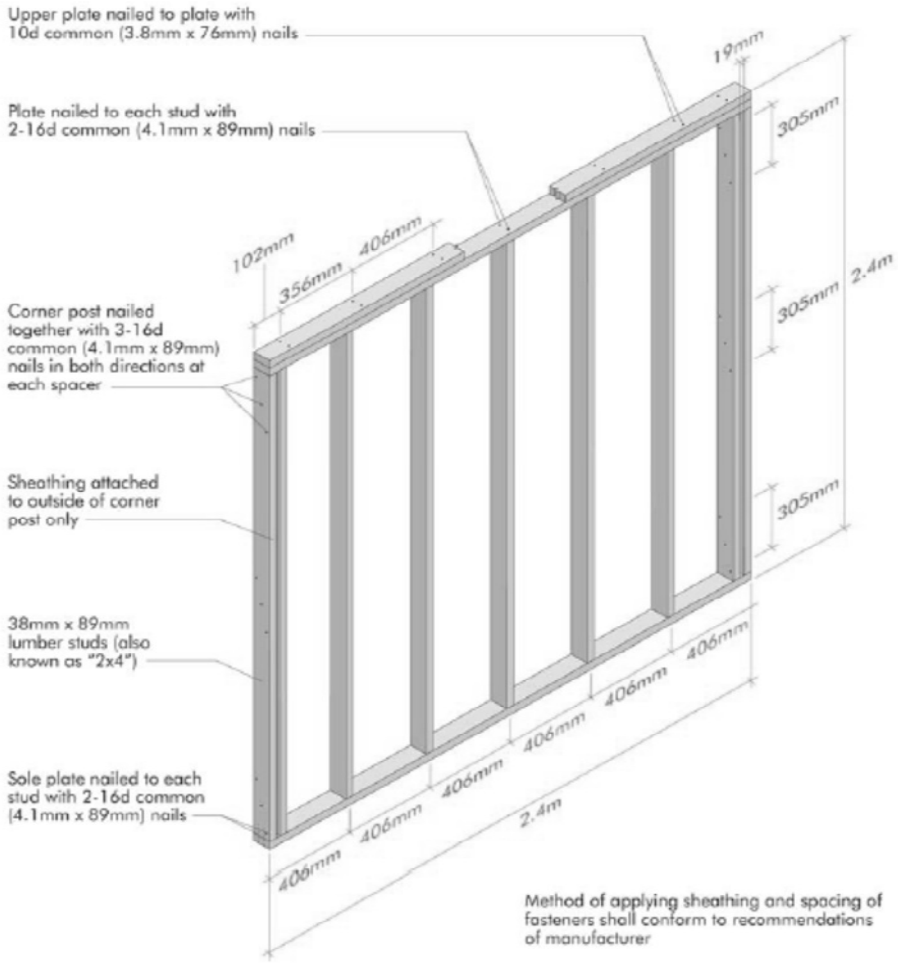

Reprinted, with permission, from ASTM E72-10 *"Standard Test Methods of Conducting Strength Tests of Panels for Building Construction",* copyright ASTM International, 100 Barr Harbor Drive, West Conshohocken, PA 49428.

Figure 11: Standard Wood Frame (ASTM E72)

ASTM E72 also specifies the loading point, the load rate, a hold down device, and the points of measurement. The load point is at the end of a timber member bolted to the double top plate. The hold down device consists of two steel rods extending

through a bearing plate with rollers above the corner post at the end where the load is applied. The rods are installed such that one is located on each side of the frame. The load rate specifies application of a uniform rate of motion to three steps: 790, 1570, and 2360 lb. The load shall be applied at the same rate for all three steps, but the first step must be loaded in no more than two minutes. Upon reaching the first load step, measurements are made at each measurement point and then the wall is unloaded. Measurements are again made after unloading to determine any permanent deformation. This process is repeated for the next two load steps. Three points of measurement are required for this test. They are all horizontal measurements. One point is located at the end of the double top plate and the remaining two are located at each end of the sole plate. The displacement measurements must be recorded to the nearest 0.01”

The purpose of ASTM E564 is to evaluate the shear capacity of any type of light framed wall supported on a rigid foundation and to determine the shear stiffness and strength of the wall (ASTM E564). The standard does not dictate a particular hold down device, but rather specifies the use of the same anchorage and applied axial loads expected in the service condition. Similarly, the framing members and fastening shall be the same size, grade and construction as anticipated in actual use.

ASTM E564 also specifies loading requirements. Although similar to ASTM E72, there are some slight differences between the standards. ASTM E564 requires an initial load equal to 10% of the anticipated ultimate load to be applied for five minutes to seat all connections. The initial load is removed and after five minutes the initial readings of displacement are recorded. The next sequence of loading is then applied in

intervals, or load steps, of 1/3, 2/3, and finally, the ultimate load. All of the load steps are applied at the same rate which is equal to reaching the anticipated ultimate load in no less than five minutes. At each of these intervals the load step is applied up to the specified load and held for one minute. The displacements are then recorded, and then the specimen is unloaded. After five minutes of unloading, the displacements are again recorded. The process is then repeated until the last load step and ultimate failure is reached. Ultimate failure may be a displacement limit rather than a load limit.

ASTM E564 provides a method for reporting both the global shear stiffness of the wall and the internal shear stiffness of the wall as well as the ultimate strength. The internal shear stiffness of the wall does not include uplift, or rotation, of the entire wall, but rather only the distortion of the wall itself. The ultimate strength is reported as an ultimate unit shear strength which is simply the ultimate load divided by the wall width.

ASTM E564 requires testing a minimum of two wall assemblies. If after testing two assemblies either the shear stiffness or the ultimate strength are not within 15% of each other, then a third test is required. The strength and stiffness values reported are then the average of the two weakest specimen values.

3.2 Wall Testing

The following summarizes the test procedure and results of the 25 wood shear walls used for the reliability analysis. The shear wall testing was conducted at the Structural Building Components Research institute in Madison, WI in March 2011. The tests were performed in accordance with ASTM E564. Details of the testing are presented in Appendix A.

3.2.1 Test Facility

The SBCRI test facility has an ACLASS accreditation, Appendix B. ACLASS is one of two brands of the ANSI-ASQ National Accreditation Board. The accreditation is for testing full scale construction assemblies and is accredited to ISO/IEC 14025:2005. Of particular interest, the accreditation specifically encompasses ASTM E564 and ASTM E72 testing.

The SBCRI test facility is capable of testing both single components and entire structures up to 30’ wide x 32’ tall x 90’ long. Completely adjustable frames allow for a large variation of test configurations.

3.2.2 Wall Construction

3.2.2.1 Wall Matrix

The 25 shear walls were constructed identically, except for the anchorage, and tested identically. The shear walls were grouped in five groups of five walls each for the testing. See Table 11 for a summary of walls tested. Illustrations of the test setups are shown in Figure 12, Figure 13, and Figure 14 at the end of this chapter.

Group A walls were tested first to determine the hold down force. The average hold down force was used to calculate the restraining force for Groups B to D. More details of the test program are presented in Appendix A.

Table 11: Test Matrix

Group	A	B	C	D	E
No. of Tests	5	5	5	5	5
Size	4'x8'	4'x8'	4'x8'	4'x8'	4'x8'
OSB Sheathing Thickness	$^{15}/_{32}$"	$^{15}/_{32}$"	$^{15}/_{32}$"	$^{15}/_{32}$"	$^{15}/_{32}$"
2x4 Plate Material	Stud Grade SPF-S	Stud Grade SPF-S	Stud Grade SPF-S	Stud Grade SPF-S	Stud Grade SPF-S
2x4 Stud Material	#2 Grade SPF-N	#2 Grade SPF-N	#2 Grade SPF-N	#2 Grade SPF-N	#2 Grade SPF-N
2x4 Stud Spacing	16"	16"	16"	16"	16"
8d Common Nail Spacing	6:12	6:12	6:12	6:12	6:12
Restraint	Mechanical Hold down	1104 lb (¼ Hold Down Force)	2208 lb (½ Hold Down Force)	3312 lb (¾ Hold Down Force)	No added restraint
Anchor Bolt	None	$^{5}/_{8}$" 12" from load edge	$^{5}/_{8}$" 12" from load edge	$^{5}/_{8}$" 12" from load edge	$^{5}/_{8}$"12" from load edge

3.3 Test Results

3.3.1 Data Results

The hysteresis curve for a typical wall tested to failure is shown in Graph 7.

From the test results, the ultimate unit shear capacity of each wall was found. A summary of these results is shown in Table 12, including the average hold down force for wall Group A. The restraining force shown for wall groups B, C, and D is ¼, ½, and ¾ of the average hold down force from Group A. The SDPWS value was determined from the tabulated 730 plf which reduces to 628 plf for SPF-S (G=0.36). The Report 154 value was determined from APA Report 154 which tabulates an average fully restrained ultimate unit shear capacity of 913 plf, which reduces to 786 plf for SPF-S (G=0.36). The species reduction factor is (1-(0.5-0.36)) = 0.86. The restraining force for

SDPWS and APA Research Report 154 is the unit shear multiplied by the wall height of 8 feet. The normalized section indicates the fraction of the fully restrained hold down force, calculated from the APA Research Report 154 average ultimate unit shear value, and the resulting fraction of the Report 154 ultimate value.

Graph 7: Hysteresis Curve for Wall A1

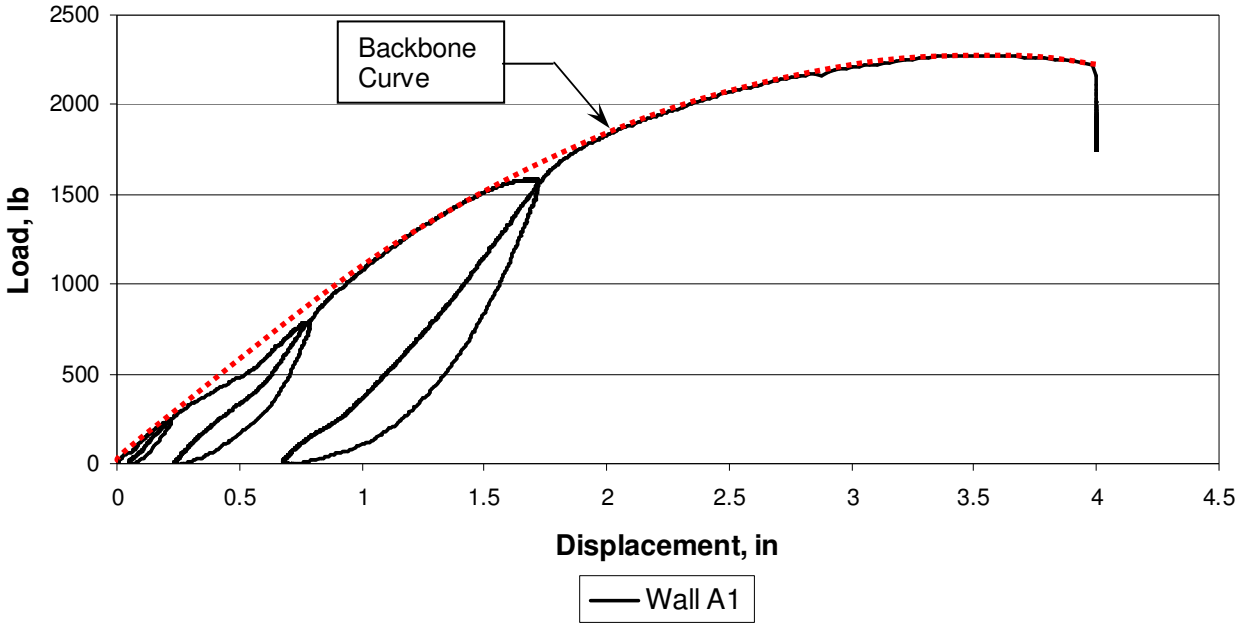

The load deformation curves tor the five different wall sets were averaged (Graph 8). Note the difference in the behavior of Wall A, the wall type with a mechanical hold down, compared with the other partially restrained walls. Also note that there is nearly a linear relationship between the peaks of Wall B, Wall C, and Wall D - the three walls with an applied dead load for restraint. Considering Walls B-E, the relationship is no longer linear, as illustrated in Graph 8.

In addition to the wall ultimate unit shear capacity and hysteresis curve, the load-deformation curves for the nails were also created for Group A as shown in Graph 9. These curves were derived from the calculated differential displacement between the

Table 12: Summary of Wall Ultimate Unit Shear Capacity

	A	B	C	D	E	SDPWS	Report 154
Wall Restraint	4416	1104	2208	3312	0	5024	6288
Ultimate Capacity, plf							
1	569	314	502	607	190		
2	538	337	500	656	181		
3	562	323	474	594	158		
4	549	372	516	590	142		
5	558	377	489	628	137		
Avg.	555	345	496	615	162	628	786
Std. Dev.	12	29	16	27	23		
COV	0.022	0.083	0.032	0.044	0.145		
Min.	538	314	474	590	137		
Max.	569	377	516	656	190		
Normalized							
$P_{hold\ down}$	0.702	0.176	0.351	0.527	0.000		1
V_{cap}(%)	0.706	0.438	0.631	0.782	0.206		1

Graph 8: Summary of Wall Tests

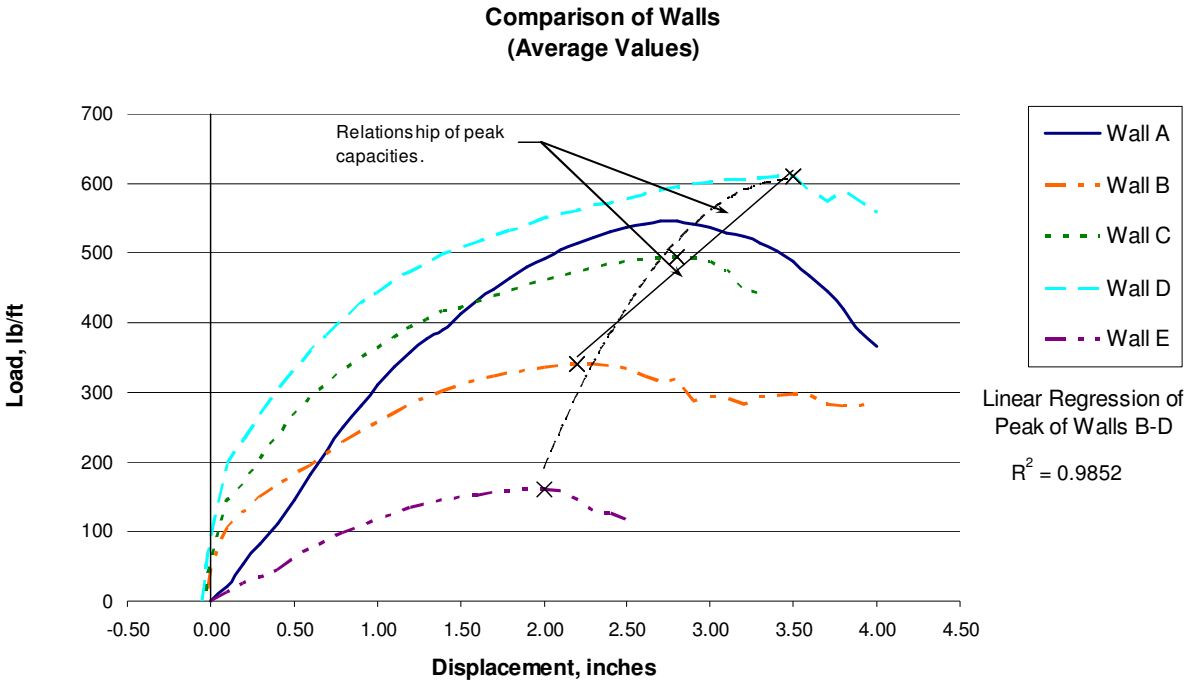

Graph 9: 8d Common Nail Curves from Wall Group A

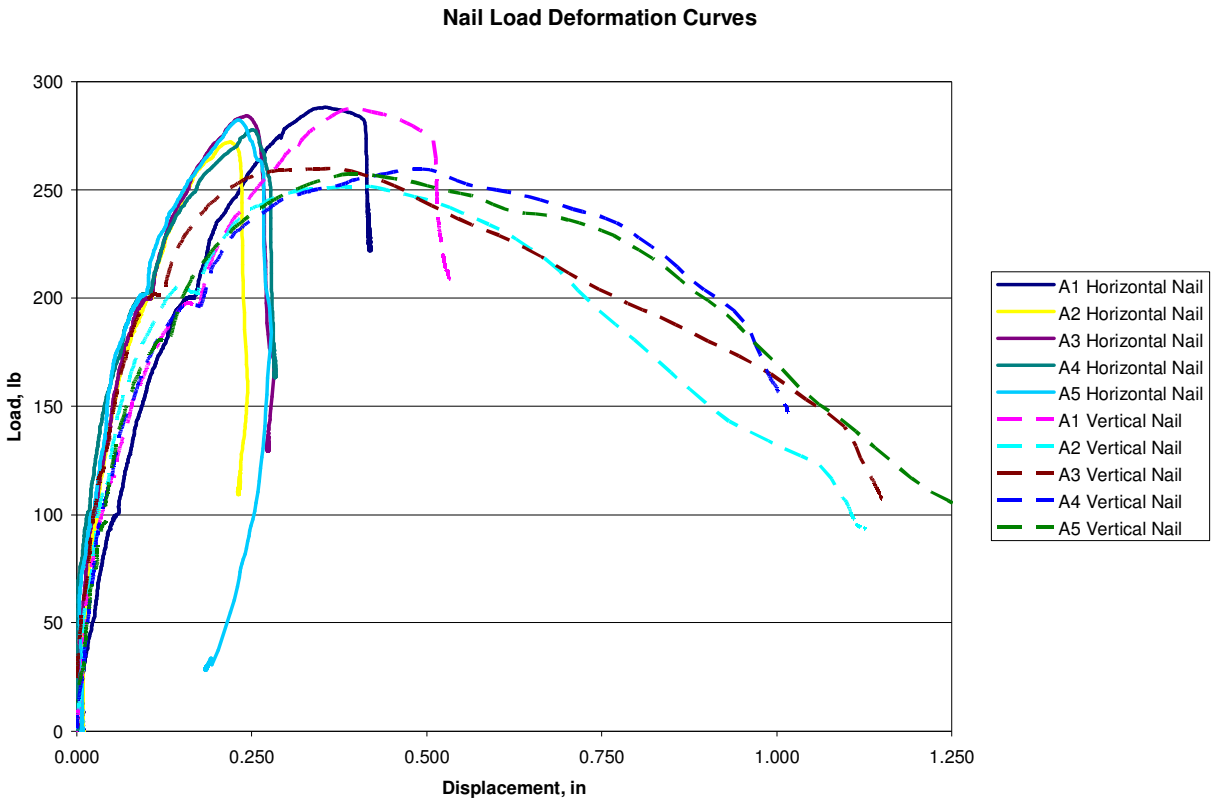

OSB sheathing and the studs from the test results. The load was calculated by dividing the force in the stud or plate by the effective number of nails along that member. The effective number of nails considered only a portion of the corner nails, assuming that they were directed to the center of the wall. This is reasonable since the nails are loaded primarily in one direction in a shear wall restrained with a hold down. "The wall specimen, as a whole, will experience the 'average' nail behavior." wrote Dolan and Madsen 1992. The curves were created for both the nails in the bottom plate as well as the nails in the tension or compression end stud, depending upon which stud experienced nail failure. The dominant failure of the walls was nail failure along the

tension stud, with one specimen failing along the compression stud. Therefore, the vertical nail curve was used to determine the average nail stiffness.

The vertical nail curves were separated and a curve was fit to describe the nonlinear behavior of the fasteners. For comparison, an additional curve is shown as Dolan. This curve uses Eq. 8 along with the following parameters:

K_1 = 4870.0 lb/in
P_0 = 180.0 lb
K_2 = 240.0 lb/in
D_{max} = 0.5
K_3 = -240.0 lb/in

These parameters are from Table 1 of Dolan and Foschi 1991, except K_3 which is from Judd 2005, for 8d Common nails with $^3/_8$" plywood and SPF studs. It is recognized that Judd chose to use $K_3 = -K_2$, which is taken from Table 3 of Dolan and Madsen 1992.

Graph 10: 8d Common Nail Curve Model

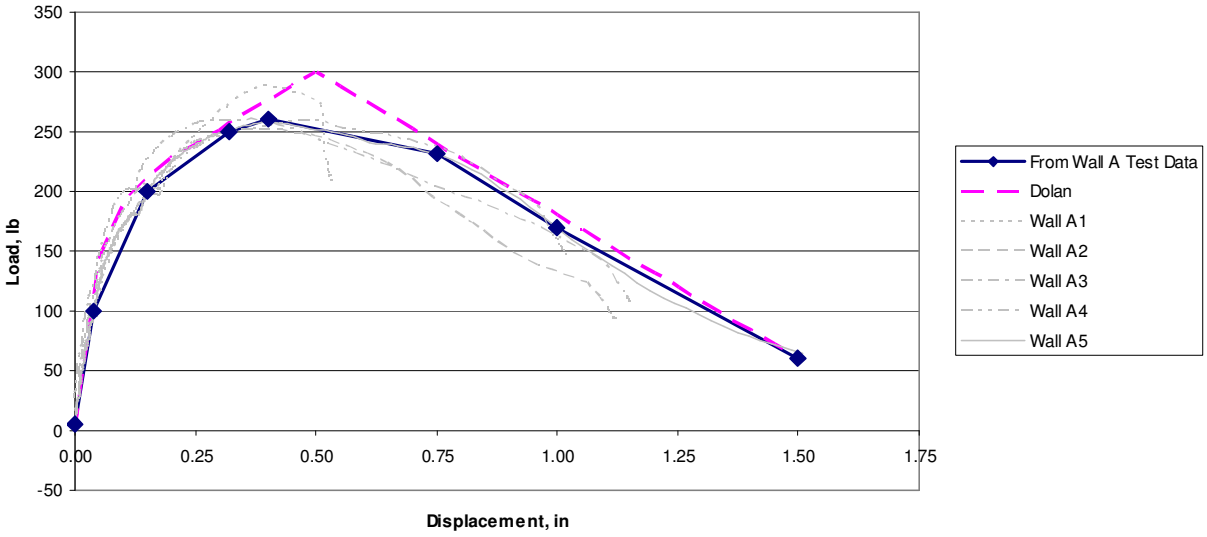

As shown in Graph 10, the curve fit from the Wall A test is very close to Dolan's model. The largest difference is in the change from the peak load to the softening branch. Rather than a sharp peak, the nails exhibited a gentler transition to the

softening branch. The softening branch of the fit curve is slightly above the average data. This matches wall A6, which had the longest softening branch.

The peak nail values for each of the five walls from Group A are tabulated in Table 13. The stud designation, Axx.1 refers to wall type A, test 'xx', and stud 1, the tension stud. Stud 4 is the compression stud. Table 13 also includes the specific gravity, G, (see section A6 in APPENDIX A) the thickness of the sheathing, t_s, the thickness of the stud, t_m, and the NDS yield limit capacity, $P_{calculated}$. The NDS yield limit capacity was calculated as the minimum of Eq. 4, Eq. 5 and Eq. 6 for modes I_m, I_s, II, III_m, III_s and IV. Mode III_s governed in all cases.

The peak nail capacity from the test results are very close to the NDS yield limit values. The difference is only 8.3%. If the NDS yield limit nail capacity is modified by the diaphragm factor, C_{di}, the difference is only 3.9%. In Table 13, C_{di} was taken as the ratio of the average $P_{test}/P_{calculated}$, or 1.09, compared with 1.10 as specified in the NDS.

Table 13: Nail Values from Wall Group A

						Failure Stud			With C_{di}	
Stud	G_s	G_m	t_s	t_m	$P_{calculated}$	P_{test}	Difference	% Difference	Difference	% Difference
A5.1	0.60	0.45	0.533	3.5	254	258	3	1.3%	19	7.2%
A4.1	0.62	0.38	0.515	3.5	248	260	12	4.7%	10	3.8%
A3.1	0.57	0.35	0.534	3.5	238	260	22	9.4%	2	0.7%
A2.1	0.50	0.34	0.529	3.5	218	252	34	15.6%	15	6.0%
A1.1	0.56	0.33	0.523	3.5	230					
A5.4	0.60	0.38	0.533	3.5	248					
A4.4	0.62	0.35	0.515	3.5	245					
A3.4	0.57	0.40	0.534	3.5	242					
A2.4	0.50	0.32	0.529	3.5	216					
A1.4	0.56	0.40	0.523	3.5	237	262	25	10.4%	4	1.6%
Average					238	258		8.3%		3.9%

The load deflection behavior and stiffness of the hold downs were determined from tests by use of a load cell at the hold down and string potentiometer measuring displacement of the tension stud. This data is shown in Graph 11, demonstrating the

slip that occurs before the linear behavior of the hold down is achieved. Note that walls A1 through A4 utilized a Simpson HDU14 while wall A5 utilized a Simpson HDU8. While the stiffness of the HDU14 is consistent, the slip varies. Unexpectedly, the HDU8 was stiffer than the HDU14.

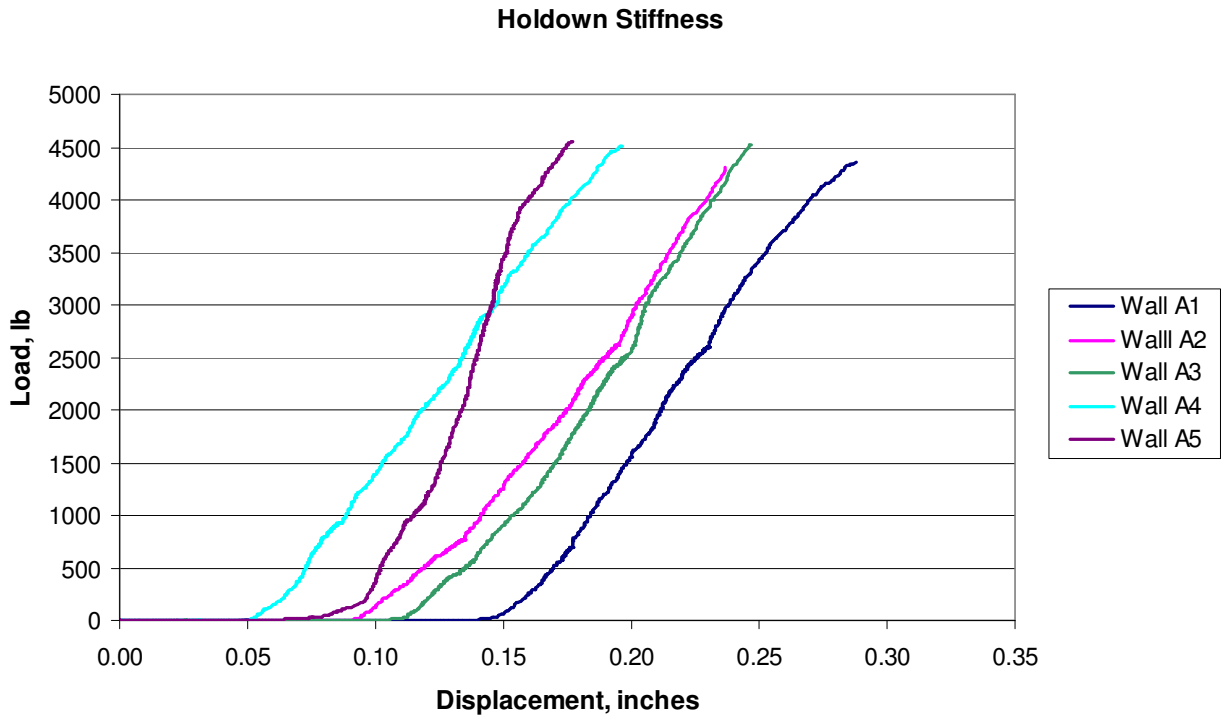

Graph 11: Hold down Stiffness from Test Results

3.3.2 Discussion of Wall Failures

Nearly all of the walls failed as expected. The failure mode of four of the test specimens, walls A2, A3, A4, and A5 in wall Group A, was nail failure along the tension stud. The failure mode of one wall from wall Group A, wall A1, was nail failure along the compression stud.

The nails typically failed in mode III_s with some in mode IV, Figure 8. The III_s mode failure is a single yielding of the nail along with rotation of the nail in the

sheathing. Mode IV is a double yielding of the nail. Mode IV was observed only a few times.

The hold down didn't fail, but did elongate more than expected. Wall A5 was the first wall tested and, as noted earlier, the hold down on this wall was installed tight to the bottom plate. As the hold down elongated, the inner tip of the hold down was tight to the bottom plate. The bottom plate then began to separate from the tension stud as the load increased. Believing that prying action occurred on this test, the hold down was installed 1" above the bottom plate on subsequent tests on the remaining walls in Group A to eliminate prying action. These walls behaved similarly at the hold down in that the hold down elongated and the bottom plate began to separate from the tension stud. Photo 1 shows the separation of the stud and bottom plate on wall A5. This photo was taken after failure so the separation closed. Note the location of the bottom of the sheathing in Photo 1 as well. The nails located in the tension stud on this wall all failed and the stud was completely free from the sheathing after failure. The top plate also separated from the tension stud on wall A1.

Photo 1: Stud/Plate Separation at Hold Down

For wall Groups B, C, D, & E, failure typically initiated at the corner nail in the bottom plate on the tension side. Since the anchor bolt 12" from the end was the only mechanical hold down, the bottom plate bent upward at the tension end of the wall as a cantilever beam from the anchor bolt.

3.3.3 Partial Restraint Effect

The test results shown in Table 12 are plotted in Graph 12. This graph shows the relationship of the restraining force and the ultimate unit shear capacity of the shear wall. Both a linear and second order curve was fit to the data. The second order fit is obviously the best with R^2=1. The line representing the SDPWS nominal value is only shown as a point of reference and is not intended to indicate that it is constant for all values of the restraining force. SDPWS requires a restraining force proportionate to the height of the wall and the nominal unit shear capacity.

Note that the curve shown in Graph 12 is a different shape than as presented in Graph 2 from previous research (Ni and Karacabeyli 2000). There are two reasons for this difference. First, the previous research considered a sole plate restrained by ½" diameter anchor bolts at 16" o.c. with the first bolt 8" from the end. This provides much greater restraint than the Group A unrestrained walls presented here. Second, the curve in the previous research was fit to the nominal unit shear capacity and not the ultimate unit shear capacity. The latter is required to understand the true relationship of the partial restraint.

Graph 12 and Table 12 also show that a mechanical hold down does not provide the same restraining effect as a restraint at the top of the wall above the tension side of the wall. In fact, the mechanical hold down can only generate 70.6% of the fully restrained ultimate unit shear capacity.

The second order equation shown in Graph 12 is the partial restraint factor for the ultimate unit shear capacity, $C_{pr\text{-}u}$. This equation is shown below as Eq. 13. The

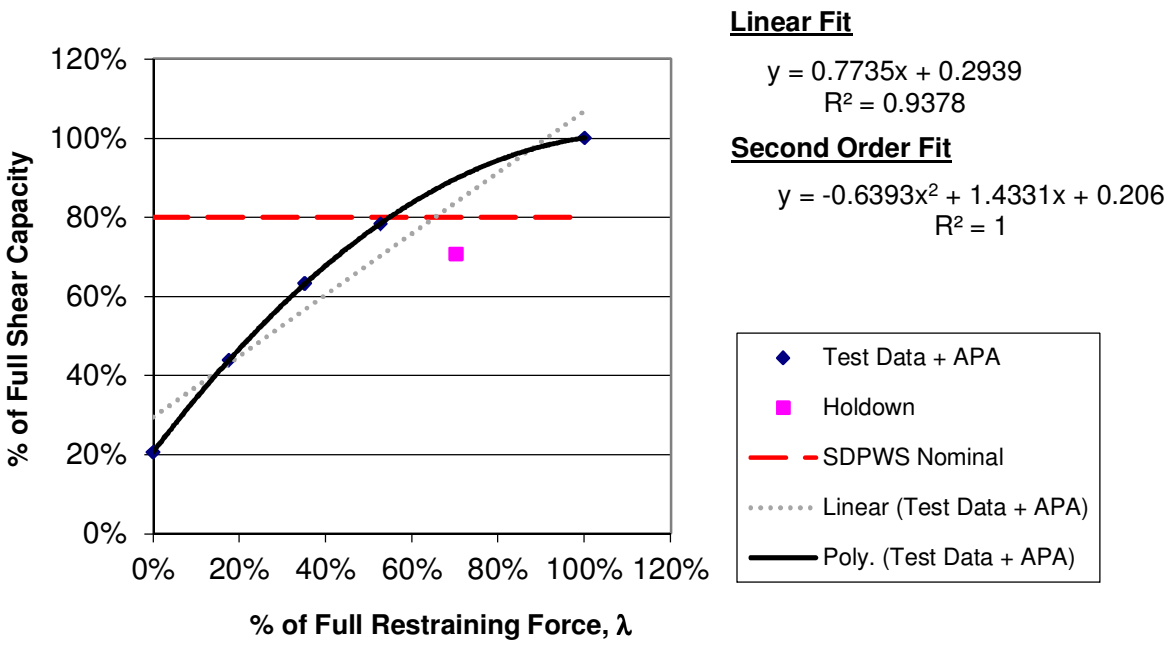

Graph 12: Partial Restraint Effect on Strength

ultimate unit shear capacity of a partially restrained wall can now be determined from Eq. 14:

$$C_{pr\text{-}u} = -0.6393\lambda^2+1.4331\lambda+0.206 \le 1.0$$

and **Eq. 13**

$C_{pr\text{-}u} = 0.706$ for a mechanical hold down

Where,

$$\lambda = \frac{P_D}{V_{ult} \times h}$$

P_D = restraining force

V_{ult} = ultimate unit shear capacity

h = shear wall height

$$V_{pr}=C_{pr\text{-}u}V_{ult}$$ **Eq. 14**

3.3.4 Probability Distribution of Unit Shear Capacity

To determine the likely probability distribution of the ultimate unit shear capacity from the test data, distribution paper was used. The two possible distributions considered were normal and log-normal. This was done for Groups A-E. For consideration of normal distribution for wall Group A, the distribution calculations are shown in Table 14. The probabilities from Table 14 are plotted against the wall capacity on normal probability paper in Graph 13.

Table 14: Wall Group A Normal Distribution Probability

m	1	2	3	4	5
V, plf	538	549	558	562	569
m/(n+1)	0.167	0.333	0.500	0.667	0.833

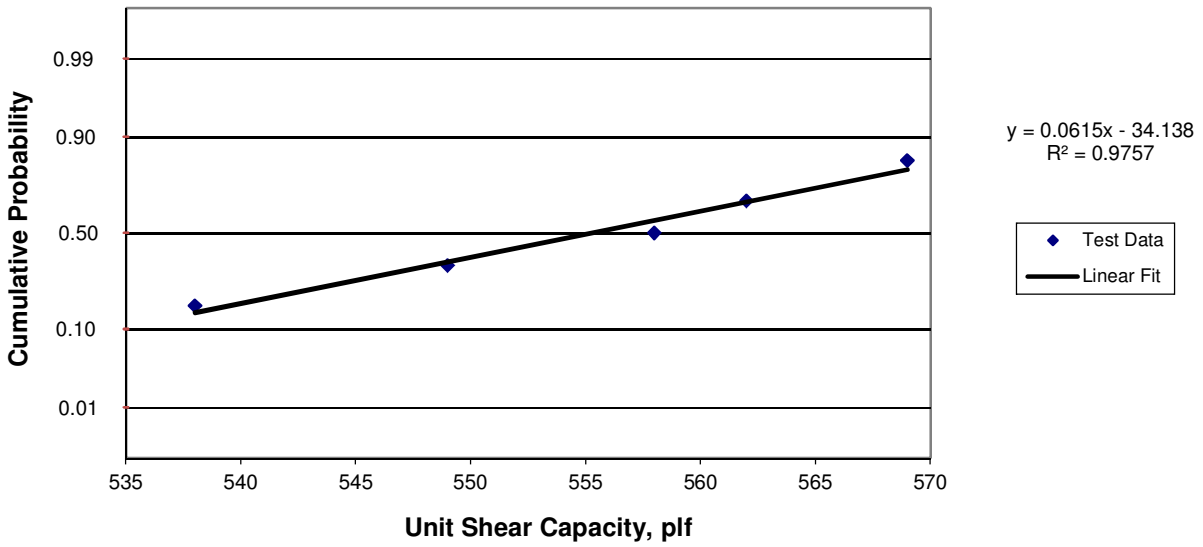

Graph 13: Unit Shear Capacity of Wall A on Normal Probability Paper

For consideration of log-normal distribution for wall Group A, the distribution calculations shown in Table 14 are plotted against the wall capacity on log-normal probability paper in Graph 14.

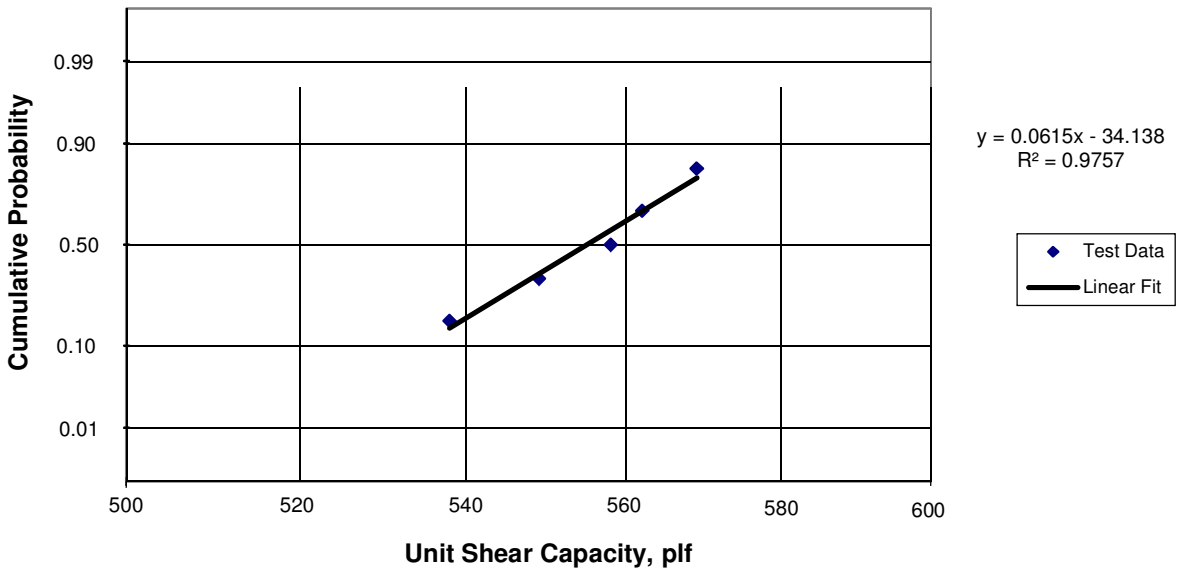

Graph 14: Unit Shear Capacity of Wall A on Log-Normal Probability Paper

While both graphs indicate a close fit and very similar result (equation of the line is the same for both and R^2 is the same for both), log-normal distribution will be used. Log-normal distribution does not allow negative values, so it is preferred over normal distribution. The remaining walls resulted in similar conclusions.

The Chi-square test is another method for determining the best matching distribution. However, a Chi-square test should have a minimum of 25-30 samples and at least five bins (Ang & Tang 1975). Since the sample size is only five, it is not feasible to use the Chi-square test for this data.

Similarly, another goodness-of-fit test is the Kolmogorov-Smirnov test for distribution. With having only five samples, the results of this test are the same for

normal and log-normal distribution at the 5% significance level. Thus no conclusions can be made from the K-S test.

3.3.5 Probability Distribution of Specific Gravity

Samples of each member were taken from the test specimens and specific gravity tests were conducted for each piece in accordance with ASTM 2395. The results of the test are shown in section A6 in APPENDIX A and summarized in Table 15.

Two distributions for specific gravity were considered, normal and log-normal. The two distributions were compared with a Chi-Squared Test. Although both were valid distributions, log-normal was selected because it always yields a positive value.

Table 15: Summary of Specific Gravity Tests

	Member	Studs		Plates		Sheathing	
	Description	2x4 Stud Grade SPF-S		No. 2 Grade SPF-N		$^{15}/_{32}$" OSB	
	Number of Pieces Tested	100		75		25	
		Exp.	Ref.	Exp.	Ref.	Exp.	Ref.
Specific Gravity	Average, G	0.36	0.36[1]	0.40	0.42[1]	0.58	0.50[3]
	Std. Dev.	0.03	0.036[2]	0.03	0.042[2]	0.03	
	Prob. Dist	Log-normal		Log-normal		Log-normal	
Moisture Content	Average, MC	15.1%		16.2%		4.7%	
	Std. Dev.	1.5%		2.1%		0.4%	
Thickness	Average, t (in)					0.511	
	Std. Dev.					0.017	

Exp. = Experimental Value; Ref. = Reference Value
[1] NDS (2005)
[2] ASTM D2555 – 06
[3] PDS (2004)

3.3.6 Wall Restrained with Hold Down

The ultimate unit shear strengths were calculated using the APA Research Report 154 (2004) tabulated average ultimate value along with the modification required for specific gravity, as shown in footnote C of Table 6, using the weighted average of the specific gravity of the actual materials. The calculated results were compared with the test values for Group A walls and are tabulated in Table 16 and shown in Graph 15.

The results were good with an average percent error of 0.07% between the average experimental values and the average calculated values. As seen in both Table 16 and Graph 15, walls A3, A4, and A5 were the most consistent to their respective anticipated values with an average percent error of -0.6%. Walls A1 and A2 are the outlying values producing percent errors of 5.1% and 2.8% respectively.

Graph 15 illustrates the correlation between the wall unit shear capacity and the average specific gravity of the wall framing members. The test results are compared against the expected values calculated from the APA Research Report 154 (2004) tabulated average ultimate value along with the modification required for a specific gravity. The bandwidth shown is $\pm\sigma$, or one standard deviation, of the experimental wall capacity. All but wall A1 lie within the bandwidth.

Although a linear regression of the results from walls A1 to A5 do not correspond to the expected relationship of the wall unit shear strength to the specific gravity, G, the data fits relatively well within the bandwidth. This result can be expected with a small sample size.

Table 16: Effectiveness of Hold Down

Wall	G_{ave} Plates and Studs	Experimental Wall Capacity	APA Report 154 Capacity	Holdown Reduction	APA Report 154 Adjusted for Holdown	% Error
A1	0.344	569	771	0.702	541	5.1%
A2	0.363	538	788	0.702	553	-2.8%
Walls A3, A4, and A5						
A3	0.379	562	802	0.702	564	-0.3%
A4	0.364	549	789	0.702	554	-0.9%
A5	0.377	558	800	0.702	562	-0.7%
Average	0.373	556	797	0.702	560	-0.6%
Std. Dev.		6.7				
Walls A1, A2, A3, A4, and A5						
Average	0.365	555	790	0.702	555	0.07%
Std. Dev.	0.0137	12.0			8.8	

Graph 15: Correlation of Wall Strength to Specific Gravity

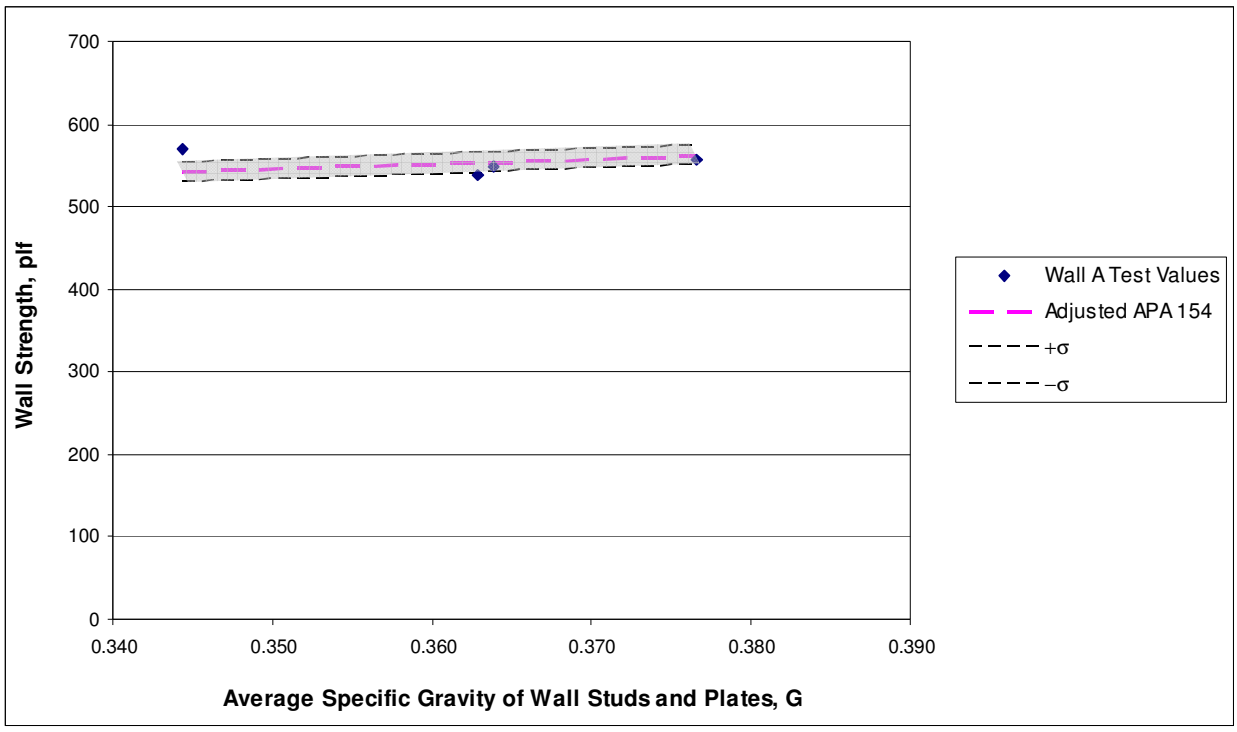

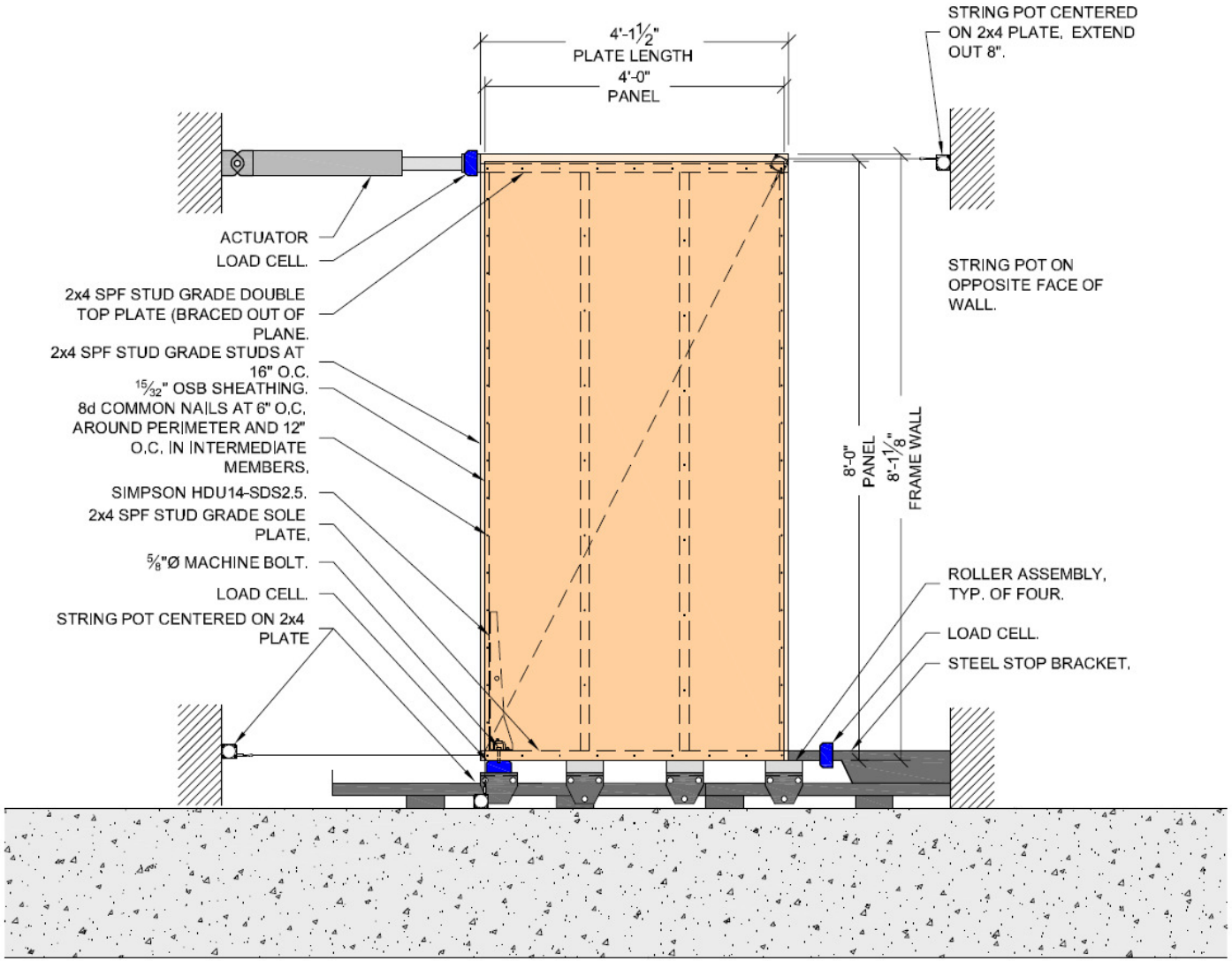

Figure 12: Test Assembly Wall A

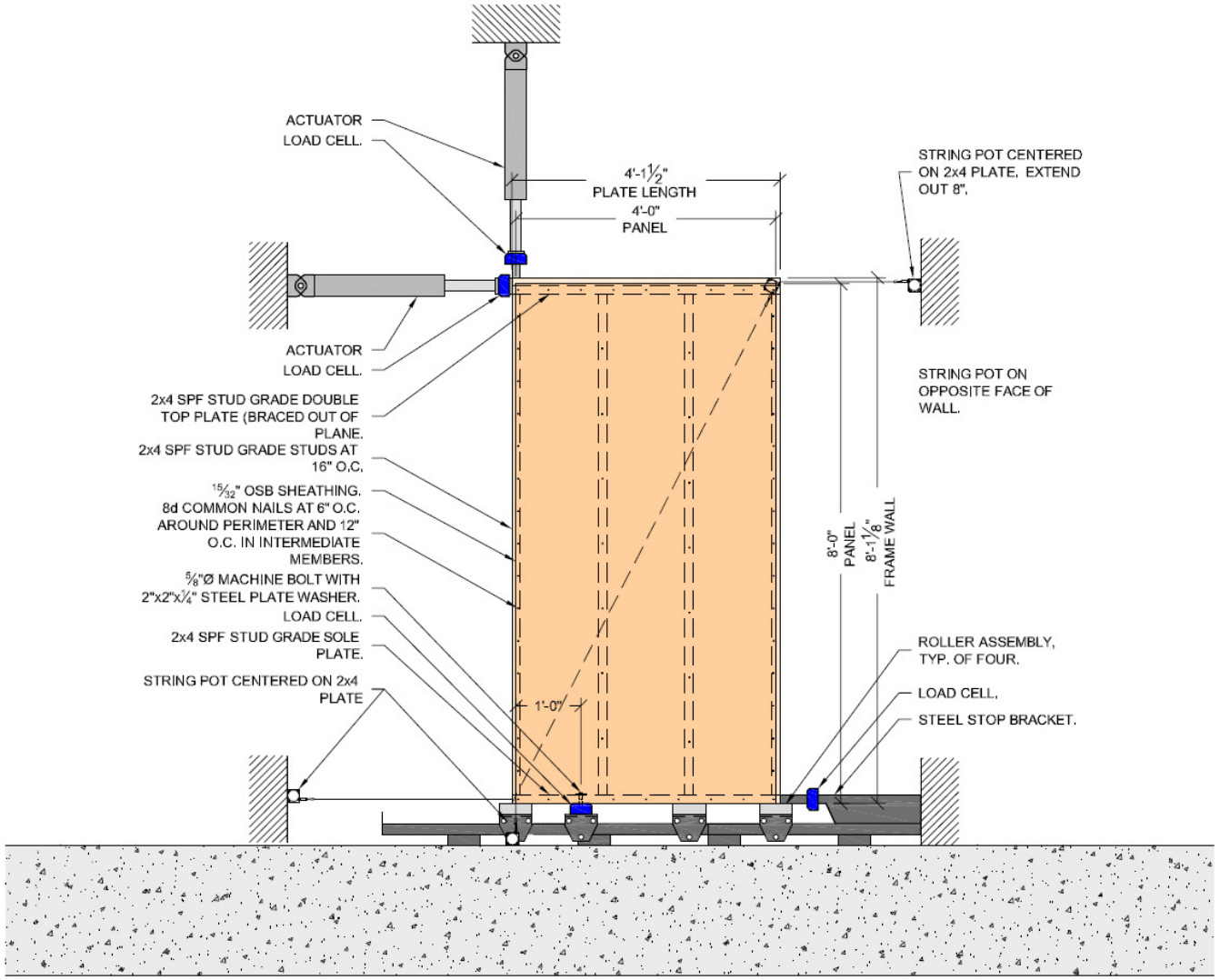

Figure 13: Test Assembly Walls B, C and D

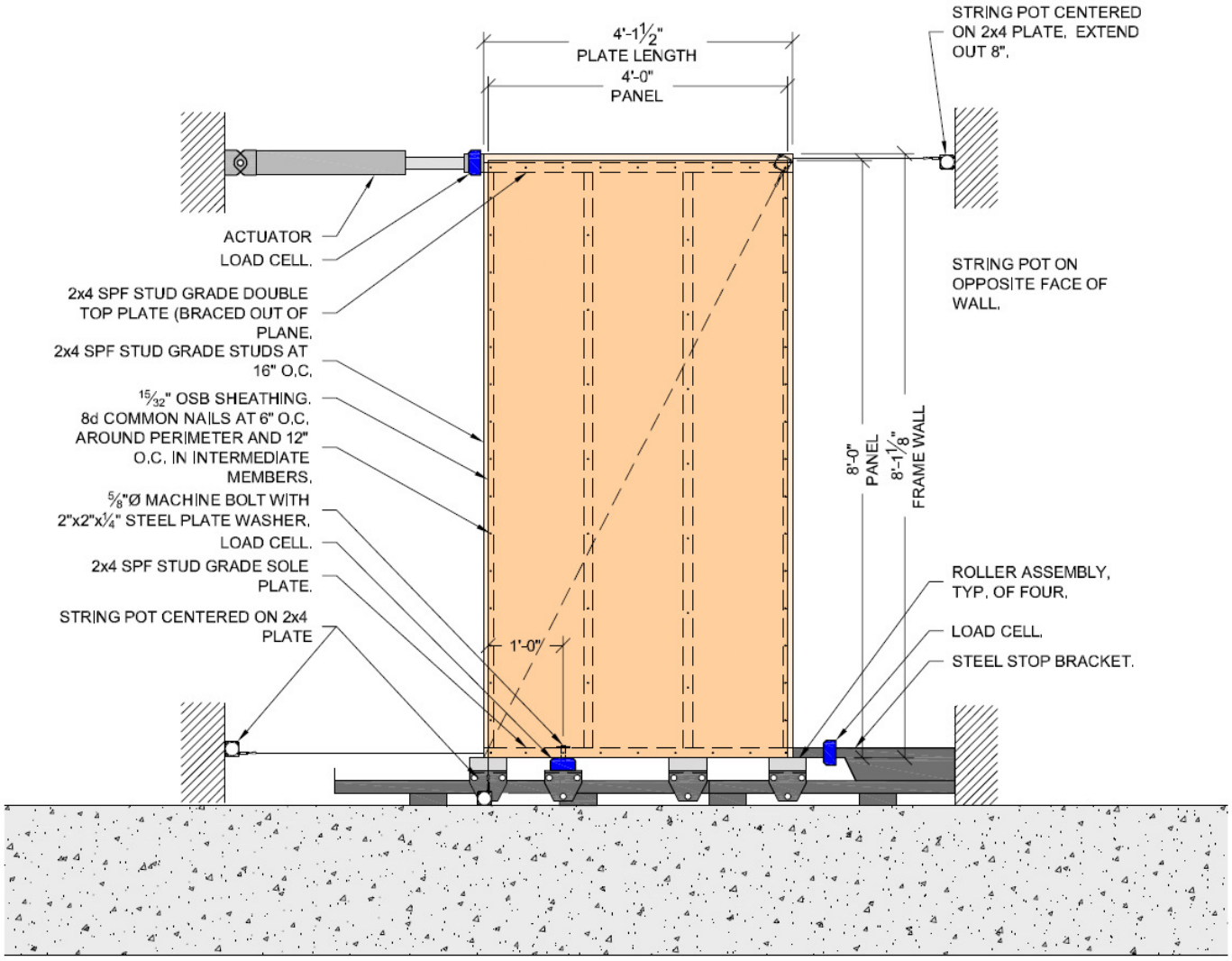

Figure 14: Test Assembly Wall E

CHAPTER 4

FINITE ELEMENT MODELING

A finite element model was created to offer a better understanding of the behavior of the walls with varying restraint conditions. The model includes a nonlinear finite element analysis. The load deformation curves are compared to the test results for accuracy of the model.

4.1 Finite Element Model

The finite element model (FEM) was constructed in HYPERMESH and analyzed in ABAQUS, a commercial finite element solver. The model was constructed to replicate as much detail as possible of the walls tested. The model used:

- Beam elements for the framing members
- Four node quadrilateral shell elements
- Two orthogonal springs connecting framing members, one linear and one nonlinear
- Two uncoupled orthogonal nonlinear springs (or spring pair) connecting the sheathing to the framing elements
- Compression-only beam elements at the supports that cannot resist tension
- And a nonlinear spring for the hold down.

Initially, the model was constructed with a single 1D nonlinear spring element that was free to rotate (a SpringA element in ABAQUS). However, this element created difficulties solving. It was extremely difficult to obtain convergence in the early steps of the analysis. ABAQUS had difficulty in these early steps as the springs rotated to their initial displacement path. The uncoupled nonlinear spring pair overcame this difficulty and created a model that was easier to converge during the initial steps.

The uncoupled nonlinear spring pair is a common model that is commonly found in other literature (Cassidy 2002, Dolan and Foschi 1991, and Folz and Filiatrault 2001). As stated in Chapter 2, the uncoupled nonlinear spring pair is sufficient for determining the ultimate load and displacement for monotonic loading.

4.1.1 Elements

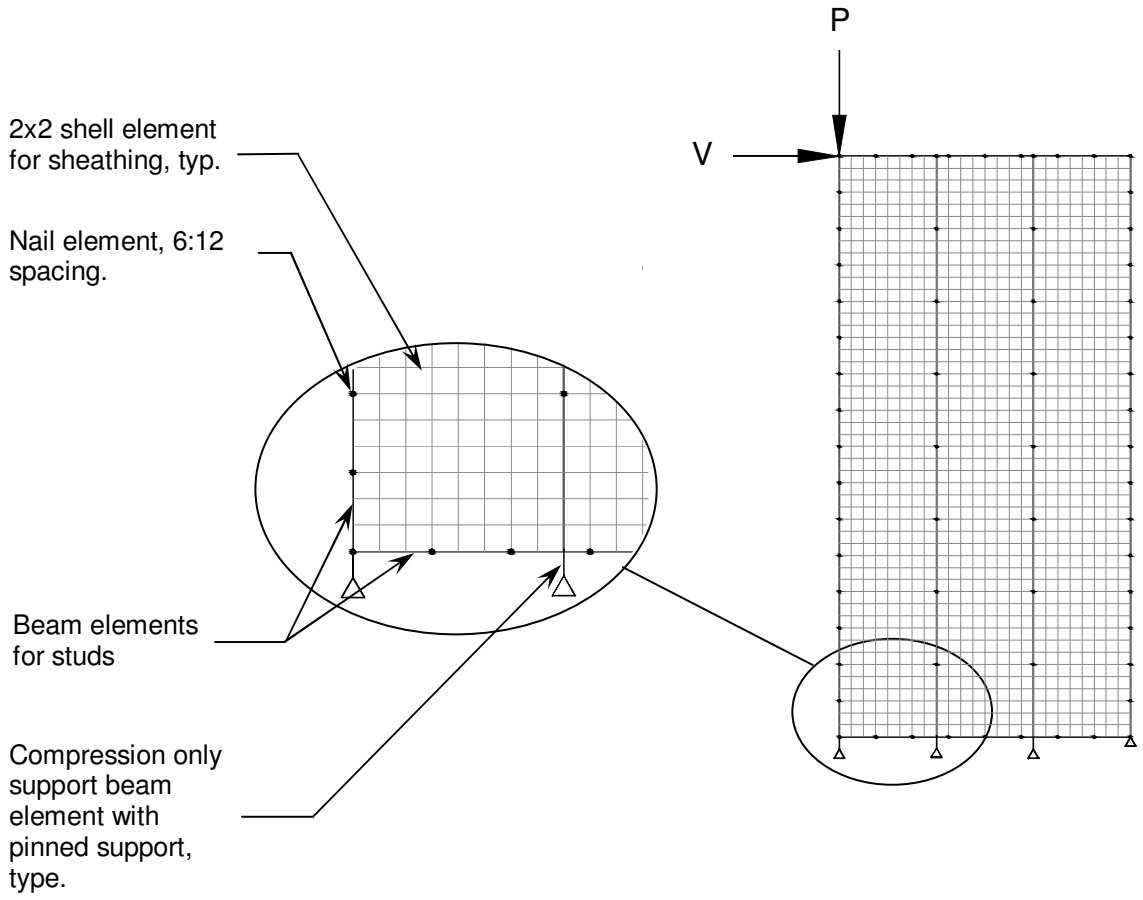

Figure 15: Finite Element Model

The FEM model is shown in Figure 15. A description of the actual elements used in the ABAQUS software model follows. For more information regarding these elements, please refer to the "*ABAQUS Analysis User's Manual*" (ABAQUS 2010).

4.1.1.1 Framing Members

The framing members, studs and plates were modeled as type B31 two node three-dimensional beam elements. This element uses linear interpolation. B31 elements have six degrees of freedom at each end. These elements can be defined by different geometric shapes. For this model, a rectangular shape was used to model a 2x4 framing member.

The second top plate of the wall was fastened only to the first top plate of the wall. This was deemed insignificant to the strength and stiffness of the wall since it was not fastened to the sheathing. It is common for models in the literature (Cassidy 2002, Judd 2005) to use both plates as one member of equal dimension. This would create additional stiffness that does not exist for the walls tested in this research.

Material properties for the B31 element are defined in the material properties card. The material properties used are explained in the Materials section of this chapter.

The length of the elements for the studs was 6” and the length of the elements for the sole and top plate was 2”. These lengths worked well for the nail and framing geometry and for the behavior of the wall as well.

4.1.1.2 Nails

The framing members were connected with two orthogonal springs (or spring pair), one linear and one nonlinear, as shown in Figure 16. As noted earlier, these springs are each one dimensional spring elements. These springs are modeled as Spring2 elements in ABAQUS. The spring used for lateral movement, or shear, was a linear spring while the spring used for end grain withdrawal was a nonlinear spring.

The sheathing was connected to the framing members with two orthogonal springs (or spring pair) as shown in Figure 16. As with the framing members these were one dimensional spring elements modeled as Spring2 elements in ABAQUS. This spring pair contains uncoupled, nonlinear springs with equivalent properties.

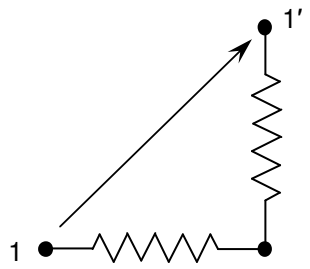

Figure 16: Spring Pair

As shown in Figure 16, the spring pair allows the node to move from point 1 to point 1′. This allows a two dimensional movement of the node replicating the nail displacement. As explained in Section 2.9.1, the spring pair model provides correct results for peak load and displacement for monotonic loading. The spring properties for these elements are explained later in Section 4.2.

4.1.1.3 Sheathing Members

The sheathing was modeled as four node quadrilateral shell elements. The general purpose S4 element was used. This element has six degrees of freedom at each node. The element size was 2” x 2” for ease of geometric construction. An element size of 4” x 4” is acceptable to model the sheathing. Cassidy modeled 16”, 8”, 4” and 2” elements and found convergence with 4” elements. He also used 2” elements to simplify the geometry for other nail patterns. (Cassidy 2002)

4.1.2 Materials

The material properties for the FEM were taken from available literature as well as from data obtained from the test. The stud and plate properties were taken from the *NDS* (2005) and the *Wood Handbook* (1999). Sheathing properties were taken from the

Plywood Design Specification (2004). Sheathing nail data and hold down data was obtained from the test results for the Group A walls. Stud to framing nail data was taken from the literature (Cassidy 2002).

Although wood is an orthotropic material, it is typically modeled as an isotropic material for wood shear walls (Judd 2005, Cassidy 2002). For the elements used, the modulus of elasticity and Poisson's ratio were required. The following values were used for the analysis:

Table 17: Framing Material

Material	Size[a] (in)	MOE[a] (psi)	Poisson's Ratio[b] υ
Studs – SPF-S	1.5 x 3.5	1×10^6	0.3
Plates – SPF-N	1.5 x 3.5	1.4×10^6	0.3

[a] From the NDS (2005)
[b] Estimated from orthotropic properties (Wood Handbook 1999)

For compression only support members, the material properties for the studs were used, but without tension. ABAQUS allows a "no tension" command to be added to a material property. This command does not allow tension stresses to occur in that material. Convergence of the model using this method worked better than using springs to model these supports.

The OSB sheathing material properties were taken from the *Plywood Design Specification* (2004). The following values were used for the analysis:

Table 18: Sheathing Material

Material	Thickness[a] (in)	MOE[a] (psi)	Shear Modulus[a] (psi)	Poisson's Ratio[b] υ
$^{15}/_{32}$" OSB	0.469	0.738 x10^6	0.178 x10^6	0.3

[a] From the PDS (2004)
[b] From literature (Judd 2005)

4.2 Connections

The properties for the sheathing nail spring pairs are the one dimensional spring element spring constants or the nonlinear load deformation nail curve data. The nonlinear load deformation nail curve data was taken from the test results as explained earlier in Section 3.3.1. The data was reciprocated in the negative region from the positive data to provide the same stiffness in the event that the spring moved in the negative direction. The same nail data was used for both orthogonal springs in the spring pair.

The nail data from the test results, shown in Graph 10, were calibrated in the model so the model behaved similarly to the test results for all five wall types. The values used in the FEM are tabulated in Table 19 and they are also shown in Graph 16. For comparison, the nail data from the test results of wall A are also shown in Graph 16.

In order to help with convergence, the stiffness at zero displacement is 5 lb. This was chosen as a small value so the spring doesn't have zero force at the beginning of the analysis.

The properties for the stud to plate nail elements were also spring constants, or the load deformation curve data. This connection also consists of two orthogonal springs. The stiffness of the springs for this connection is not the same in both

Table 19: Sheathing Nail Data

Displacement (in)	Load (lb)
-1.500	-37
-1.000	-148
-0.720	-213
-0.540	-250
-0.369	-240
-0.180	-200
-0.042	-100
0.000	5
0.042	100
0.180	200
0.369	240
0.540	250
0.720	213
1.0	148
1.5	37

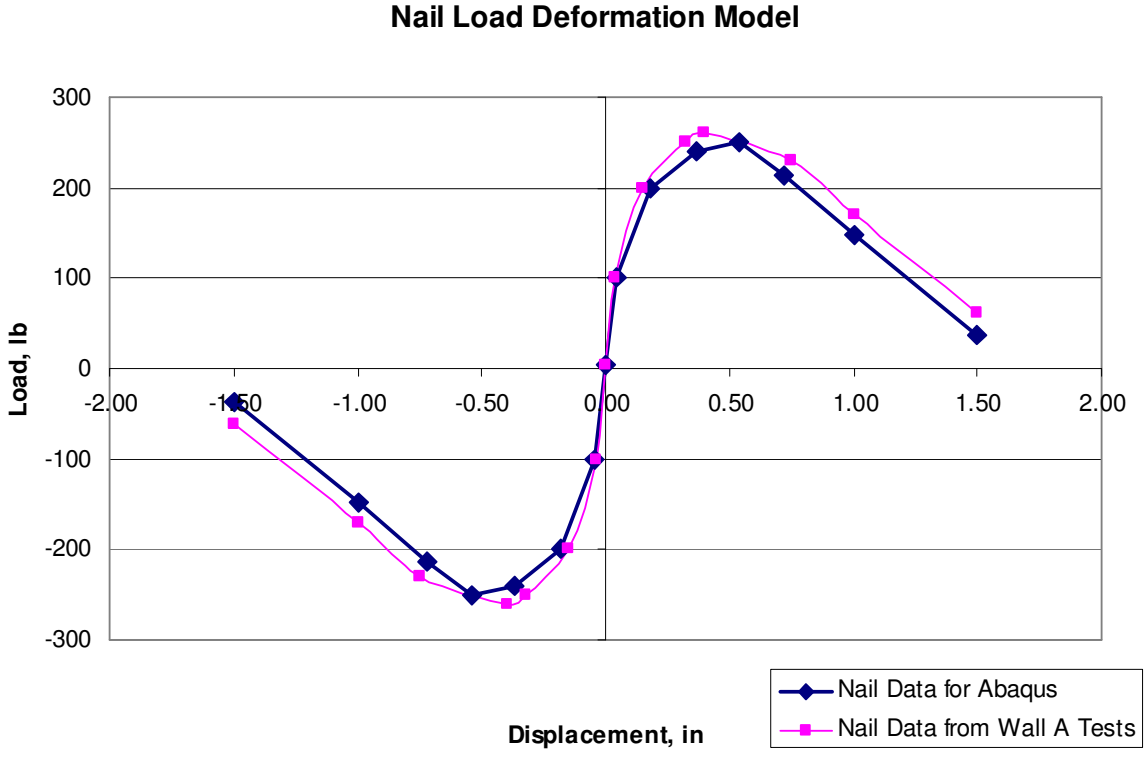

Graph 16: Sheathing Nail Data for ABAQUS

directions. The two directions considered are perpendicular to the stud in the plane of the wall and parallel to the stud in the plane of the wall. The latter is a withdrawal load from the end grain of the stud. For the direction perpendicular to the stud, a linear spring stiffness of 12,000 lb/in was used, which was used by Cassidy (2002) and published by Dolan *et. al.* (1995). For the direction parallel to grain, a nonlinear spring stiffness was used. The nonlinear spring stiffness was modified from the values used by Cassidy (2002). The modification was made on the tension value due to observations made during testing and dismantling the walls. It was observed that nail withdrawal from the end grain of the stud was not linear. The connection remained intact and then abruptly withdrew. The exact magnitude of this response is not known. A parametric study was conducted with the FE model until the load deformation curve reasonably met the test results. Recall that Cassidy (2002) used an arbitrary tension stiffness of 100 lb/in. As noted above, the compression stiffness was not altered and a value of 41,000 lb/in was used as modeled by Cassidy (2002). The values used in the FEM are tabulated in Table 20 and they are also shown in Graph 17.

Table 20: Stud to Plate Vertical Nail Data

Displacement (in)	Load (lb)
-1.0	-41,000
0.0	5
0.094	200
3.0	450

In order to obtain convergence of the model, the spring pairs for the framing member connections were used for the two studs closest to the leading edge only (where tension will result). The other two studs were simply connected to the plate

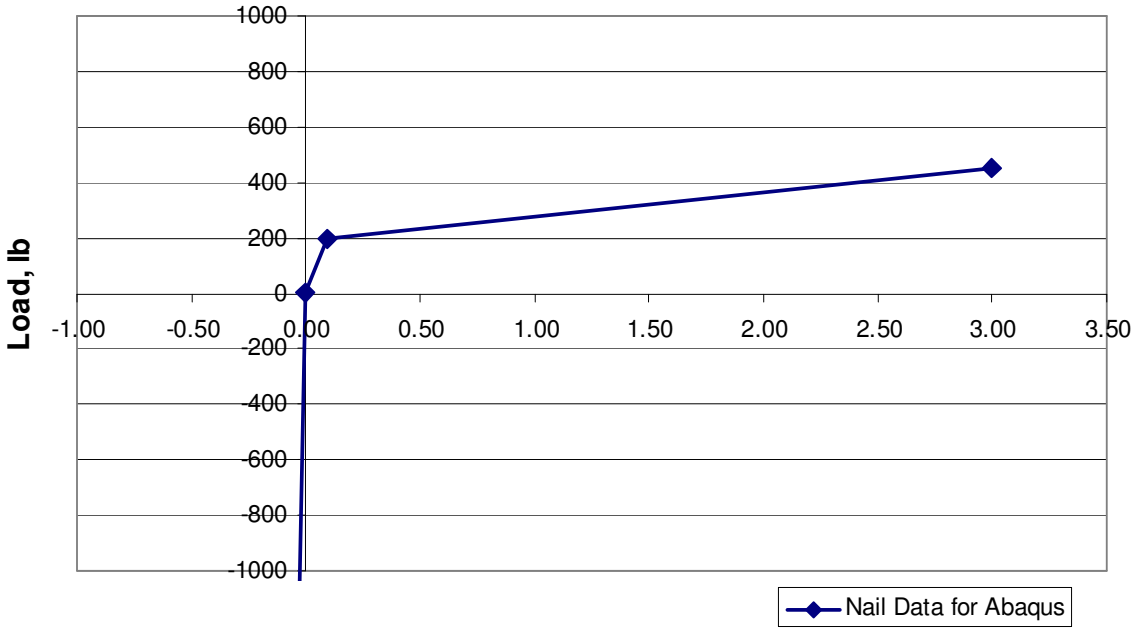

Graph 17: 16d Stud Withdrawal Nail Data for ABAQUS

nodes. It was discovered that this is a good modeling technique to capture the behavior of the framing connections.

It was recognized that the connection of the stud to the plate is neither an ideal pinned connection nor a rigid connection. This joint is in fact a semi-rigid joint. When the stud is in tension and the framing nails are withdrawing from the end grain of the stud, the rotational stiffness of the joint is only the stiffness of the two 16d nails. However, when there is a compression force in the stud, rigidity is created at the joint.

To illustrate the rigidity of the joint due to compression in the stud, a finite element model was created, Figure 17, to observe the behavior of the joint. The model consisted of a 2x4 member 6" tall. Since the base is supported on the sole or top plate, compression only springs were used with the same stiffness as the compression bearing shown in Table 20. RAM Elements was used for the FEA.

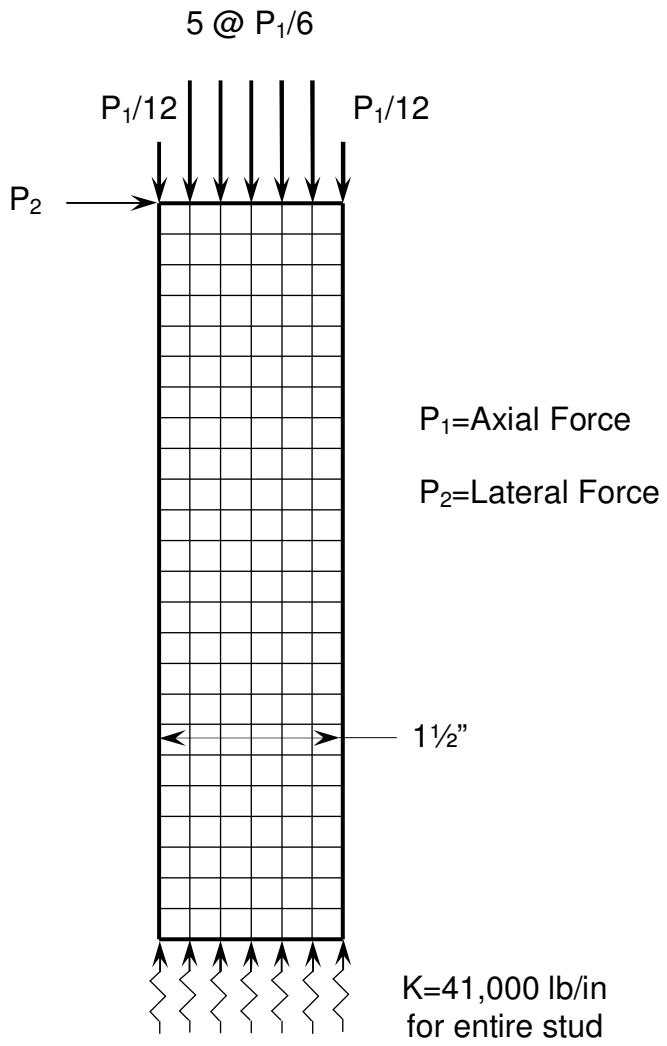

Figure 17: FEM of Stud Connection

From statics it is known that the eccentricity of a load, see Figure 17, cannot exceed b/2 or ¾". Therefore, it is possible to develop a moment equal to P_1 x ¾" at the ends of the compression studs. The results of this model are shown in Graph 18. Note the rotational stiffness is a constant 13,850 in-lb/radian in the linear range and the linear range is extended to a greater rotation as the axial force increases.

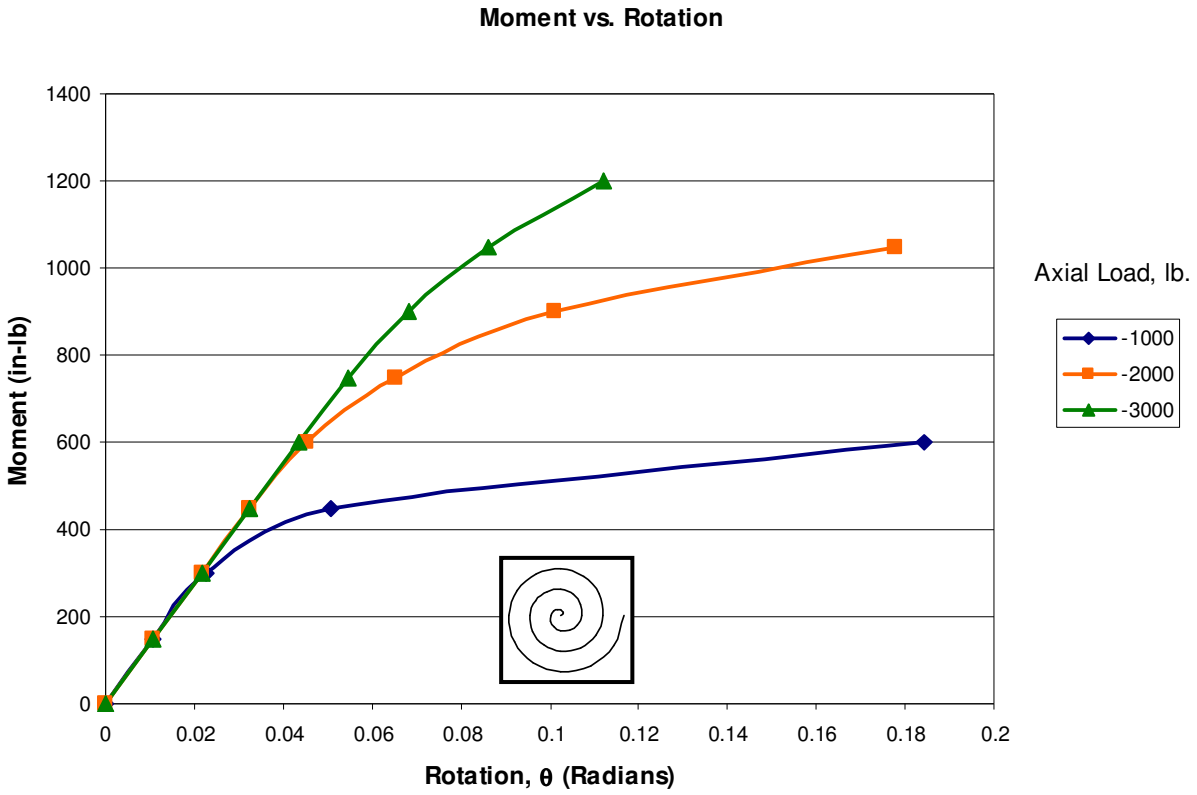

Graph 18: Effect of Axial Load on Stud Connection Rigidity

Figure 18 shows some of the results from the FEM with the 3,000 lb axial load and a 100 lb lateral load. Figure 18 (a) shows the reactions, (b) shows the deformed shape and (c) shows the axial stress.

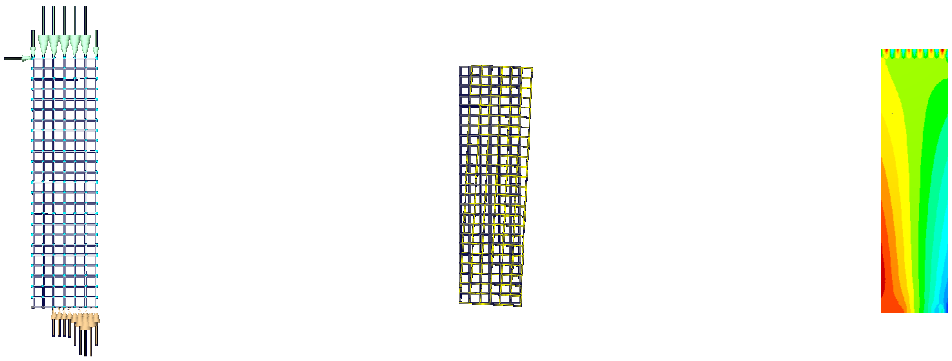

(a) (b) (c)

Figure 18: FEM Results of Stud Connection Rigidity

The model developed for this thesis models the semi-rigid connections by using one half of the connections as rigid and the other half pinned. As noted earlier, specifically the connections on the two studs at the leading edge of the wall were hinged in anticipation of the resulting tension in these studs. This, combined with the spring pair framing connection, allowed separation of the studs from the plates at these locations as observed in the test specimens.

The hold down was modeled as a nonlinear spring to account for the slip in the connection. It is recognized by the manufacturer and in SDPWS (2005) that there is slip in a hold down. This was observed and recorded during the tests. The nonlinear spring data used in the FEM was taken from the test data. The values used in the FEM are tabulated in Table 21 and they are also shown in Graph 19. This data creates a slip of 0.114" and then provides a tension stiffness of 39,562 lb/in.

Table 21: Hold Down Stiffness Data

Displacement (in)	Load (lb)
0.0	5
0.114	200
1.0	35,063

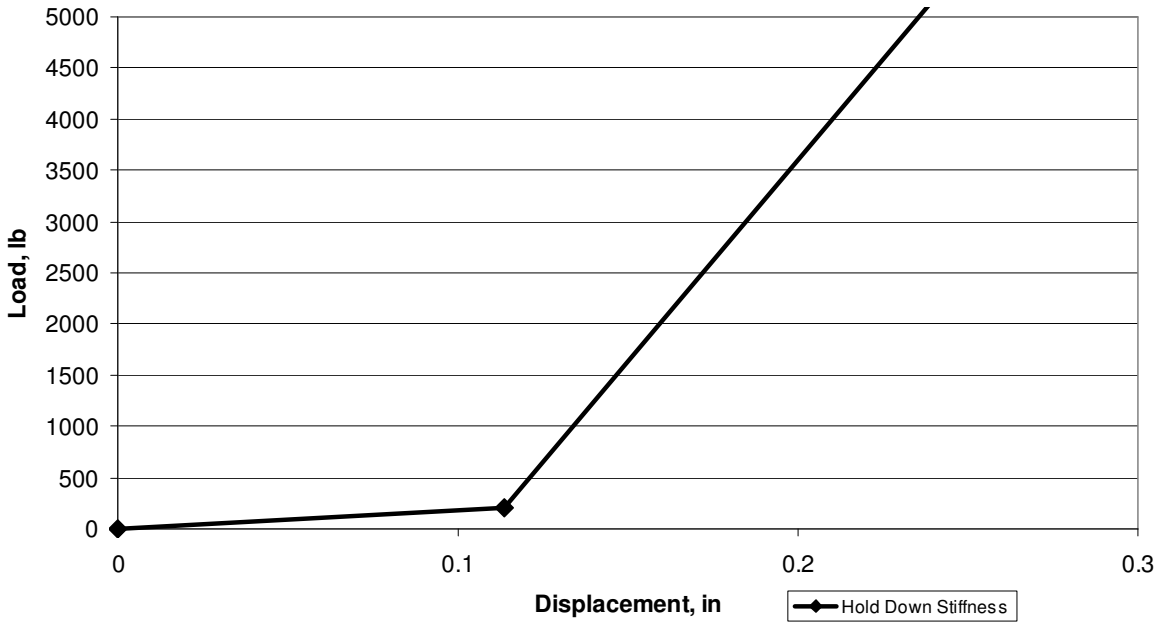

Graph 19: Hold Down Stiffness for ABAQUS

4.3 Modeling

The FEM used displacement control in the load steps. Nonlinear geometry control was used with the solver. The solver also used the Newton-Raphson method for calculating the stiffness matrix. The ABAQUS line search control parameter was used to help with convergence using the Newton-Raphson method.

The analysis utilized time steps to solve the model. The use of nonlinear geometry required that a time step analysis was used. For convergence, the solver automatically chose the step increment. An initial suggested step increment of $^1/_{1000}$ was used with a maximum of $^1/_{50}$. The solver was set to use smaller increments if necessary. To further aid the convergence, a discontinuous analysis control was used. This allows an increased number of iterations before divergence is checked. While this can increase computational time, it was often necessary for convergence.

In addition to the constraining force, *P*, as shown in Figure 15, the dead load of the wall was included in the analysis. This was applied as four 25 lb loads at the top of the wall to account for the weight of the sheathing and framing members.

4.4 Finite Element Analysis Results

The model utilized the same boundary conditions and restraining force as the five different sets tested, as well as one additional model with full constraint. The uplift boundary constraints and restraining forces are summarized in Table 22. The additional model with full constraint consisted of supports at 8" on center, along the top and bottom. The supports along the top were connected to a rigid beam that was constrained in both the vertical and out-of-plane directions. The supports directly above and below the studs, as well as between the studs along the top plate, were no tension elements. The supports between the studs along the bottom could resist tension. The latter model is for illustration of a fully restrained wall. The results of all of the FE models are shown on the following graphs and are each plotted along with the corresponding test results.

Table 22: Summary of FE Model Constraints

Wall	A	B	C	D	E	Full Constraint
Restraining Force, P (lb)	None	1104	2208	3312	None	None[1]
Mechanical Hold Down	Y[2]	N[3]	N[3]	N[3]	N[3]	N[4]

[1]Rigid beam across top of wall preventing any uplift.
[2]Simulated mechanical hold down as used in actual tests.
[3]Simulated $^5/_8$" diameter bolt 12" from tension edge.
[4]Simulated $^5/_8$" diameter bolt at 8", 24", and 40" from tension edge.

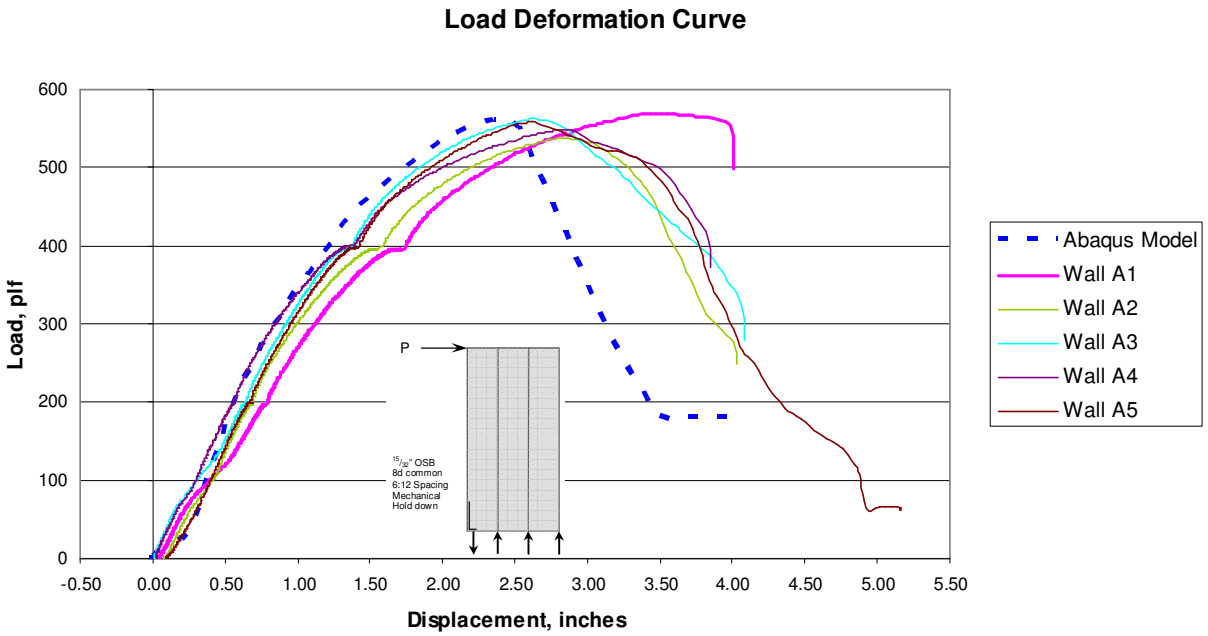

Graph 20: FE Comparison for Wall A

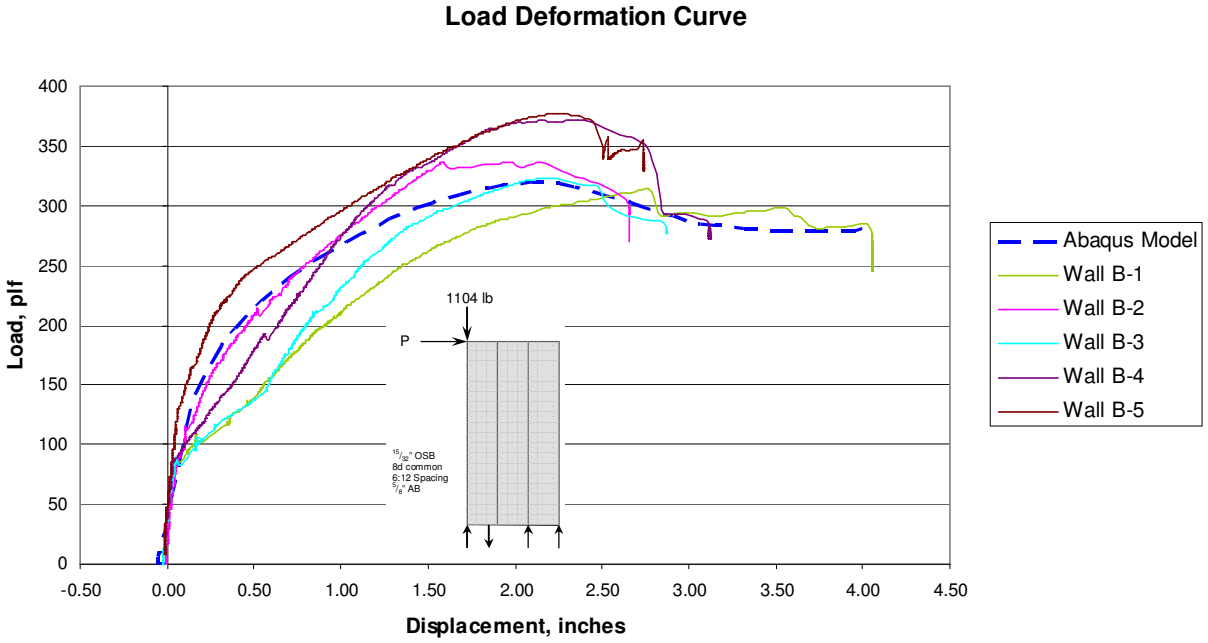

Graph 21: FE Comparison for Wall B

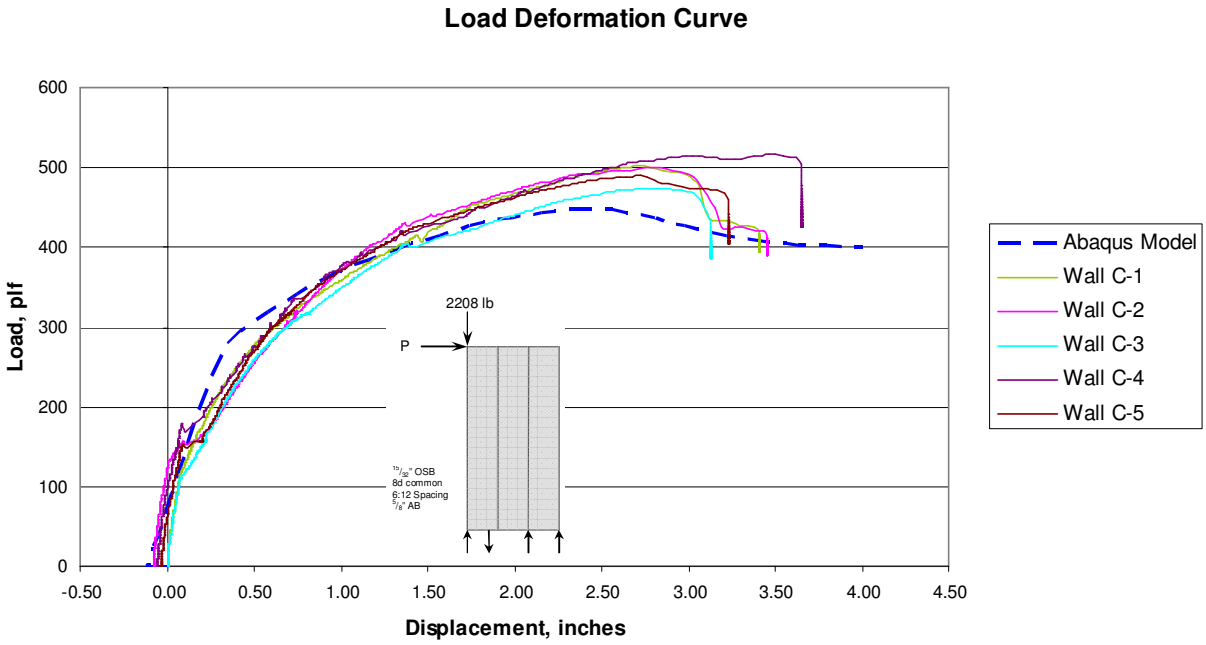

Graph 22: FE Comparison for Wall C

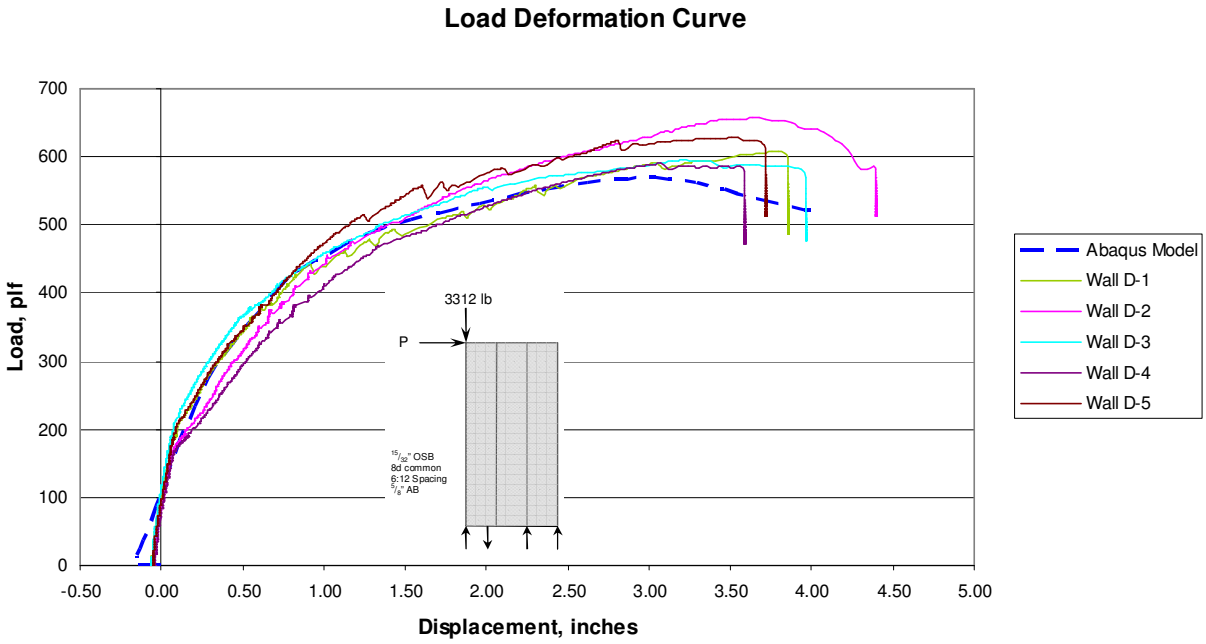

Graph 23: FE Comparison for Wall D

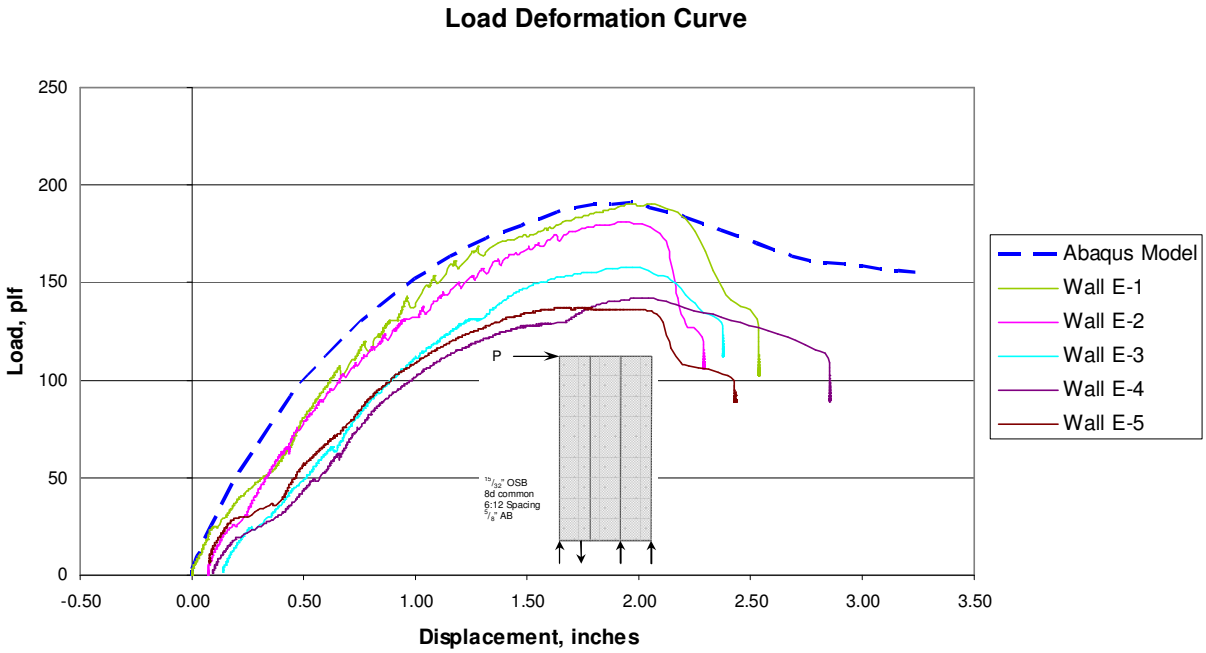

Graph 24: FE Comparison for Wall E

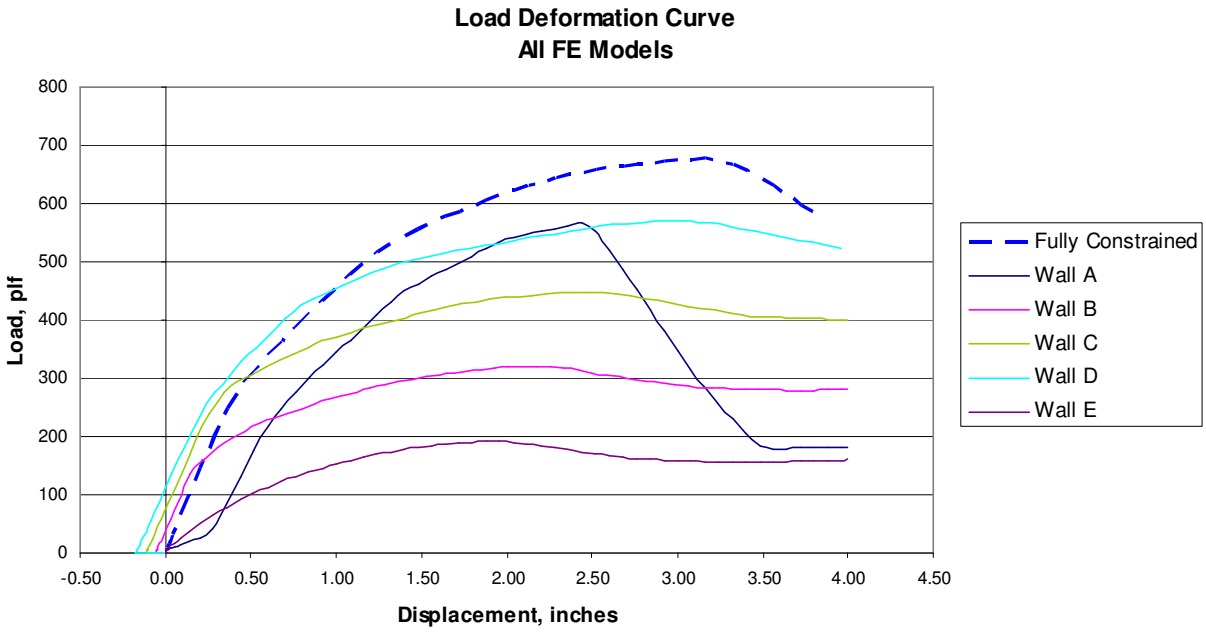

Graph 25: FE Model of Fully Restrained wall Compared to FE Model of Walls A-E

The results of the FE model are good in comparison to the test values for all five wall sets. Graph 25 shows the result of the fully constrained FE model compared to the results of the other five FE models. This graph also compares well with the summary of the actual test results shown in Graph 8.

The results are further summarized in Table 23 and Graph 26. It is apparent that wall A (with the mechanical hold down) has the least variability. The data from APA Research Report 154 has the greatest variability. For all of the comparisons, the FE model results fit well between the minimum and maximum values. Wall E and the APA Research Report 154 comparison have the largest percent error. However, the average of the errors is only -2.5%. If the comparison includes only the tested walls, the average percent error is -0.3%. This makes sense recognizing that wall E has the greatest variability of the walls tested. APA Research Report 154 doesn't offer an explanation for the large variation in the published values.

Table 23: Comparison of FE Model to Test Results

	Test Results						
	Wall A	Wall B	Wall C	Wall D	Wall E	APA 154[1]	
Average	555	345	496	615	162	785	
Min	538	314	474	590	137	593	
Max	562	377	516	656	190	888	
	ABAQUS Results						
ABAQUS	569	322	449	571	193	678	
							Average
% Error	2.5	-6.6	-9.5	-7.2	19.4	-13.7	-2.5

[1]Values in APA 154 modified to a specific gravity of 0.36.

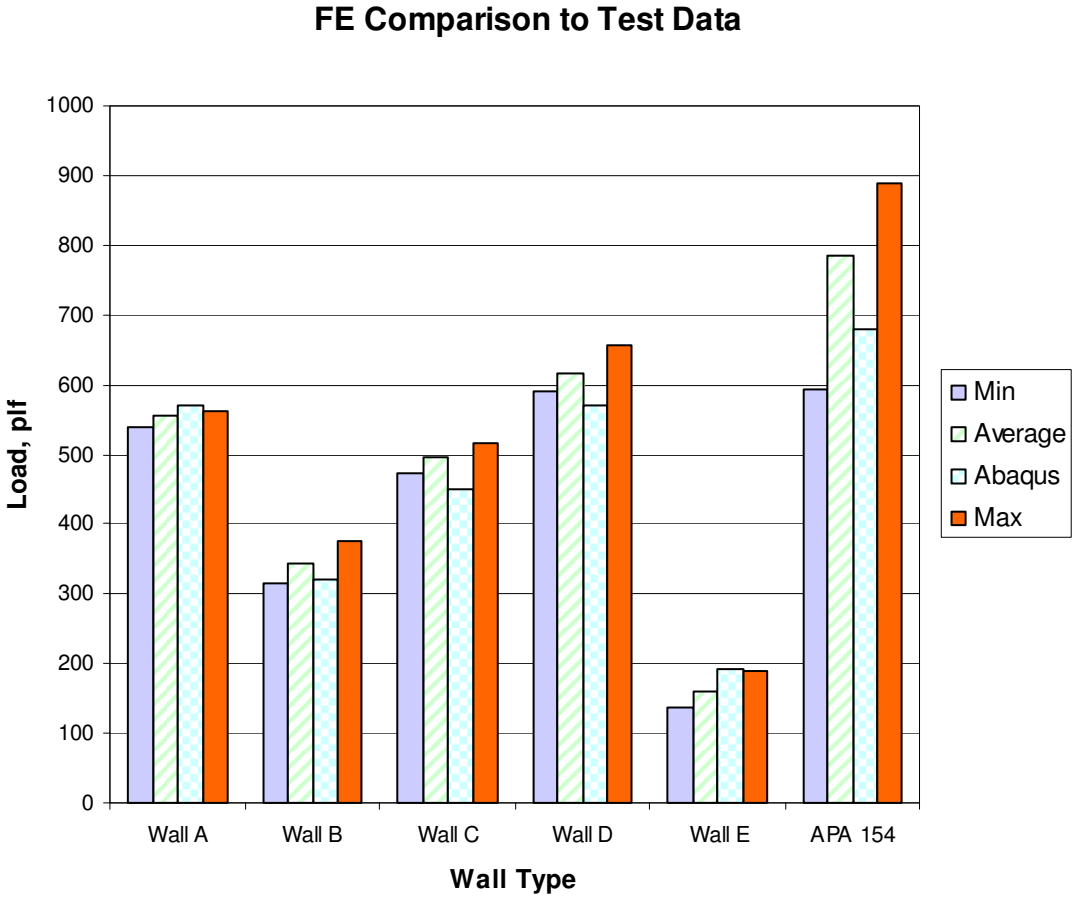

Graph 26: Comparison of FE Model to Test Results

Walls B, C and D have a negative movement initially due to the application of the restraining force P. This was observed in the test walls as well. There is a P-Δ effect that occurs when the restraining force, P, is applied since it is eccentric to the centroid of the wall. There is also a prestess that occurs with an added restraining force, P. The prestress, along with the added clamping action that keeps the plates from separating from the studs, increases the unit shear capacity of the wall.

The partial restraint effect of a single anchor bolt 12" from the end of the wall is best observed by viewing the sole plate as the wall is loaded. Figure 19 shows the

deformation of the sole plate as well as the sheathing and the nails at the base of wall E as it is loaded. Horizontal dashed lines are added to these figures as a reference to observe the deformation of the sole plate. The arrows pointing upward indicate compression only supports while the downward arrow represents the anchor bolt capable of resisting tension.

The view shown in (i) is at the early stages of the pushover analysis. As the load progresses, the tip of the sole plate continues to lift off the support. Between stages (iii) and (iv) the end stud separates from the sole plate, the sole plate to the end stud nails withdraw, and the corner nail must then resist more load. The peak load occurs when

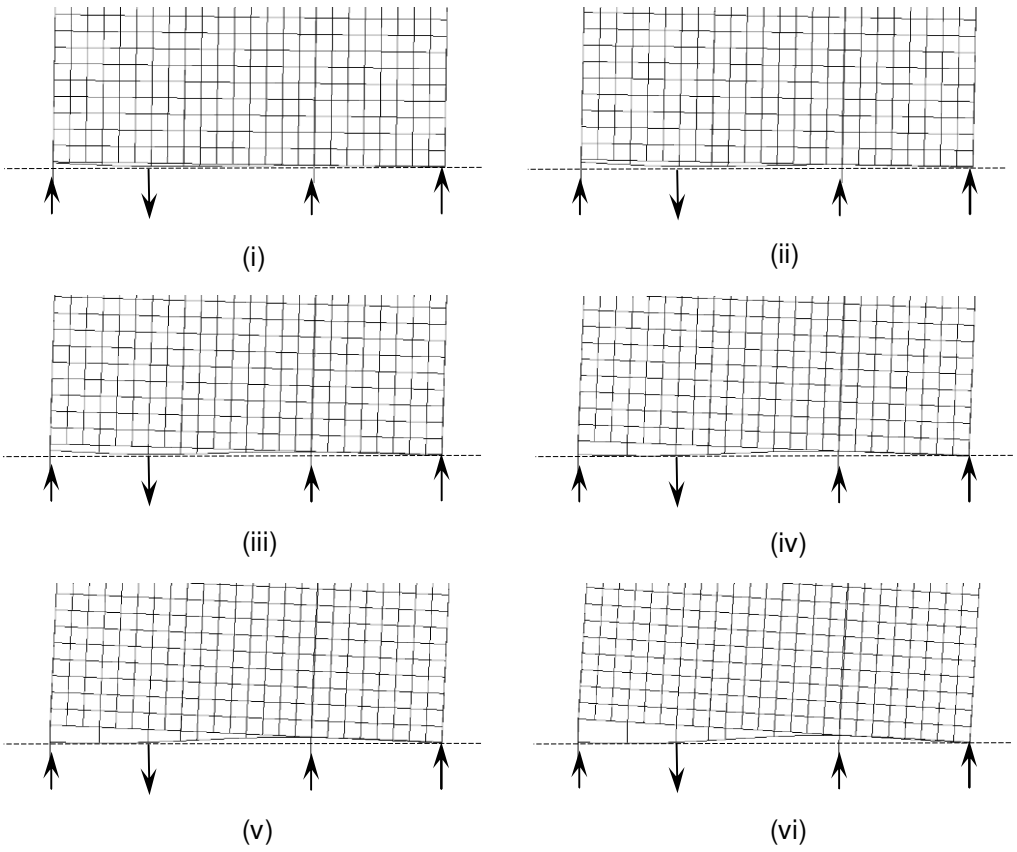

Figure 19: Sole Plate Deformation of Wall E

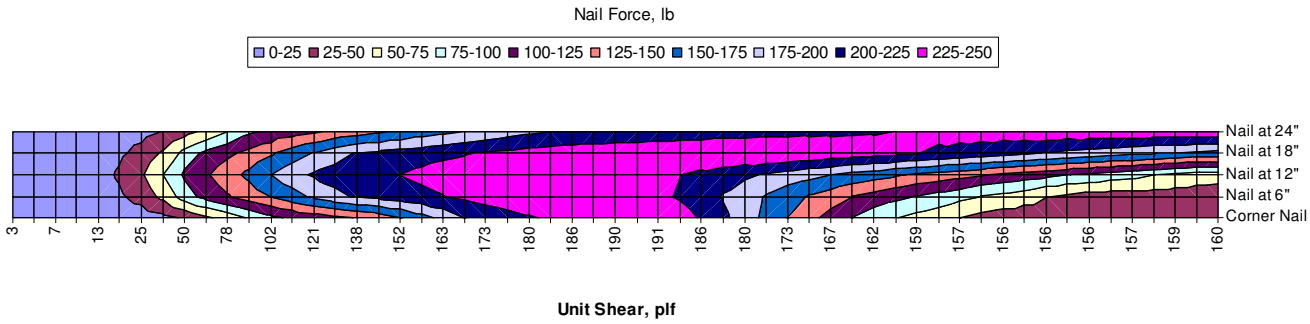

Graph 27: Contour Plot of Corner Nail Vertical Force, Wall E

the first three nails reach their peak capacity and the fourth nail is near its peak capacity. Graph 27 illustrates this clearly. It also shows that maximum force occurs first in the nail closest to the anchor bolt. The two neighboring nails then resist more load until they too yield and eventually all three reach their peak capacity. Note also in Figure 19 that the sheathing nails are nearly all vertical. This behavior was observed in the tests as well. This behavior can also be observed in the SBCRI 12' x 30' test structure shown in Figure 10.

The sole plate deformation and corner sheathing nail failure in the FE model is the same for walls B, C and D as shown for wall E in Figure 19. It just occurs at a greater unit shear load due to the restraining force.

Wall A exhibits a different failure mode due to the mechanical hold down. The deformation of the overall wall is shown in Figure 20. The top plate separates from the tension stud and then the sheathing nails in the tension stud reach their peak loads when the wall reaches its peak capacity. The same reference line and support locations are shown along the sole plate. The hold down kept the tension stud near the sole plate, but did allow some separation. There is some uplift of the sole plate at this

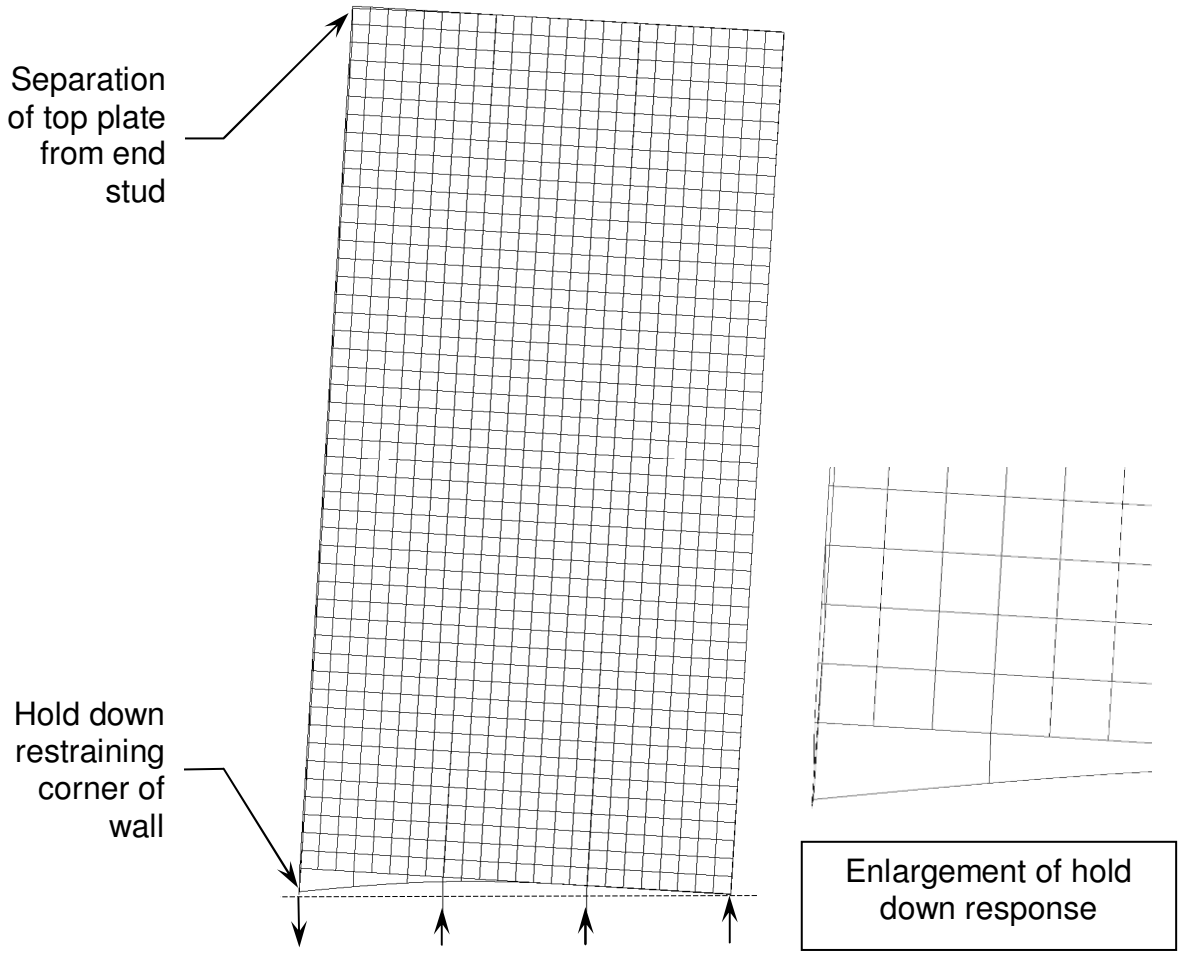

Figure 20: Deformation of Wall A FE Model

point due to slip and elongation of the hold down. This behavior was observed in the tests as well.

The fully restrained FE model illustrates the behavior of the wall when the plates are not allowed to separate from the studs. This can occur if a test apparatus utilizes a stiff load beam bolted to the top, if anchor bolts are used in each stud space, and if hold down rods are used to anchor the load beam to the foundation as illustrated in ASTM E72, Figure 22.

For the fully restrained FE model, the peak load was reached when the peak capacity of the nails in the compression stud was reached. The deformation of the studs can be seen in Figure 21. At peak load the studs transferred 869 lb of shear at the top plate and 894 lb of shear at the sole plate. This is an average force of 220 lb per stud connection or 220 plf of additional unit shear capacity beyond the sheathing edge nail contribution. This can add a significant increase to the wall unit shear capacity when the wall is fully restrained. This also explains the difference in the nail load deformation curves shown in Graph 9.

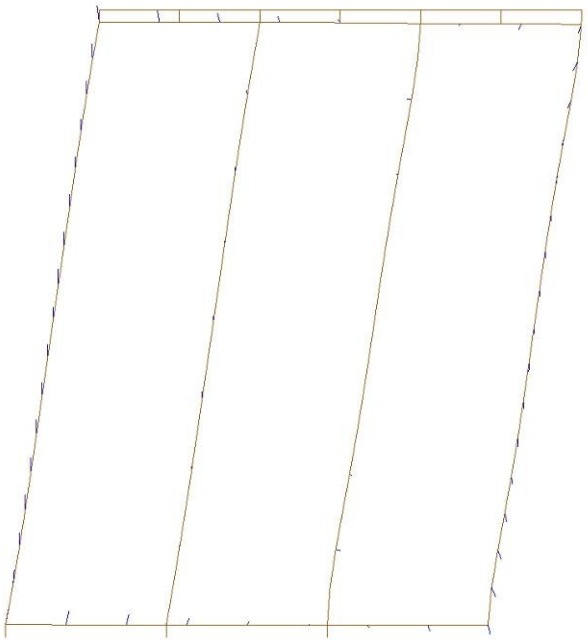

Figure 21: Deformation of Fully Restrained FE Model Frame

The contributing effect of the wall studs to the unit shear capacity was also observed in the other wall models, but to a lesser degree. The full benefit of the stud resistance cannot be achieved without a full constraint condition or other mechanical means of keeping the studs from separating from the plates.

The sheathing is not shown in Figure 21 for clarity to show the framing deformation. The rigid beam along the top of the wall is also shown in Figure 21.

CHAPTER 5

RELIABILITY ANALYSIS

The calibration using a reliability analysis was conducted in stages to fully understand the effect of each random variable and load combinations. It was necessary to first determine the reliability of the current industry standard, SDPWS, so a target reliability index could be used to determine the correct bias factors to produce the proper nominal values. The end result is verification of the nominal unit shear value used in SDPWS along with modifications for specific gravity, and proposed modification factors for the restraint type and partial restraining force; all of which are calibrated to the target reliability index.

At the two extremes of a partially restrained shear wall are unrestrained and fully restrained. The unrestrained shear wall is not restrained by any special mechanical hold down device or restraining force. The unrestrained shear wall is only restrained by the ½" diameter anchor bolt 12" from the end as required by the IRC. The fully restrained shear wall is restrained completely by an applied restraining force at the top of the wall. This load is so large that it produces a righting moment such that the overturning force will never overcome it. The failure modes of these two shear wall conditions have nothing to do with the variability of the restraining force and thus are only dependent upon their unit shear strength and the specific gravity of the lumber.

The load combinations of ASCE 7 and the IBC will have an effect on the partially restrained conditions between the two extremes explained in the preceding

paragraph. The calibration stage process presented will clearly illustrate the effect of these load combinations.

5.1 Code Required Load Combinations

Both ASCE 7-05 and IBC 2009 provide requirements for load combinations that a structure must meet. SDPWS provides the required ASD safety factor and LRFD resistance factor, (section 2.6). The governing load combinations for wood shear walls with wind load, the corresponding ASD safety factor and LRFD resistance factor are summarized in Table 24.

Table 24: Load Combinations

ASD		LRFD	
Load Combination	Safety Factor, Ω^1	Load Combination	Resistance Factor, ϕ^1
D+W	2.0	1.2D+1.6W	0.8
0.6D+W	2.0	0.9D+1.6W	0.8

[1] From SDPWS
D=Dead Load
W=Wind Load

5.2 Reliability of SDPWS Nominal Unit Shear Capacities

It is necessary to understand the reliability of the current unit shear capacities in order to calibrate the partially restrained shear wall unit shear capacities. To accomplish this, the origination of the SDPWS values was researched. The values in SDPWS originate from APA Research Report 154.

The test results, shown in Table 12, indicate that a mechanical hold down device at the bottom tension corner is not sufficient to achieve the fully restrained shear wall capacity. Therefore, to determine the capacity of a fully restrained shear wall, the values published in APA Report 154 were used and are indicated here for the $^{15}/_{32}$"

WSP as used for the test samples. The nominal design unit shear capacity for $^{15}/_{32}$" WSP are based on the results of seven tests, Table 25. The seven test results are a combination of three tests using $^{19}/_{32}$" plywood and four tests using $^{5}/_{8}$" plywood. The panel thickness has little influence on the ultimate capacity of the shear wall (van de Lindt and Rosowsky 2005). Therefore, it is reasonable to use the test results shown in Table 26 as the ultimate unit shear capacity for $^{15}/_{32}$" WSP.

Table 25: Excerpt from APA Report 154, Table A1

Fastener		Panel Thickness[(a)] (in)	No. of Tests	Ultimate Loads (plf)			Target Design Shear	Load Factor[(b)]
Size	Spacing (in)			Min.	Max.	Avg.		
RATED SHEATHING								
8d	6	$^{15}/_{32}$	7	689	1033	913	260	3.5

(a) Minimum panel thickness for design shear, some walls sheathed with thicker panels.
(b) The load factor is determined by dividing the average ultimate load by the target design shear.

A summary of the reported test results shown in Table 25 and Table 26 are shown in Table 27. Since all four tests are not reported for the $^{5}/_{8}$" WSP, the two missing values were estimated with equal weight.

Table 26: Excerpt from APA Report 154, Table A2

Fastener		Panel		No. of Tests	Ultimate Loads (plf)			Target Design Shear	Load Factor[(a)]
Size	Spacing (in)	Type	Thickness (in)		Min.	Max.	Avg.		
RATED SHEATHING									
8d	6	Plywood	$^{19}/_{32}$	3	950	1033	992	260[(b)]	3.8
			$^{5}/_{8}$	4	689	1000	854	260[(b)]	3.3

(a) The load factor is determined by dividing the average ultimate load by the target design shear.
(b) Design shear increased for "over-thick" panel, studs 16" o.c. or panel placed with 8' length perpendicular to framing.

Table 27: Summary of APA Report 154

Panel Thickness (in)	Ultimate Capacity (plf)
$^{19}/_{32}$	950
	992
	1033
$^{5}/_{8}$	689
	1000
	863.5 [1]
	863.5 [1]
Average	913
Standard Deviation	119
COV	0.13

[1]Estimated from data in APA Report 154.

The standard deviation and distribution of the APA wall tests are needed to calculate the reliability of SDPWS. Table 27 includes one of these two parameters. The distribution is expected to be lognormal as found with the test results reported in Section 3.3.4. To verify the accuracy of the COV in Table 27, it was compared with the 5% lower exclusion value for the data from APA Report 154. Table 28 shows that the calculated standard deviation is very close to the 5% lower exclusion value. Since the 5% lower exclusion value is commonly used for timber design values, the actual standard deviation of ultimate unit shear capacity from the APA test data is more accurately 112 plf.

Table 28: Comparison of SDPWS Nominal Unit Shear to the 5th Percentile

	APA Data + 2 Estimated Points	Values to Match SDPWS
Average	913	913
COV	0.130	0.123
Standard Deviation	119	112
5th Percentile	718	728

5.2.1 Reliability Model

The reliability model begins with the limit state equation. A basic limit state equation is given in Eq. 11 which is repeated here. Failure occurs when $g(x) < 0$. This results in the basic design equation shown in Eq. 15. The load factors are given in ASCE 7 (2005).

$$g(x) = R - S \qquad \textbf{Eq. 11}$$

$$\phi R_n \geq \sum_{i=1}^{m} \gamma_i Q_{ni} \qquad \textbf{Eq. 15}$$

Where,

R_n = Nominal Strength for a Given Failure Mode

Q_n = Nominal Design Load

ϕ = Resistance Factor

γ = Load Factor

Since R and S are random variables, or multiple random variables, statistical parameters must be known for each. The distribution function must be known. For the distributions used in this thesis, two statistical parameters, the mean and the standard

deviation, are needed. Additionally the random variables must be identified. The wind load, the shear wall strength, the dead load restraining force, and the specific gravity of the framing lumber have been identified as random variables. Of these four random variables, the parameters are known for wind load (van de Lindt and Rosowsky 2005), the dead load (Ellingwood, et al 1980), and the specific gravity (ASTM D2555). The parameters for the shear wall unit shear strength were determined from the wall testing presented in this thesis. Table 29 summarizes the parameters known thus far.

Table 29: Summary of Distributions

Item	$\bar{X}/X_n$	v_x (cov)	DF
Dead Load	1.05	0.1	Normal
Wind Load	0.8	0.35	Type 1
Specific Gravity, G	1.0	0.1[1]	Lognormal[2]
Shear Wall Capacity	Unknown	Varies[3]	Lognormal[3]

[1]From ASTM D 2555
[2]From specific gravity test of lumber from samples
[3]From shear wall test results

The formation of the limit state function, *g(x)*, then includes the unit shear strength of the shear wall, *V*, the specific gravity of the framing lumber, *G*, the wind load, V_W, and the dead load, *P*. For the limit state of shear:

$$\phi V_n \geq V_u \qquad \textbf{Eq. 16}$$

$$V_n = V_{tab}(1-(0.5-G)) \qquad \textbf{Eq. 17}$$

$$V_u = \gamma_W V_W = \phi V_n$$

$$V_W = \frac{\phi V_n}{\gamma_W}$$

$$\overline{V}_W = a_1 V_W = \frac{a_1 \phi V_n}{\gamma_W} \qquad \textbf{Eq. 18}$$

Where,
V_{tab} = SDPWS unit shear values
G = Specific gravity
a_1 = *Wind* load bias factor
V_W = Unfactored shear load due to wind
$\overline{V}_W$ = *Average* shear load

Eq. 18 shows the relationship of the average shear load to the bias factor, resistance factor, load factor, and the nominal unit shear strength.

5.2.2 Reliability Analysis Results

Since the SDPWS shear wall is considered as fully restrained, only two of the four random variables are considered to determine the reliability of the SDPWS unit shear capacity. The two random variables are the wall shear strength and the wind load. These two random variables were applied to Eq. 11. Using the first order second moment, FOSM, reliability method the reliability index β was determined to be 3.27 for the $^{15}/_{32}$" shear wall tabulated in SDPWS for a fully restrained condition. Recall from Section 2.6 that the SDPWS values are 2.8 times the APA Report 154 target design shear. Therefore, as determined by the quotient of the average ultimate load, 913 plf, in

Table 25 and the nominal unit shear capacity, 730 plf, in SDPWS, Table 6, the bias factor used in SDPWS is 1.25. The calculations are shown in Appendix D.

The target reliability index, β, for the calibration of the partially restrained shear walls tested will be 3.25 since the SDPWS nominal unit shear capacity has a reliability index of 3.27. This is reasonable based on other literature (van de Lindt and Rosowsky 2005).

5.3 Base Calibration of Partially Restrained Unit Shear Capacities

The reliability index of the unit shear capacity of the unrestrained shear wall was calculated next. Using the mean unit shear capacity of wall E, 162 plf, from Table 12, the reliability index was calculated using the FOSM method. The calculations are shown in Appendix E for a bias factor of 1. With a bias factor of 1, the reliability index, β, was determined to be 2.59, Table 30. The calculations were iterated changing the bias factor, Table 30, and the results were plotted in Graph 28. The calibrated bias factor was determined from the graph and verified again with calculation. A summary of the results is shown in Table 30.

This procedure was repeated for the remaining partially restrained walls A, B, C, and D. A summary of the results are shown in Table 31. Note that the calibrated values shown in Table 31 simply calibrate all of the partial restraint conditions from the tests and the SDPWS (APA) values to the target reliability index, β=3.25. This is appropriate for the ASD load combination D+W with a safety factor, Ω=2.0. For the mechanical hold down, Group A walls, the unrestrained Group E walls, and the SDPWS

(APA) fully restrained wall, this is also appropriate for the LRFD load combination 1.2D+1.6W with a resistance factor, ϕ=0.8.

Table 30: Nominal Unit Shear Calibration for Unrestrained Wall E

V(Strength)				Vw(Load)				β
u_{VN} plf	a_V	u_V plf	σ_V Plf	u_{VwN} plf	a_{Vw}	u_{Vw} plf	σ_{Vw} plf	
162.0	1.00	162	23.5	81.0	0.8	64.8	22.7	2.59
154.3	1.05	162	23.5	77.1	0.8	61.7	21.6	2.72
147.3	1.10	162	23.5	73.6	0.8	58.9	20.6	2.84
140.9	1.15	162	23.5	70.4	0.8	56.3	19.7	2.96
135.0	1.20	162	23.5	67.5	0.8	54.0	18.9	3.07
129.6	1.25	162	23.5	64.8	0.8	51.8	18.1	3.19
126.6	***1.28***	***162***	***23.5***	***63.3***	*0.8*	***50.6***	***17.7***	***3.25***
124.6	1.30	162	23.5	62.3	0.8	49.8	17.4	3.3
120.0	1.35	162	23.5	60.0	0.8	48.0	16.8	3.39
115.7	1.40	162	23.5	57.9	0.8	46.3	16.2	3.49
111.7	1.45	162	23.5	55.9	0.8	44.7	15.6	3.59
108.0	1.50	162	23.5	54.0	0.8	43.2	15.1	3.69
104.5	1.55	162	23.5	52.3	0.8	41.8	14.6	3.78

The reason that the nominal unit shear values shown in Table 31 are appropriate for the ASD and LRFD load combinations stated is that the dead load will not affect the wall strength in these load combinations. There are additional load combinations (Table 24) which require a reduced load factor for the dead load. This insures that dead load will not be a limiting factor and these combinations are addressed in section 5.4. Therefore, the unit shear capacity of the wall is the only random variable on the strength side considered for this step.

To illustrate the relationship between partial restraint and nominal unit shear strength, the results shown in Table 31 are graphed in Graph 29. Note that the shape of the graph is similar to Graph 12. The difference between these two graphs is shown in Graph 30. Note that the fully restrained wall has 100% unit shear capacity in both the

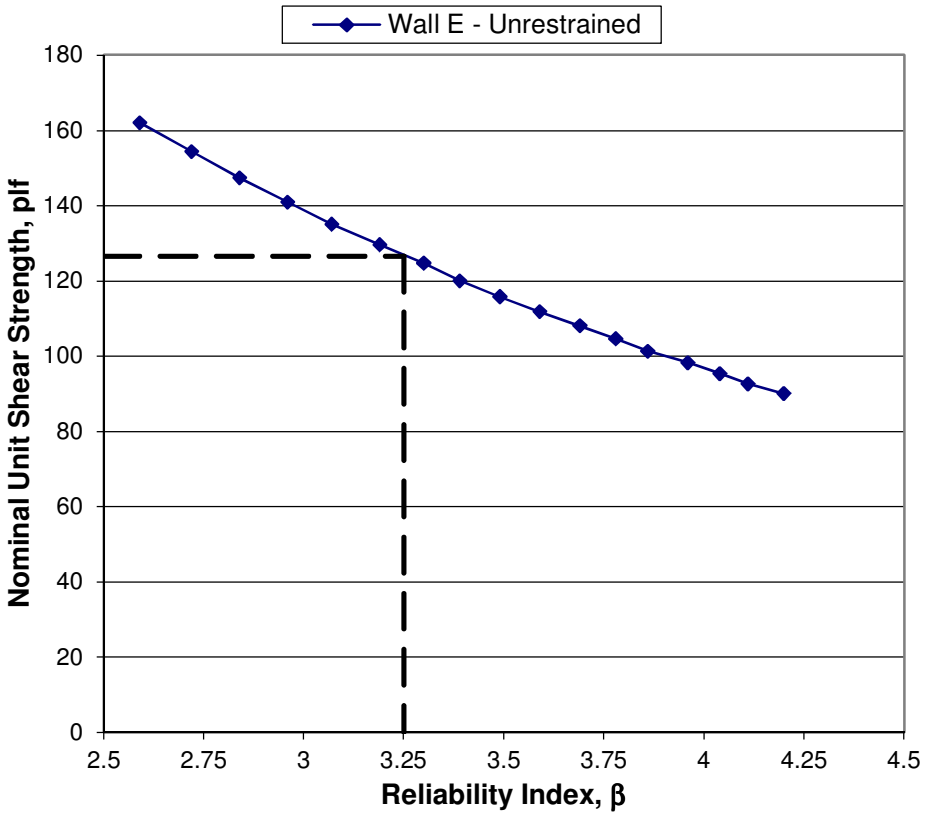

Graph 28: Calibration of Unrestrained Shear Wall

nominal, calibrated, the ultimate and test result. They are the same due to the normalization. The unrestrained wall is nearly the same as well. The larger difference occurs for walls B, C, and D. This difference is due to the shift in the percent of full restraint. The mechanical hold down cannot achieve the same unit shear capacity as a wall restrained from the top. This was discussed in Section 3.3.3. The difference in the two points in Graph 30 is from the calibration as well as the percent of full restraint occurring in the normalization process.

Table 31: Calibrated Shear Wall Capacities

Calibrated Wall Values[1]						
	A	B	C	D	E	SDPWS[2]
Wall Restraint (lb)	4416	1104	2208	3312	0	5051
Ultimate Unit Shear Capacity (from tests), plf						
	555	345	496	615	162	786
Bias Factor						
a_2	1.15	1.19	1.16	1.16	1.28	1.25
Nominal Unit Shear Capacity, plf						
	483	289	428	529	127	631
Normalized						
$P_{hold\ down}$	0.874	0.219	0.437	0.656	0.000	1
V_{cap}(%)	0.764	0.458	0.678	0.838	0.200	1.000

[1]Calibrated for ASD load combination D+W
[2]From SDPWS and APA Report 154
a_2 = Unit shear capacity bias factor

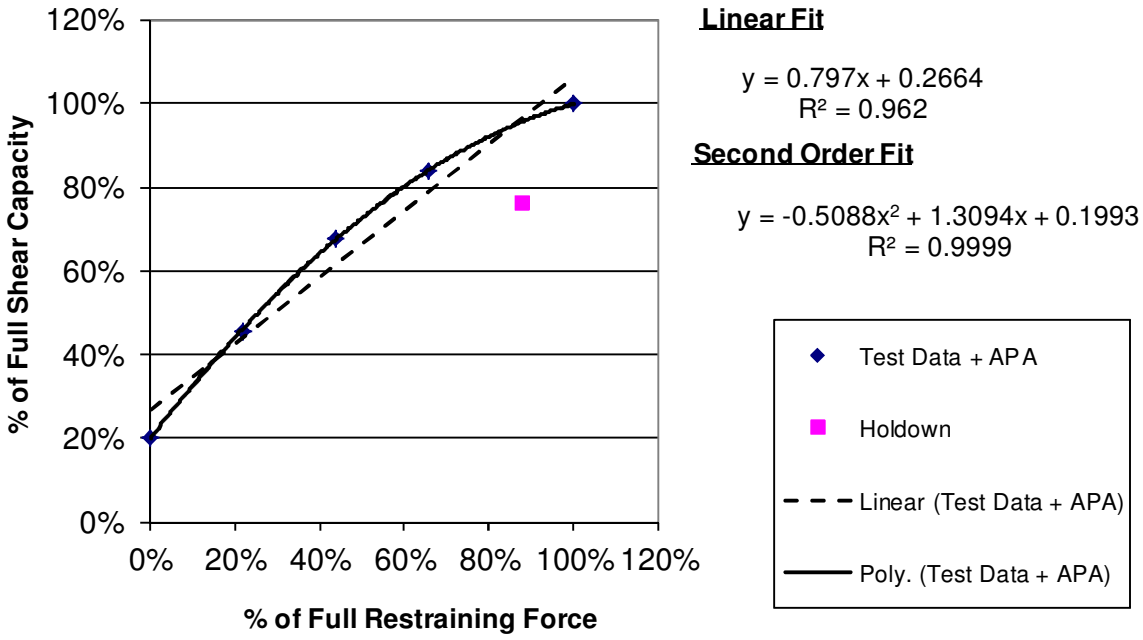

Graph 29: Partial Restraint Effect on Strength - Calibrated

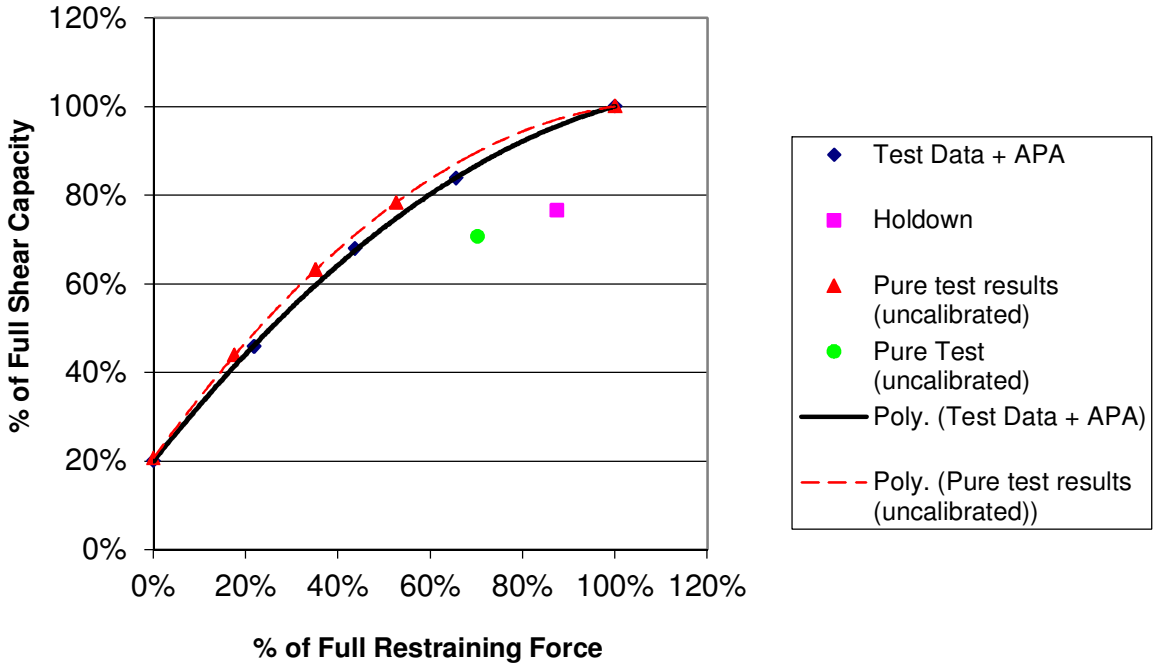

Graph 30: Comparison of Calibrated Partial Restraint Effect

5.4 Extended Calibration of Partially Restrained Unit Shear Capacities

5.4.1 Calibration with Reduced Dead Load Combinations

Next, the unit shear capacities were calibrated for the ASD and LRFD load combinations that have a dead load factor, γ_D, less than 1. This is a critical part of the calibration to consider since the partially restrained shear walls use a dead load applied to the top of the wall to resist the lateral wind load.

5.4.2 Calibration without a Variation in the Specific Gravity

First, the calibration was performed without considering the specific gravity of the framing lumber as a random variable. The random variables for this calibration are the

unit shear capacity, V, the wind load, V_W, and the dead load, P. These random variables are defined in Table 29.

The shear wall ultimate unit shear capacity is a function of the restraining force. As shown in Eq. 14, the ultimate unit shear capacity of a partially restrained shear wall is related to the fully restrained shear wall unit shear capacity by the partial restraint factor, $C_{pr\text{-}u}$. This relationship was used for the second calibration. Since the restraining force, P_D, is a random variable, then $C_{pr\text{-}u}$ varies. However, $C_{pr\text{-}u}$ cannot be greater than 1. This limit cannot be accounted for in a FOSM model. Therefore, for the second calibration, a Monte Carlo simulation was used.

The Monte Carlo simulation was conducted in Excel 2010. To adequately capture the target reliability index, β, of 3.25 (p_f = 5.77e-4), four million simulations were used. This was done by repeating 100,000 simulations 40 times for each increment of bias factor studied. The calibration consisted of varying the bias factor to achieve the target reliability index, β=3.25; similar to what was done with the first calibration with the test data. The results were graphed to determine the calibrated bias factor similar to Graph 28. The value from the graph was then confirmed with 4 million simulations. The Monte Carlo simulation is described below.

5.4.3 Random Variables used for Calibration

The nominal shear capacity of the wall is:

$$\frac{\overline{V}}{V_n} = a_2$$

$$V_n = \frac{\overline{V}}{a_2}$$

or,

$$V_n = \frac{\overline{V}(1-(0.5-G))}{a_2}$$

Where,

a_2 = Shear Capacity bias factor

Since V is a random variable, V_n is a random variable as well. For this step, the specific gravity, G, is considered a constant.

Recall from Eq. 14 that the partially restrained unit shear capacity is the fully restrained unit shear capacity modified by the partial restraint factor (Eq. 13) which is repeated here:

$$C_{pr\text{-}u} = -0.6393\lambda^2 + 1.4331\lambda + 0.206 \leq 1.0 \qquad \textbf{Eq. 13}$$

$$\lambda = \frac{P_D}{V_{ult} \times h}$$

P_D = restraining force (random variable)

V_{ult} = average ultimate unit shear capacity

h = shear wall height

Therefore,

$$V_n = \frac{C_{pr-u}\,\overline{V}(1-(0.5-G))}{a_2} \qquad \textbf{Eq. 19}$$

The mean dead load restraining force applied to the wall is:

$$\frac{\overline{P}_D}{P_n} = a_3$$

$$\overline{P}_D = a_3 P_D$$

Adding the load factor:

$$\overline{P}_D = \frac{a_3 P_D}{\gamma_D} \qquad \textbf{Eq. 20}$$

Where,

a_3 = Dead load bias factor

γ_D = Dead load factor

The nominal wind load is taken as the nominal capacity of the shear wall. Therefore, the nominal wind load is calculated as shown here:

$$V_{Wn} = \frac{\phi V_n}{\gamma_W} \qquad \textbf{Eq. 21}$$

$$\overline{V}_W = a_1 V_{Wn}$$

or,

$$\overline{V}_W = \frac{a_1 \phi V_n}{\gamma_W} \qquad \textbf{Eq. 22}$$

Where,

V_{Wn} = nominal wind load unit shear (random variable)

$\overline{V}_W$ = mean wind load unit shear (random variable)

a_1 = Wind load bias factor

ϕ = resistance factor

γ_W = Wind load factor

And, for a partially restrained shear wall, the limit state equation is:

$$g(V_W, V) = V - V_W \qquad \textbf{Eq. 23}$$

Where,
V_W = wind load unit shear
V = unit shear capacity of the wall

5.4.4 Random Variable Distributions

Although Eq. 23 only indicates two random variables, keep in mind that there is a third random variable, P_D, included in the partial restraint factor, $C_{pr\text{-}u}$. Table 34 summarizes the three random variables necessary for Eq. 23 and the Monte Carlo simulation. The bias factor for V is indicated as "unknown" because this is what is being determined by the calibration.

Table 32: Summary of Distributions

Random Variable	Item	$\bar{X}/X_n$	v_x (cov)	DF
P_D	Dead Load	1.05	0.1	Normal
V_W	Wind Load	0.8	0.35	Type 1
V	Shear Wall Capacity	Unknown	0.12[3]	Lognormal[4]

[1]From ASTM D 2555
[2]From specific gravity test of lumber from samples
[3]From Table 28
[4]From shear wall test results

5.4.5 Steps used for Monte Carlo Simulation

The Monte Carlo simulation was conducted with the following steps:

1. Begin with the restraining force. This is the restraining force from walls B, C, and D; 1104 lb, 2208 lb, and 3312 lb respectfully.
    a. Calculate the mean dead load restraining force, $\bar{P}_D$, using Eq. 20 and its bias factor shown in Table 32.

2. Calculate the partial restraining factor, $C_{pr\text{-}u}$, Eq. 13 using the restraining force from step 1.
3. Determine the mean ultimate unit shear strength, $\overline{V}$, from APA Report 154, and its statistical properties.
4. Start with a trial bias factor, a_2=0.8.
5. Calculate the nominal unit shear strength, V_n, using Eq. 19, with the specific gravity of the wall framing members, G=0.36 for SPF –S.
6. Calculate the nominal wind load, V_{Wn}, using Eq. 21.
7. Calculate the mean wind load, $\overline{V}_W$, using Eq. 22 and its statistical properties.
8. Monte Carlo Simulation
    a. Use a random number generator to generate a random probability between 0 and 1 and calculate the inverse of the CDF (normal distribution) for the dead load, P_D, at the random probability.
    b. Using the result of step 8.a, calculate $C_{pr\text{-}u}$ using Eq. 13.
    c. Use a random number generator to generate a random probability between 0 and 1 and calculate the inverse of the CDF (lognormal distribution) for the unit shear capacity, V, at the random probability.
    d. Calculate the partially restrained unit shear capacity of the wall by modifying the unit shear capacity, V, from step 8.c by the partial restraint factor, $C_{pr\text{-}u}$, from step 8.b.
    e. Use a random number generator to generate a random probability between 0 and 1 and calculate the inverse of the CDF (Type I extreme value distribution) for the wind load, V_W, at the random probability.
    f. Using Eq. 23 calculate the survival of the function ($g(x)>0$ for survival). Set a flag equal to zero for survival or one for failure.
    g. Repeat steps 8.a to 8.f 100,000 times, and add the number of failures in step 8.f.
9. Repeat step 8 forty times and sum the total number of failures from step 8.g. Calculate the reliability of the 4,000,000 samples and then calculate the reliability index, β as shown:

$$R = 1 - p_f$$

$$R = 1 - \frac{\#\text{ of failures}}{4{,}000{,}000}$$

$$\beta = \Phi^{-1}(1 - R)$$

10. Plot the bias factor, a_2, and the reliability index, β, from step 9.
11. Increase the bias factor, a_2, increment (0.1 was used) and repeat steps 5 to 11 until $\beta \geq 3.25$.
12. Using the graph from step 10, determine the correct bias factor, a_2, to obtain the target reliability index β=3.25.
13. Repeat steps 5 to 9 to validate the bias factor, a_2, determined in step 12.
14. Make correction to the bias factor a_2 if necessary and repeat steps 5 to 9.
15. Repeat entire procedure for next wall set (restraining load).

An illustration of the Excel spreadsheet used for the Monte Carlo simulation is shown in Appendix F.

5.4.6 Calculations for Monte Carlo Simulation

The known distributions of each random variable were used in the MCS to generate random values to evaluate Eq. 11. As shown in Table 32 and again in Table 34, three distributions were used, Normal, Log-Normal, and Type I. The cumulative distribution function, CDF, for each of these was used along with a random number generator to generate values of the random variables. The random number generator is used to generate a probability which can then be evaluated with the CDF to determine the random variable value at the generated probability.

For normal distribution, denoted as N(μ, σ), the PDF is given as:

$$f_X(X) = \frac{1}{\sigma\sqrt{2\pi}} exp\left[-\frac{1}{2}\left(\frac{x-\mu}{\sigma}\right)^2\right] \qquad -\infty < x < \infty$$

Where,
μ=mean of the variate
σ=standard deviation of the variate

The CDF is then given as the integral of the PDF and is commonly referred to as $F_X(x)$. The CDF, $F_X(x)$, is given as:

$$F_X(x) = \frac{1}{\sigma\sqrt{2\pi}} \int_{-\infty}^{x} exp\left[-\frac{1}{2}\left(\frac{x-\mu}{\sigma}\right)^2\right] dx$$

Where,
$F_X(x)$=the probablity that $-\infty < X \leq x$
μ=mean of the variate X
σ=standard deviation of the variate X

For the standard normal distribution, denoted as N(0,1), the CDF is commonly noted as $F_S(s) = \Phi(s)$. And the value of a standard normal variate at a cumulative probability, *p*, is $\Phi^{-1}(s)$. $\Phi(s)$ and $\Phi^{-1}(s)$ are commonly tabulated. With the use of the table of $\Phi(s)$, probabilities can be easily determined for any normal distribution by substituting:

$$s = \left(\frac{x-\mu}{\sigma}\right)$$

As described above for a standard normal variate, for a given probability, any normal variate can be determined using:

$$\left(\frac{x-\mu}{\sigma}\right) = \Phi^{-1}(x)$$

Therefore, for any given probability, $\Phi(x)$, the value of x can by calculated. A random number generator is used to generate the probability $\Phi(x)$ for which a given value for the random variate X is calculated using $\Phi^{-1}(x)$. Therefore, if *p* is a random probability, $\Phi(x)$, the value of the random variate is calculated as:

$$P(-\infty < X \le x) = p$$
$$p = \Phi(x)$$
$$\Phi^{-1}(p) = x$$

Since the CDF is tabulated for the standard normal distribution,

$$x = \sigma s + \mu$$

Where,
p= probability that $-\infty < X \le x$, and is randomly generated
μ=mean of the variate X
σ=standard deviation of the variate X

The use of this for the MCS is illustrated in Appendix F.

For lognormal distribution, the PDF is given as:

$$f_X(x) = \frac{1}{\sigma\sqrt{2\pi}\zeta x}\exp\left[-\frac{1}{2}\left(\frac{\ln x - \lambda}{\zeta}\right)^2\right] \qquad 0 \le x < \infty$$

Where,

$$\lambda = E(\ln X)$$
$$\zeta = \sqrt{Var(\ln X)}$$

The parameters λ and ζ are related to the mean μ and the standard deviation σ of the variate as (Ang and Tang, 1975):

$$\lambda = \ln \mu - \frac{1}{2}\zeta^2$$
$$\zeta^2 = \ln\left(1 + \frac{\sigma^2}{\mu^2}\right)$$

If σ/μ is ≤ 0.30, then,

$$\zeta \approx \frac{\sigma}{\mu}$$

The CDF is then given as the integral of the PDF and is given as:

$$P(a < X \le b) = \frac{1}{\sigma\sqrt{2\pi}\zeta x}\int_a^b \exp\left[-\frac{1}{2}\left(\frac{\ln x - \lambda}{\zeta}\right)^2\right]dx$$

Where,
P=the probability that X is between a and b
λ=mean of the lognormal of the variate X
ζ=standard deviation of the lognormal of the variate X

The lognormal distribution of a random variable X is a normal distribution of the natural logarithm of X. Therefore, the commonly tabulated values of $\Phi(s)$ and $\Phi^{-1}(s)$ for standard normal distribution can be used similarly to the description earlier where:

$$s = \left(\frac{\ln x - \lambda}{\zeta}\right)$$

And also similar to the explanation above for normal distribution, for a given probability, the normal variate can be determined using:

$$\left(\frac{ln\, x - \lambda}{\zeta}\right) = \Phi^{-1}(x)$$

Therefore, for any given probability, $\Phi(x)$, the value of x can by calculated. A random number generator is used to generate the probability $\Phi(x)$ for which a given value for the random variate X is calculated using $\Phi^{-1}(x)$. Therefore, if *p* is a random probability, $\Phi(x)$, the value of the random variate is calculated as:

$P(-\infty < X \le x) = p$

$p = \Phi(x)$

$\Phi^{-1}(p) = x$

Since the CDF is tabulated for the standard normal distribution,

$x = exp\left(\Phi^{-1}(x)\zeta + \lambda\right)$

Where,
p= probability that $-\infty < X \le x$, and is randomly generated
λ=mean of the lognormal of the variate X
ζ=standard deviation of the lognormal of the variate X

The use of this for the MCS is illustrated in Appendix F.

For the Gumbel Type I distribution, the CDF is given as Eq. 9 and is repeated here:

$$F_{X_n}(x) = exp[-exp(-\alpha(x-u_n))] \qquad -\infty < x < \infty \qquad \textbf{Eq. 9}$$

Where,
u_n = location parameter
α_n = scale parameter

The location and scale parameters are related to the mean and standard deviation of the random variable X as:

$$\alpha_n = \frac{\pi}{\sigma_x\sqrt{6}}$$

$$u_n = \mu_x - \frac{\gamma}{\alpha_n}$$

Where,
α_n = scale parameter
u_n = location parameter
σ_x = standard deviation of random variable X
μ_x = mean of random variable X
γ = Euler's Constant = 0.577216

Since the CDF is given directly in Eq. 9, the probability that $-\infty < X \leq x$ is $F_{X_n}(x)$. Eq. 9 can be rearranged, Eq. 24, to solve for the value of x at a random probability:

$$x = u_n - \frac{1}{\alpha_n} ln\left[- ln\left(F_{X_n}(x)\right)\right] \qquad \textbf{Eq. 24}$$

Where,
u_n = location parameter
α_n = scale parameter
$F_{X_n}(x)$ = probability of X_n, and is randomly generated

The use of this for the MCS is illustrated in Appendix F.

5.4.7 Results of the Monte Carlo Simulation for ASD

The results of the MCS for the ASD load combination 0.6D+W are summarized in Table 33 for wall Groups A, B, C, D, E, and SDPWS. The values for A, E, and SDPWS are from the FOSM analysis summarized in Table 31. For these walls, the restraining force was not the limit state of failure and was not modeled in the MCS. The ASD load combination will assure there is enough dead load for these conditions.

Table 33 summarizes the restraining force, the average unit shear capacity from the test results and SDPWS, the bias factor from the calibration, and the resulting nominal unit shear capacity. The nominal unit shear capacity was then normalized to the SDPWS nominal unit shear capacity. Similarly, the ratio of the restraining force to the SDPWS restraining force was also tabulated to achieve the nominal unit shear capacity.

Table 33: Summary of MCS for ASD without Specific Gravity

Calibrated Wall Values						
Wall	A	B	C	D	E	SDPWS
Restraint, $\gamma_D P_D$	4416	1104	2208	3312	0	5051
Ultimate Unit Shear Capacity (from tests), plf						
	555	345	496	615	162	786
Bias Factor, a_2						
	1.150	0.944	0.941	1.001	1.280	1.245
Nominal Unit Shear Capacity, plf						
	483	364	527	615	127	631
Normalized						
$P_{hold\ down}$, λ'^{1}	0.874	0.219	0.437	0.656	0.000	1.000
V_{cap}(%)	0.764	0.577	0.834	0.974	0.200	1.000

$$^{1}\lambda' = \frac{\gamma_D P_D}{P_{n-SDPWS}} = \frac{\gamma_D P_D}{V_n C_G h}$$

Just as before, a wall restrained with a hold down (wall A) only has a nominal unit shear capacity equal to 76% of a fully restrained wall. Wall E has a nominal unit shear capacity equal to 20% of a fully restrained wall. A curve was fit to the normalized results of Table 33 (zunzun.com) to create a function for the partial restraint factor $C_{pr\text{-}n}$. The equation that best fit is the Bleasdale-Nelder with offset, Eq. 25. The R^2 value is 1.0 for this equation. The specific equation that fits Table 33 is shown in Eq. 26 and is applicable for values of $0 < \lambda' \leq 1$. The normalized results of Table 33, Eq. 26, and the test results, from Graph 12, are shown graphically in Graph 31.

$$y = (a + bx^c)^{-1/d} + \text{Offset} \qquad \textbf{Eq. 25}$$

Partial Restraint Factor for $0 \le \lambda' \le 1$,

$$C_{pr-n} = (9.491 + 0.153\lambda'^{-7.738})^{-1/10.129} + 0.200 \qquad \textbf{Eq. 26}$$

For $\lambda'=0$,

$C_{pn\text{-}n} = 0.20$

For $\lambda'>1$,

$C_{pn\text{-}n} = 1.0$

As expected, the partial restraint function is shifted up and to the left of the actual test result relationship. This is due to the ASD load combination requiring the use of only 60% of the applied dead load restraining force. In other words, the actual restraining force on the shear wall with this load combination is 167% of the factored load, $\gamma_D P_D$.

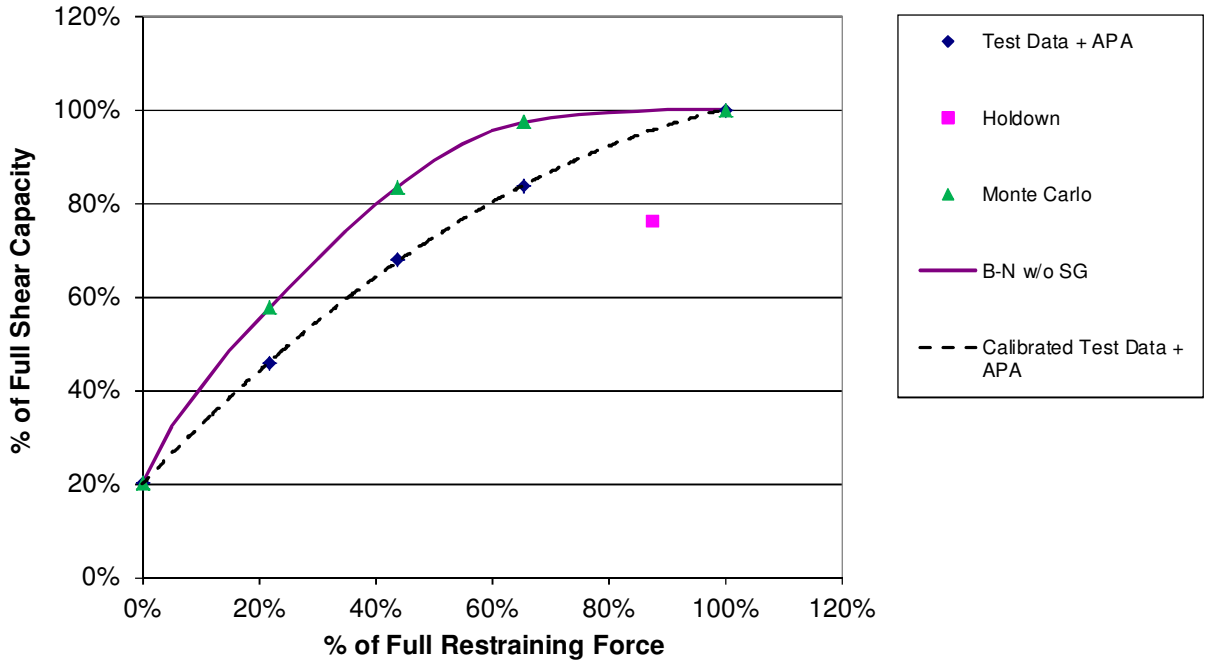

Graph 31: Partial Restraint Effect, ASD, without Specific Gravity

5.4.8 Calibration with a Variation in the Specific Gravity

Next, the calibration was performed considering the specific gravity of the framing lumber as a random variable, G. Specific gravity is also a random variable as discussed earlier. The MCS was performed as previously explained for Sections 5.4.2 through 5.4.6 with the added random variable for specific gravity, G. Table 34 summarizes the random variables and their distributions.

Table 34: Summary of Distributions

Random Variable	Item	$\overline{X}/X_n$	δ_x (cov)	DF
P_D	Dead Load	1.05	0.1	Normal
V_W	Wind Load	0.8	0.35	Type 1
G	Specific Gravity, G	1.0	0.1[1]	Lognormal[2]
V	Shear Wall Capacity	Unknown	0.12[3]	Lognormal[4]

[1]From ASTM D 2555
[2]From specific gravity test of lumber from samples
[3]From Table 28
[4]From Test Results

The distribution parameters for specific gravity were modified for the number of framing members. Since the framing members are all fastened together with nails to a single WSP, the specific gravity for the system can be the average for the framing members.

Therefore,

$$\overline{G} = \frac{1}{n}\sum_{i=1}^{n} G_i \qquad \textbf{Eq. 27}$$

The average value, Eq. 27, for the specific gravity for the same species of lumber, is simply the published value for the species.

Assuming G_1 through G_n are statistically independent and from the same population, the variance is (Ang and Tang 1975):

$$\mathrm{Var}(\overline{G}) = \frac{1}{n^2}\mathrm{Var}\left(\frac{1}{n}\sum_{i=1}^{n} G_i\right)$$

$$\mathrm{Var}(\overline{G}) = \frac{1}{n^2}\left(n\sigma^2\right) = \frac{\sigma^2}{n} \qquad \textbf{Eq. 28}$$

Therefore, from Eq. 28, the standard deviation for the random variable G, is equal to $\sigma/\sqrt{n}$, where σ is the standard deviation of the samples. Using Eq. 28, the coefficient of variation, δ, of random variable G can be calculated as $\delta_G = \delta/\sqrt{n}$, where δ is the coefficient of variation of the samples. Using this principle, the coefficient of variation for the wall assembly is adjusted as a weighted value. Recalling that for the test samples, the two sole and top plates are nominally half the length of the four wall studs, the weighted coefficient of variation is calculated as shown:

$$\delta = \frac{\sigma_G}{\overline{G}} = \frac{0.1}{\sqrt{4 + 2\left(1/2\right)}} = 0.045$$

Therefore, the coefficient of variation for random variable G is 0.045. For the MCS, the coefficient of variation, 0.045, is used instead of 0.1 as indicated in Table 34.

5.4.9 Results of the Monte Carlo Simulation for ASD

As before, without the random variable G in the MCS, the results of the MCS for the ASD load combination 0.6D+W are summarized in Table 35 for walls A, B, C, D, E and SDPWS. For this simulation, all of the unit shear values were calibrated considering the addition of the random variable G.

Table 35 summarizes the results as explained in Section 5.4.7 for Table 33.

Table 35: Summary of MCS for ASD with Specific Gravity

Calibrated Wall Values						
Wall	A	B	C	D	E	SDPWS
Restraint, $\gamma_D P_D$	4416	1104	2208	3312	0	5051
Ultimate Unit Shear Capacity (from tests), plf						
	555	345	496	615	162	786
Bias Factor, a_2						
	1.150	0.947	0.944	1.003	1.245	1.248
Nominal Unit Shear Capacity, plf						
	483	363	524	613	130	629
Normalized						
$P_{hold\ down}$, λ'[1]	0.877	0.219	0.439	0.658	0.000	1.000
V_{cap}(%)	0.767	0.577	0.833	0.974	0.207	1.000

[1] $\lambda' = \frac{\gamma_D P_D}{P_{n-SDPWS}} = \frac{\gamma_D P_D}{V_n C_G h}$

Just as before, a wall restrained with a hold down (wall A) only has a nominal unit shear capacity equal to 76% of a fully restrained wall. Wall E has a nominal unit shear capacity equal to 21% of a fully restrained wall. A curve was fit to the normalized results of Table 35 (zunzun.com) to create a function for the partial restraint factor $C_{pr\text{-}n}$. The equation that best fit is the Bleasdale-Nelder with offset, Eq. 25. The specific equation that fits Table 35 is shown in Eq. 29 and is applicable for values of $0<\lambda'\leq 1$. The R^2 value is 1.0 for this equation. The normalized results of Table 35, Eq. 26, and the test results, from Graph 12, are shown graphically in Graph 32.

Partial Restraint Factor for $0 < \lambda' \leq 1$,

$$C_{pr-n} = (10.642 + 0.163\lambda'^{-7.925})^{-1/10.288} + 0.207 \qquad \textbf{Eq. 29}$$

For $\lambda'=0$,

$C_{pn\text{-}n} = 0.21$

For $\lambda'>1$,

$C_{pn\text{-}n} = 1.0$

As expected, the partial restraint function is shifted up and to the left of the actual test result relationship. This is due to the ASD load combination requiring the use of only 60% of the applied dead load restraining force. In other words, the actual restraining force on the shear wall with this load combination is 167% of the factored load, $\gamma_D P_D$.

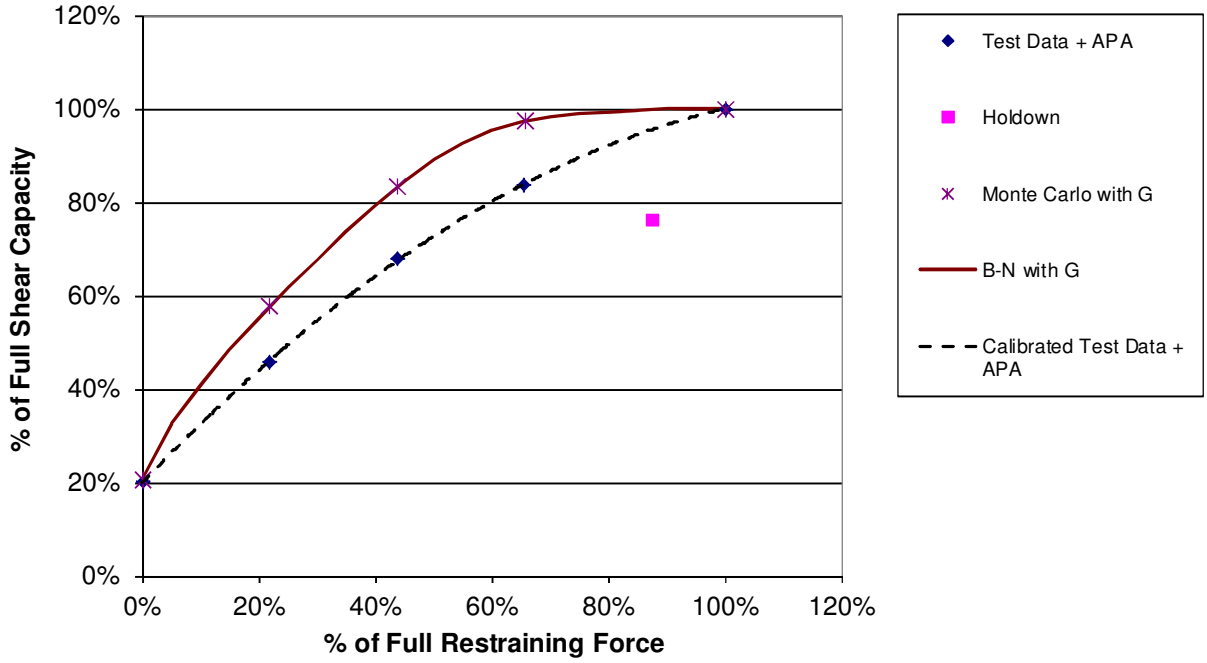

Graph 32: Partial Restraint Effect, ASD, with Specific Gravity

5.4.10 Results of the Monte Carlo Simulation for LRFD

The procedures explained for the MCS for ASD were repeated for LRFD. Since the resistance factor, ϕ=0.8, is already utilized by SDPWS, the bias factor was adjusted to calibrate the partial restraint factor for the LRFD strength values. The results of the MCS for the LRFD load combination 0.9D+1.6W are summarized in Table 36 for walls A, B, C, D, E, and SDPWS. The values for A, E, and SDPWS are from the FOSM

analysis summarized in Table 31. For these walls, the restraining force was not the limit state of failure and was not modeled in the MCS.

Table 36: Summary of MCS for LRFD without Specific Gravity

Calibrated Wall Values						
Wall	A	B	C	D	E	SDPWS
Restraint, $\gamma_D P_D$	4416	1104	2208	3312	0	5051
Ultimate Unit Shear Capacity (from tests), plf						
	555	345	496	615	162	786
Bias Factor, a_2						
	1.150	1.167	1.166	1.170	1.280	1.245
Nominal Unit Shear Capacity, plf						
	483	295	425	527	127	631
Normalized						
$P_{hold\ down}$, λ'^{1}	0.874	0.219	0.437	0.656	0.000	1.000
V_{cap}(%)	0.764	0.467	0.673	0.834	0.200	1.000

$$^{1}\lambda' = \frac{\gamma_D P_D}{P_{n-SDPWS}} = \frac{\gamma_D P_D}{V_n C_G h}$$

Just as before, a wall restrained with a hold down (wall Group A) only has a nominal unit shear capacity equal to 76% of a fully restrained wall. Wall E has a nominal unit shear capacity equal to 20% of a fully restrained wall. A curve was fit to the normalized results of Table 36 (zunzun.com) to create a function for the partial restraint factor $C_{pr\text{-}n}$. The equation that best fit is the Bleasdale-Nelder with offset, Eq. 25. The R^2 value is 1.0 for this equation. The specific equation that fits Table 36 is

Partial Restraint Factor for $0 < \lambda' \leq 1$,

$$C_{pr-n} = (0.950 + 0.969\lambda'^{-2.539})^{-1/2.911} + 0.200 \qquad \textbf{Eq. 30}$$

For $\lambda'=0$,

$$C_{pn\text{-}n} = 0.20$$

For $\lambda'>1$,

$$C_{pn\text{-}n} = 1.0$$

shown in Eq. 30 and is applicable for values of $0 < \lambda' \leq 1$. The normalized results of Table 36 and Eq. 30 are shown graphically in Graph 33.

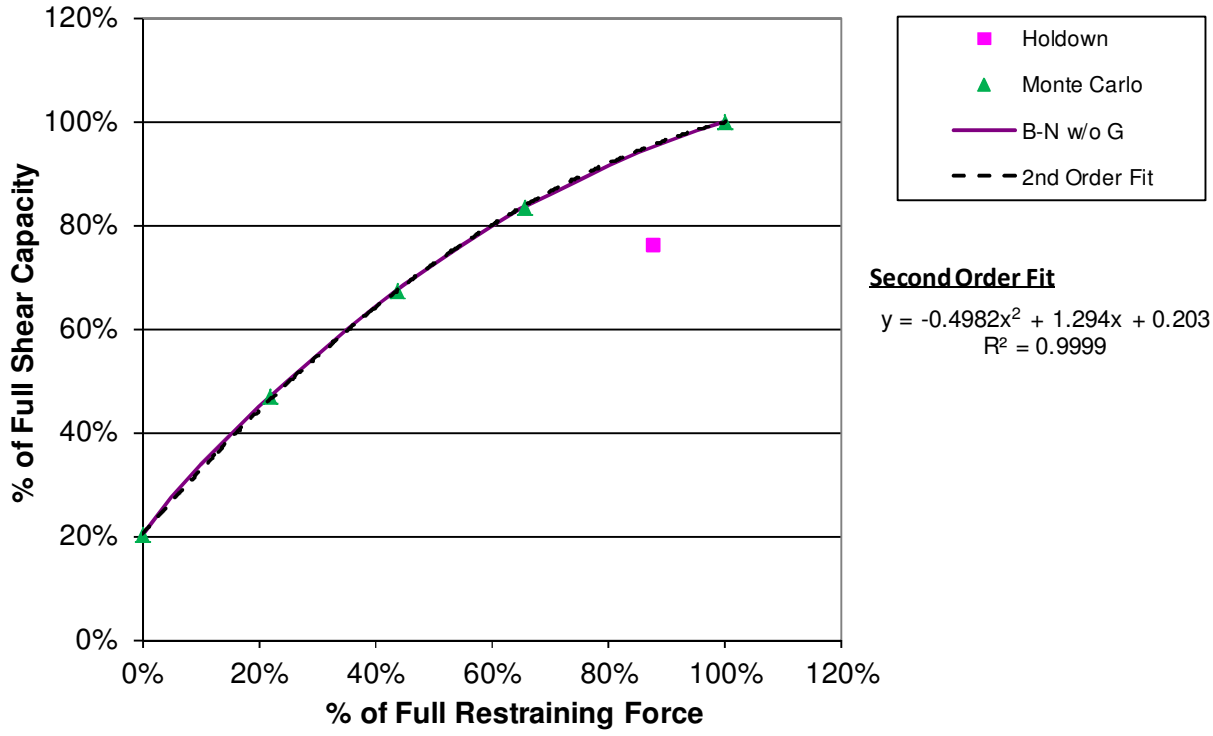

Graph 33: Partial Restraint Effect, LRFD, without Specific Gravity

Although not directly comparable, the partial restraint function utilizing Eq. 30 is extremely close to the partial restraint function shown as the second order fit equation in Graph 29. This is due to the LRFD load combination requiring the use of only 90% of the applied dead load restraining force. An additional second order curve was fit for comparison to the B-N fit. The resulting curve has an R^2 value of 0.9999. The equation for the second order curve is simpler than that of the B-N curve and is presented in Eq. 31.

Partial Restraint Factor for $0 \le \lambda' \le 1$,

$$C_{pr-n} = -0.498\lambda'^2 + 1.294\lambda + 0.203 \qquad \textbf{Eq. 31}$$

For $\lambda'=0$,

$C_{pn\text{-}n} = 0.20$

For $\lambda' \ge 1$,

$C_{pn\text{-}n} = 1.0$

5.4.11 Calibration with a Variation in the Specific Gravity

Next, the calibration was performed considering the specific gravity of the framing lumber as a random variable, G. This is the same as explained in section 5.4.8, but using LRFD.

5.4.12 Results of the Monte Carlo Simulation for LRFD

As with the previous simulation, without the random variable G, the results of the MCS for the LRFD load combination 0.9D+1.6W are summarized in Table 37 for walls A, B, C, D, E and SDPWS. For this simulation, all of the unit shear values were calibrated considering the addition of the random variable G.

Table 37 summarizes the results as explained in Section 5.4.10.

Almost identical to the previous simulation, a wall restrained with a hold down (wall Group A) only has a nominal unit shear capacity equal to 77% of a fully restrained wall. Wall E has a nominal unit shear capacity equal to 21% of a fully restrained wall. A curve was fit to the normalized results of Table 37 (zunzun.com) to create a function for the partial restraint factor $C_{pr\text{-}n}$. The equation that best fit was the Bleasdale-Nelder with offset, Eq. 25. The R^2 value is 1.0 for this equation. The specific equation that fits Table

37 is shown in Eq. 32 and is applicable for values of $0 < \lambda' \leq 1$. The normalized results of Table 37 and Eq. 32 are shown in Graph 34.

Table 37: Summary of MCS for LRFD with Specific Gravity

Calibrated Wall Values						
Wall	A	B	C	D	E	SDPWS
Restraint, $\gamma_D P_D$	4416	1104	2208	3312	0	5051
Ultimate Unit Shear Capacity (from tests), plf						
	555	345	496	615	162	786
Bias Factor, a_2						
	1.150	0.947	0.944	1.003	1.245	1.248
Nominal Unit Shear Capacity, plf						
	483	294	424	525	130	629
Normalized						
$P_{hold\ down}$, λ'^{1}	0.877	0.219	0.439	0.658	0.000	1.000
V_{cap}(%)	0.767	0.467	0.674	0.834	0.206	1.000

[1] $\lambda' = \dfrac{\gamma_D P_D}{P_{n-SDPWS}} = \dfrac{\gamma_D P_D}{V_n C_G h}$

Partial Restraint Factor for $0 < \lambda' \leq 1$,

$$C_{pr-n} = (0.826 + 0.830\lambda'^{-2.028})^{-1/2.188} + 0.207 \qquad \textbf{Eq. 32}$$

For $\lambda'=0$,

$C_{pn\text{-}n} = 0.21$

For $\lambda'>1$,

$C_{pn\text{-}n} = 1.0$

The results are only slightly different from the curve shown in Graph 33 without the added random variable, G. An additional second order curve was fit for comparison to the B-N fit. The resulting curve has an R^2 value of 0.9999. The equation for the second order curve is simpler than that of the B-N curve and is presented in Eq. 33.

Since the LRFD calibration curve shown in Graph 34 resembles the actual behavior of the actual test walls and since Eq. 33 is simpler than Eq. 32, LRFD is the preferred method for design. The partial restraint factor in LRFD will make more sense to the building designer. The calculation of the partial restraint factor is also easier for the building designer.

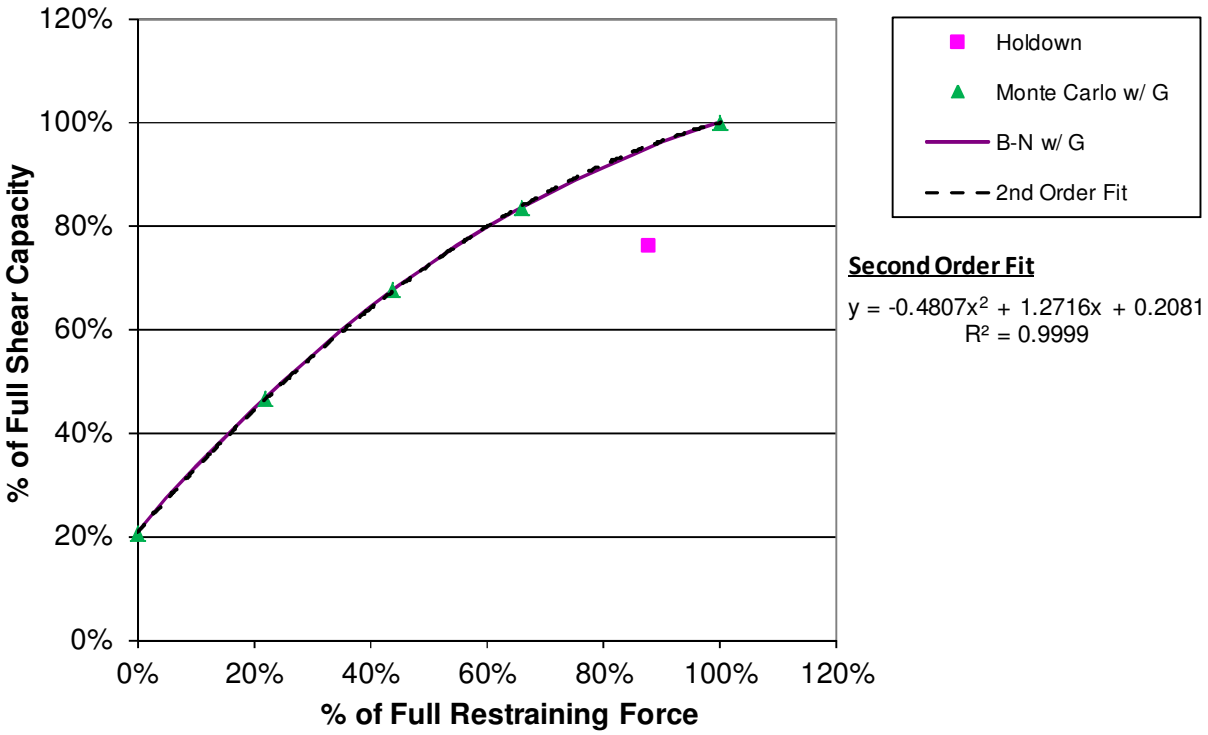

Graph 34: Partial Restraint Effect, LRFD, with Specific Gravity

Partial Restraint Factor for $0 \le \lambda' \le 1$,

$$C_{pr-n} = -0.481\lambda'^2 + 1.272\lambda + 0.208 \qquad \textbf{Eq. 33}$$

For $\lambda' > 1$,

$$C_{pn-n} = 1.0$$

CHAPTER 6

DISCUSSION OF NOMINAL UNIT SHEAR VALUES

This chapter addresses some of the conflicts that exist with current methods of determining unit shear values for wood structural panels. These conflicts directly relate to the capacity of a partially restrained shear wall as prescribed in the IRC (2009).

6.1 Difference in Method to Determine Unit Shear Values

6.1.1 SDPWS Values for Anchoring Device

The SDPWS (2005) unit shear values, based on *APA Research Report 154* (APA 2004) cannot be achieved with a conventional mechanical hold down only. The values are reportedly based upon ASTM E72. The test frame from ASTM E72 is shown in Figure 22. The clamping action of the test fixture is not equivalent to applying a conventional hold down on the tension stud as explained earlier.

APA Research Report 154 (APA 2004) indicates that a timber was used over the top of the wall and a double tie rod hold down was used to restrain the tension side of the wall. The double tie rod system over the top of the wall provides a clamping force keeping the wall plates in contact with the wall stud. This action keeps the plates and stud from separating, thus reducing the force on the corner nails at the tension side. Additionally, the second stud at each end adds additional strength and stiffness even though the sheathing is not directly attached to it.

The conventional mechanical hold down attached to the tension stud does not offer the same restraint as the clamping mechanism required by ASTM E72. The elongation of the mechanical hold down allows the tension stud to separate from the

bottom plate and there is nothing to keep the top plate from separating from the tension stud unless additional building framing exists. The result is the capacity of the wall is reduced. This was observed in the test specimens and was also observed in the FE model.

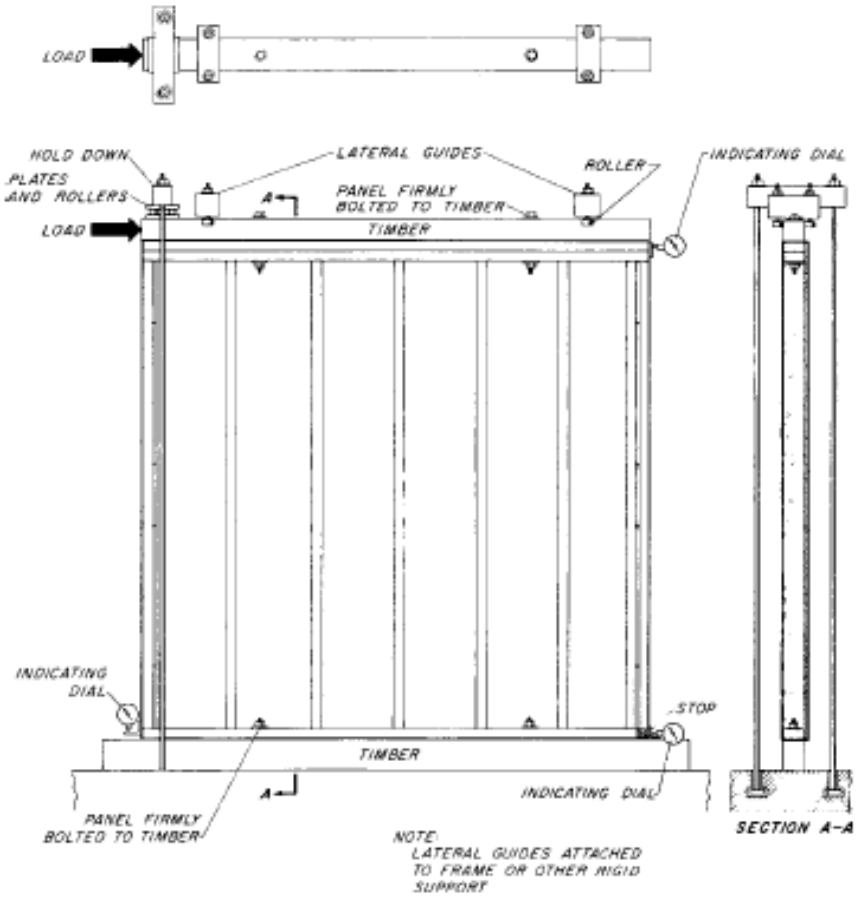

Reprinted, with permission, from ASTM E72-10 *Standard Test Methods of Conducting Strength Tests of Panels for Building Construction*, copyright ASTM International, 100 Barr Harbor Drive, West Conshohocken, PA 49428.

Figure 22: ASTM E72 Test Fixture

SDPWS (2005) requires either a dead load stabilizing moment or an anchoring device at the end of the shear wall. No difference is given to either restraining device. There is a difference between the two; the resulting unit shear strength based on the test results shown in Table 12 with an anchoring device is 13% less or 87% of the

tabulated nominal unit shear value published in SDPWS (2005). Therefore, SDPWS (2005) should at least provide an anchoring device factor, C_a, as given in Eq. 34. This value should not be confused with the value determined in Chapter 5 which was calibrated for design. The latter is preferred since it was calibrated to ASCE 7-05 and the IBC (2009) load combinations to provide a reliability index, β, of 3.25.

$$C_a = 0.87 \qquad \textbf{Eq. 34}$$

6.1.2 Use of ASTM E72

One of the intentions of ASTM E72 is to provide a test method and a test frame that can be used to compare different sheathing materials for use as shear walls to resist lateral forces, such as wind loads. The standard states that it intends to function as a shear wall that would typically be used in a building. The purpose of the standard is to provide a relative comparison of sheathing materials.

While the stated intent of the standard is good and useful, the standard does not capture the behavior of partially restrained shear walls that are prescribed in the 2009 IRC. It has been explained earlier that there is a large difference between a fully restrained shear wall and a wall only restrained in accordance with the 2009 IRC. These differences are not tested and the resulting behavior is not captured in ASTM E72.

Due to the increased forces in the corner nails in a partially restrained shear wall, as well as shear walls having no dead load along the top of the wall restrained with a hold down, wall sheathing intended as shear wall material should be tested to capture

this behavior. This will provide a relative comparison of different materials. The behavior of the sheathing material at the edges can be crucial to the strength of the wall and in fact was the focus of the research conducted by Cassidy (2002).

ASTM E72 recognizes that a prestress force can greatly influence the results of the racking test and restricts the prestress in the hold down rods to 20 lb. However, there is no requirement to report the initial hold down force or the hold down force throughout the test. Reporting of this data should be made so that the entire test method to determine the resulting unit shear values is completely transparent if these values will be used in design standards. This too will allow for a comparison of different sheathing materials.

6.1.3 Use of ASTM E564

ASTM E564 states that its use is not intended for classifying sheathing shear capacity. Thus, to this author's knowledge, it is not used in the design standards. In contrast to ASTM E72, ASTM E564 allows for walls to be constructed in dimensions intended for use and with the boundary conditions and restraining forces of the intended use. This results in data that reflects the actual construction of the wall and doesn't attempt to only make a relative comparison of sheathing material shear capacity as ASTM E72 does.

Since the failure of wood shear walls is highly dependent on the capacity and response of the fasteners as well as the initial boundary conditions, it makes sense to use ASTM E564 for codified design standards for partially restrained wood shear walls. This standard was used as the basis of the testing for this thesis as well. This would

also provide a relative comparison of sheathing material performance where edge breakout or failure is the limit state.

6.1.4 Partial Restraint Factors

It is obvious that the peak capacity of wood shear walls in a fully restrained condition is greater than the peak capacity of a wood shear wall with a mechanical hold down at the base of the wall. Therefore, when a wall is partially restrained from the top, the partially restrained capacity must be a function of the fully restrained condition (i.e. the APA Research Report 154 ultimate capacity) rather than the nominal (SDPWS – unless it is calibrated) capacity, or the mechanical hold down restrained capacity. This is best shown in Graph 35 where the partial restraint effect from this research is compared with Ni and Karacabeyli's (2000).

As explained earlier in Chapter 2, Ni and Karacabeyli (2000) assumed that a wall with a mechanical hold down at the base of the wall was fully restrained. As shown in Graph 35, there is a noticeable difference when using this assumption. The light scale represents Ni and Karacabeyli's (2000) partial restraint factor and partial restraint force. Their curve was scaled to the hold down capacity from this research to make the comparison.

Another problem with using the unit shear capacity developed with a mechanical hold down as the fully restrained unit shear capacity is that this capacity is unknown unless testing is conducted or unless a partial restraint factor for a mechanical hold down is used as proposed in this research. Therefore, a correlation must always be made to between the unit shear capacity with a mechanical hold down and the nominal value in SDPWS (2005).

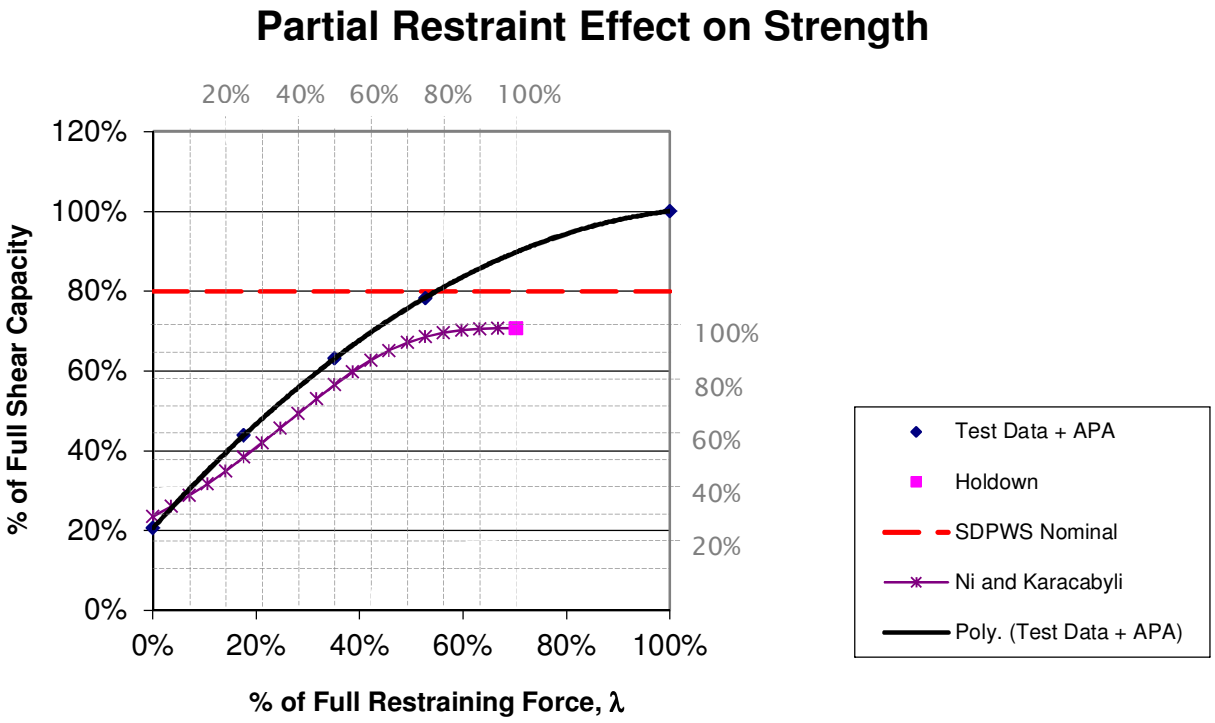

Graph 35: Comparison of Partial Restraint

CHAPTER 7

SUMMARY, CONCLUSION, AND RECOMMENDATIONS FOR FUTURE RESEARCH

7.1 Summary

The unit shear capacity of partially restrained WSP shear walls constructed in accordance with the 2009 IRC was studied in this thesis. A nonlinear finite element model was developed to understand and describe the behavior of these walls. Additionally, as a focus of this thesis, a reliability analysis was conducted to develop modification factors to fully restrained unit shear capacities. These modification factors were calibrated to provide a uniform reliability index of 3.25.

7.2 Conclusions

The following conclusions are made from this research effort:

1. The SDPWS (2005) nominal unit shear capacity, 730 plf, for $^{15}/_{32}$" WSP with 8d common nails at 6" o.c. at the perimeter and 12" o.c. at the intermediate members provides a reliability index, β=3.25, for wind load using the ASD reduction factor of 2 per SDPWS (2005) and using the LRFD resistance factor of 0.8. This was used as the target reliability index for the calibration.
2. The derivation of design values for use in SDPWS with ASTM E72 is not appropriate for walls anchored with mechanical hold downs or partially restrained IRC (2009) prescriptive walls. The ASTM E72 test frame provides a clamping action not present in partially restrained shear walls. ASTM E564 is appropriate for shear walls with these types of restraint.

3. ASTM E72 should add a requirement to record the initial and resulting hold down force for a racking test. Though it has a limit of a maximum 20 lb of initial hold down force, it does not have to be measured for the test.
4. The SDPWS (2005) nominal unit shear capacities, based on *APA Research Report 154* (APA 2004), cannot be achieved with a conventional mechanical hold down at the base of the wall for a 4' x 8' WSP shear wall.
5. For the ASD design methodology, partially restrained shear walls have an allowable nominal unit shear capacity to resist wind load, V'_n, as shown in Eq. 35. This is applicable to 4' x 8' WSP shear walls constructed in accordance with the IRC (2009) using a mechanical hold down device (i.e. Simpson HUD14) at the base of the wall.

$$V_n' = \frac{V_n C_a C_G}{C_{ASD}} \qquad \textbf{Eq. 35}$$

Where,

V_n = nominal unit shear capacity per SDPWS (2005)
C_a = anchor reduction factor
C_a = 0.77
C_G = 1-(0.5-G)
G = specific gravity of the framing lumber
C_{ASD} = 2

6. For the ASD design methodology, wood shear walls partially restrained by a dead load restraining force, P, have a nominal unit shear capacity to resist wind load, V'_n, as shown in Eq. 36. The controlling IBC (2009) load combination is 0.6D+W. This is applicable to 4' x 8' WSP shear walls constructed in accordance with the IRC (2009).

$$V_n' = \frac{V_n C_{pr} C_G}{C_{ASD}} \qquad \textbf{Eq. 36}$$

Where,

V_n = nominal unit shear capacity per SDPWS (2005)

$C_{pr} = (10.642 + 0.163 C_p^{-7.925})^{-0.097} + 0.207$

C_G = 1-(0.5-G)

G = specific gravity of the framing lumber

$C_p = \frac{P}{V_n C_G h}; 0 < C_p \leq 1.0$

$C_p = 0.207; C_p = 0$

$C_p = 1.0; C_p \geq 1.0$

h = height of shear wall

P = $0.6P_D$ [per IBC (2009)] (restraining force)

C_{ASD} = 2

7. For the LRFD design methodology, partially restrained shear walls have an allowable nominal unit shear capacity to resist wind load, $\phi V'_n$, as shown in Eq. 37. This is applicable to 4' x 8' WSP shear walls constructed in accordance with the IRC (2009) using a mechanical hold down device (i.e. Simpson HDU14) at the base of the wall.

$$\phi V_n' = \phi V_n C_a C_G \qquad \textbf{Eq. 37}$$

Where,

ϕ = strength reduction factor

ϕ = 0.8

V_n = nominal unit shear capacity per SDPWS (2005)

C_a = anchor reduction factor

C_a = 0.77

C_G = 1-(0.5-G)

G = specific gravity of the framing lumber

8. For the LRFD design methodology, wood shear walls partially restrained by a dead load restraining force, P, the nominal unit shear capacity, $\phi V'_n$, as shown in Eq. 38. The controlling IBC (2009) load combination is

0.9D + 1.6W. This is applicable to 4' x 8' WSP shear walls constructed in accordance with the IRC (2009).

$$\phi V_n' = \phi V_n C_{pr} C_G \qquad \textbf{Eq. 38}$$

Where,

ϕ = strength reduction factor
$\phi = 0.8$
V_n = nominal unit shear capacity per SDPWS (2005)
$C_{pr} = -0.481C_p^2 + 1.272C_p + 0.208$
C_G = 1-(0.5-G)
G = specific gravity of the framing lumber
$C_p = \frac{P}{V_n C_G h}; 0 < C_p \leq 1.0$
$C_p = 0.208; C_p = 0$
$C_p = 1.0; C_p \geq 1.0$
h = height of shear wall
$P = 0.9P_D$ [per IBC (2009)] (restraining force)

9. The curve generated by the partial restraint factor, C_{pr}, in Eq. 38 (LRFD method) more accurately emulates the actual shear wall behavior than the same factor in Eq. 36 (ASD method). The ASD controlling load combination creates a shift in the curve of the partial restraint factor due to use of only 60% of the dead load restraining force.
10. The IRC (2009) assumption that shear walls are partially restrained requires a dead load force applied to the top of the shear wall at the tension side as indicated in Table 38.

Table 38: Design Restraining Force for IRC Shear Wall

Wall Supporting	IRC Partial-Restraint Factor	Dead Load Required (lb)[1]
Roof Only	0.8	2,786
Roof + One Story	0.9	3,512
Roof + Two Stories	1.0	6,867

[1]Based on $^3/_8$" WSP per IRC with SPF Framing, G=0.42

11. The clamping force in shear walls constrained from the top with either external mechanical methods or dead loads allows a substantial horizontal load to transfer through the studs to the plate (220 plf for this research). For this reason, the nails in the vertical end studs always failed first for these types of shear walls. This behavior is not realized without the clamping action.
12. Finite element analysis should model the behavior of wood shear walls. It should always include the effect of the boundary conditions and should model the connection behavior of the studs to the plates. The separation of the studs from the plate can greatly reduce the unit shear capacity of the wall.

7.3 Recommendations for Future Research

Future research could extend in a number of directions. Since the coefficient of variation for wind load is so large, this is an area that could use further research. Additional research could be conducted on the effect of wall length on partially restrained walls. This could be included as a parameter to the partial restraint modification factor if it is found to be significant. Finite element modeling could be improved with further research on connections within the shear wall. Particularly the interaction of nail withdrawal and shear resistance of the framing nails. Upon improving the connection behavior in FEM, comparisons of whole building tests utilizing partial restraints can be made and the FEM can be further calibrated.

APPENDIX A

WALL TESTS

A1 Wall Testing

This appendix details further the testing procedure conducted for the 25 wood shear wall tests.

A2 Wall Materials

The material was delivered to the lab on March 11, 2011. The following material was received and inventoried:

Table 39: Lumber Materials

Quantity	Description
100	2x4x92 5/8" SPF NSLB[1] Stud Grade Precut Studs
25	2x4x14' SPF NLGA[2] No. 2 Plate Material
25	32/16 APA Rated Sheathing, ½" Category Oriented Strand Board (OSB), t_{min}=0.483"

[1]National Lumber Softwood Bureau; SPF South, G=0.36
[2]National Lumber Grades Authority; SPF North, G=0.42

Photo 2, Photo 3, Photo 4 and Photo 5 show the stamps recorded from the material.

The 2x4x14' plate material was cut into three pieces each 49½" long for the wall plates. The groups of three plates were maintained such that all three plates from the same 14' board were used in one wall. During the cutting procedure, the 16" o.c. stud locations were marked. After cutting all of the plates, a ¾" diameter hole was drilled in each bottom plate, five at 3" from one end and twenty 12" from one end. The former

Photo 2: Wall Stud

Photo 3: Wall Plate

Photo 4: OSB Sheathing

Photo 5: OSB Sheathing

Photo 6: Digital Scale for OSB

Photo 7: Digital Scale Monitor

Photo 8: Thickness of OSB

was for the Group A walls with the hold down while the latter was for the $^{5}/_{8}$" diameter anchor bolt for Groups B to E.

The OSB sheathing was further inventoried by weighing each piece, measuring the thickness of each side of each piece, marking the wall number, marking the nail locations, and performing an out-of-plane stiffness test on each piece. Each sheet was

Photo 9: Wall Identification

Photo 10: Nail Layout

carefully weighed with a Pelouze Model 4010 digital scale to one-tenth of a pound, Photo 6 and Photo 7 recorded. The thickness of each side of each sheet was measured with a dial caliper to 0.001" along with two pieces of $^{3}/_{8}$" x $^{5}/_{8}$" x 4" tool steel Photo 7. The tool steel was used to provide an average thickness of the OSB. Some of the wood flakes are thicker than others creating high and low areas. The tool steel averaged these high and low areas allowing a more accurate measurement. The identification was marked on each sheet of OSB Photo 9. Next, each sheet was placed on a pair of sawhorses spaced 7'- 8½" apart, center-to-center, and tied together with a pair of 2x4 strong-backs. The location of the sawhorses was marked on the floor as a reference.

The nail locations were marked on the face of each sheet using a piece of OSB as a story pole Photo 10. An out of plane stiffness test was also conducted as a way to compare each sheet against one another. The test was conducted simply by supporting each end of each piece of OSB such that it was spanning the long, 8 ft, length. Once the sheet was set in the fixture, the center was marked. An initial measurement from the long edge was made at the center of the length (measured and marked) to the concrete floor below (square to the

Photo 11: Panel Stiffness

floor and marked on the floor). After the initial measurement, a 41.4 lb weight was added to the center of the sheet and another measurement was made to the floor below, Photo 11. These measurements were recorded to obtain a flexural stiffness. The results of the OSB measurement are summarized in Table 40.

Table 40: OSB Measurements

OSB Sample	Weight (lbs)	Average Thickness (in)	Estimated Stiffness (lb-in^2/ft)
A1	50.8	0.523	152,009
A2	51.2	0.529	152,009
A3	52.4	0.534	156,912
A4	50.0	0.515	135,119
A5	51.2	0.533	152,009
B1	51.2	0.519	143,067
B2	50.0	0.510	135,119
B3	50.6	0.505	152,009
B4	50.8	0.511	147,403
B5	51.2	0.527	152,009
C1	52.2	0.526	152,009
C2	51.4	0.529	162,143
C3	52.2	0.529	162,143
C4	52.0	0.525	156,912
C5	51.8	0.519	156,912
D1	52.2	0.534	167,734
D2	51.0	0.513	147,403
D3	51.0	0.523	162,143
D4	53.2	0.538	147,403
D5	50.0	0.530	156,912
E1	53.2	0.534	135,119
E2	52.0	0.525	135,119
E3	53.2	0.535	135,119
E4	50.6	0.533	187,088
E5	52.8	0.549	152,009
Minimum	50.0	0.505	135,119
Maximum	53.2	0.549	187,088
Average	51.5	0.526	151,753
Variance	0.98	0.000	143,766,517
Std. Dev.	0.99	0.010	11,990
COV	0.02	0.02	0.08

A3 Wall Construction

After inventorying the lumber and preparing it for construction of the wall, a fixture, Photo 12, was constructed to fabricate each wall. The fixture consisted of a pair of sawhorses with LVLs and 2x4s connecting them and forming stops to construct square walls. Each wall consists of three plates (two on top and one on bottom), four studs, and one sheet of OSB.

To begin construction of the walls, the bottom plate and one top plate were placed in the fixture. Next, four studs were placed between the plates at the previously marked locations on the plates. The bottom plate was fastened to each stud, Photo 13, with 2-0.131"x3¼" smooth shank, full head nails, Photo 14 and Photo 15, with a Paslode pneumatic nail gun. The top plate was fastened to each stud the same as the bottom plate. Next, the OSB wall sheathing was placed atop the studs and plates. The bottom edge was carefully aligned with the bottom edge of the bottom plate and the stud frame was blocked tight to the fixture to square it. A gage block was made to hold the edge of the sheathing ¾" from the edge of the end studs, Photo 16. The aligned sheathing on the stud framed wall is shown in Photo 17. Once the sheathing was

Photo 12: Wall Fixture

Photo 13: Wall Stud Connection

Photo 14: Stud Fasteners

Photo 15: Stud Fasteners

Photo 16: OSB Edge Gage

Photo 17: Assembled Wall

aligned in the correct position and the wall was square, the sheathing was fastened to each stud with 8d Common (0.131”x2½” smooth shank, full head) nails, Photo 18 and Photo 19, with a Paslode pneumatic nail gun, Photo 20.

Photo 18: Sheathing Fasteners

Photo 19: Sheathing Fasteners

Photo 20: Pneumatic Nailer

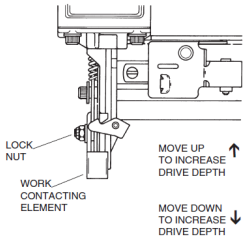

Photo 21: Nail Depth Adjustment

Photo 22: Sheathing Fastener Placement

Photo 23: Sheathing Fastener Placement

Photo 24: Edge Blow Out

Photo 25: Relocated Nail at Damaged Edge

For all nails, the nail gun depth, Photo 21, and air pressure was set so that the nail heads were set flush with the surface of the material, Photo 22 and Photo 23. In instances where the nail was not fully driven, the nails were driven flush with a hammer. No fasteners were overdriven. The placement of the fasteners was accomplished with accuracy as shown in Photo 23. Along the vertical edges, the fasteners were located

3/8" from the edge of the sheathing and 3/8" from the inside edge of the stud, Photo 22. At these locations, the fasteners were driven at an angle (about 5°). After completing the fastening of the sheathing, the back side was checked for any nails that missed the studs. If any nails missed, they were removed and a new nail was installed 1" away from the intended location. Similarly, if the edge of the sheathing was damaged (edge blow out), Photo 24, the nail was removed and a new nail was installed 1" away from the intended location, Photo 25. These instances did not occur very often and the avoidance skills were learned after two walls. Consistency of construction was easily accomplished since all walls were constructed the same day, in the same fixture, and by the same person.

For all of the walls, the sheathing fastening was the same. The perimeter nails were placed 6" o.c. (except first and last spaces) and the intermediate member nails were placed at 12" o.c. (except first and last spaces). The spacing at the first and last space was different to allow for the boundary condition. If the same spacing was used, the nails would be at the edge of the sheathing. As noted above, the nails along the vertical edges were place 3/8" from the edge of the sheathing. The nails along the bottom plate were placed ¾" from the bottom edge of the sheathing or along the centerline of the bottom plate. The nails along the top edge were placed along the centerline of the first top plate, or 1 1/8" from the top edge of the sheathing. Since there was no need to maintain a 3/8" edge distance on the corner nails, they were installed ¾" from the vertical edge, Photo 20.

For the Group A walls, a mechanical hold down was installed to create the restrained condition. A Simpson HDU8 hold down was used for wall A5, Photo 26. The

HDU8 was installed flush with the bottom plate, Photo 27, and fastened to the stud with 20-SDS ¼"x2½" screws, Photo 28. Since the screws were longer than the stud thickness of 1½" a nominal 20" long 2x4 scab was used on the outside face of the stud, Photo 27, so that the SDS screws could fasten to it as well. No other fasteners were used between the scab and the stud. The bottom of the scab was held 5¼" up from the bottom of the wall. This was duplicated for the remaining Group A walls.

After testing wall A5, it was determined that the flush installation of the hold down caused prying of the bottom plate at the end stud. This was discussed earlier in CHAPTER 3. For this reason, the hold down was held up 1" from the bottom plate on walls A1 to A4, Photo 29. Also, the hold down was changed to a Simpson HDU14 hold down, Photo 30, for these remaining walls. This was done to assure that the wall failure would not be a result of the hold down or hold down fastener slippage. The HDU14 was installed 1" above the bottom plate and fastened to the stud with 36-SDS ¼"x2½" screws. The Simpson catalog states "Tension values are valid for hold downs flush or raised off of sill plates." They do not indicate a preferred method for installation.

Photo 26: Simpson HDU8 Hold Down

Photo 27: Simpson HDU8 Hold Down

Photo 28: SDS ¼" x 2½" Screw

Photo 29: Simpson HDU14 Hold Down

Photo 30: Simpson HDU14 Hold Down

A4 Test Setup

A4.1 Test Fixture Setup

The test fixture was setup within the Structural Building Component Research Institute's test lab. The fixture was fabricated such that each wall specimen could be easily removed and the next one installed. An overall view of the test fixture setup is shown in Figure 23.

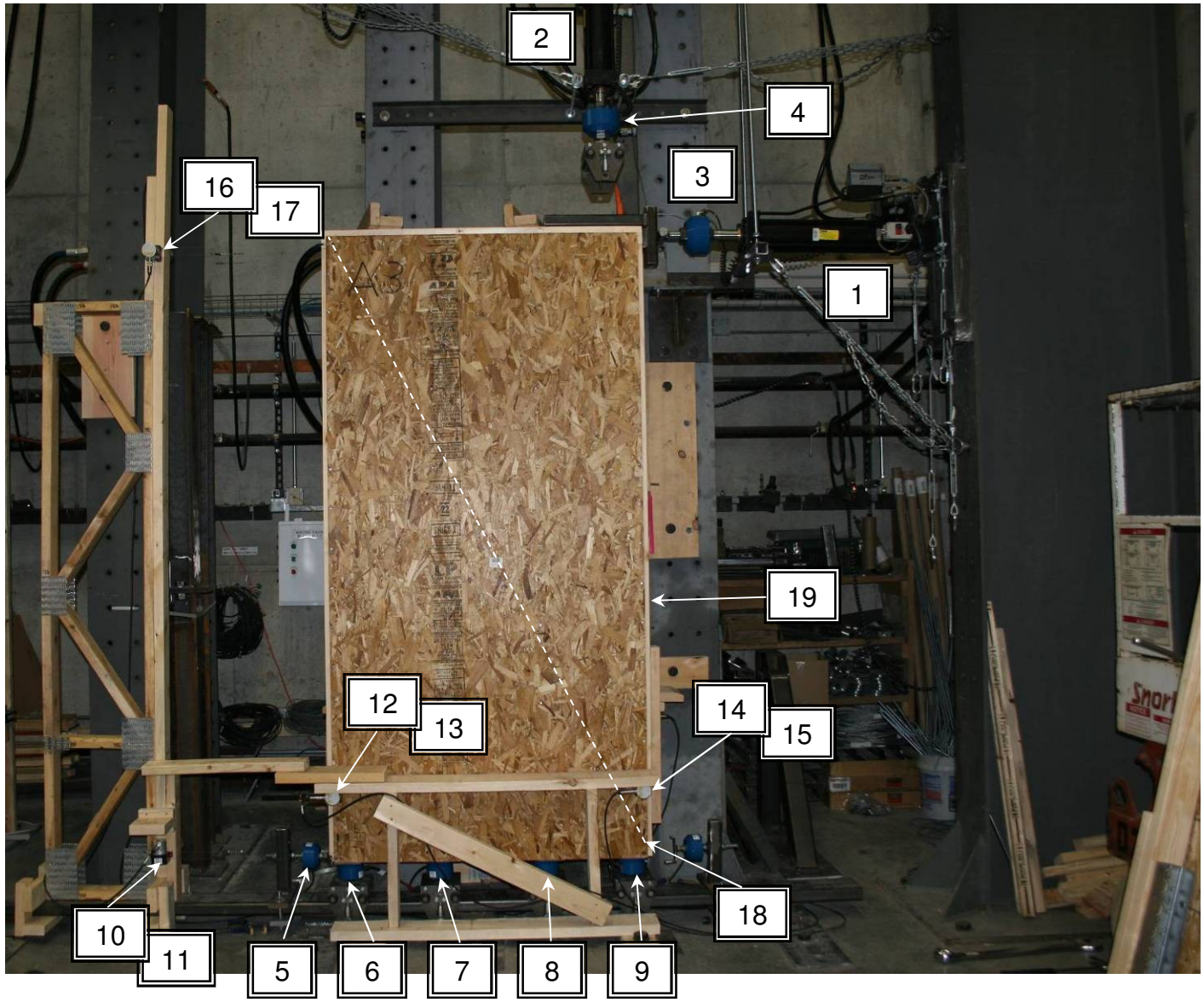

Figure 23: Test Setup

Key:

1. Horizontal actuator
2. Vertical actuator
3. Horizontal actuator load cell
4. Vertical actuator load cell
5. Horizontal load cell
6. Vertical load cell at stud
7. Vertical load cell at stud
8. Vertical load cell at stud
9. Vertical load cell at holdown
10. Horizontal string pot at base of sheathing (front)
11. Horizontal string pot at bottom plate (back)
12. Vertical string pot at base of sheathing (front)
13. Vertical string pot at bottom plate (back)
14. Vertical string pot at base of sheathing (front)
15. Vertical string pot at bottom plate (back)
16. Horizontal string pot at top of sheathing (front)
17. Horizontal string pot at top plate (back)
18. Diagonal string pot (back)
19. Wall test specimen

A4.2 Test Frame

The test frame utilized two portal test frames and one cantilevered column. All columns were W36x135's which were anchored to a strong floor. The two portal frames were used to support the vertical actuator utilizing a W6x25 beam supported by brackets on the columns. The W6x25 was installed parallel to the columns. The cantilevered column was used to support the horizontal actuator. This column was oriented 90° to the portal columns.

The base of the test frame consisted of an HSS6x2x¼ welded to bearing plates

Photo 31: Base Roller

Photo 32: Base Bearing Plate

Photo 33: Alignment of Frame

Photo 34: Alignment of Frame

Photo 35: Alignment of Horizontal Actuator

Photo 36: Restraint of Actuators

that were anchored to the strong floor. This tube supported four roller bearings, Photo 31, one below each wall stud. The roller bearings consisted of two steel rollers atop the tube and two nylon rollers along the bottom, below the tube. Therefore the rollers could resist compression and tension forces. A load cell with a bearing plate was mounted on each roller, Photo 32.

The HSS6x2 was aligned with the W6 above using a plumb bob and both were parallel with the portal frame columns. The plumb bob was also used to set the vertical actuator, Photo 33 and Photo 34. The horizontal actuator was aligned with a string along the centerline of the wall and leveled in place, Photo 35. Both vertical and horizontal actuators were anchored to resist translation at the wall, Photo 36

The actuators were both hydraulic piston, 25,000 lb capacity, with a 20" stroke. The actuators each have internal load cells and LVDT's for control. The vertical actuator was connected to a roller where it loaded the wall, Photo 38 and Photo 39. This was the same roller as the base of the wall but with the nylon rollers removed. The horizontal actuator had a 1½" diameter T-bar that pushed against the wall bar. This T-bar was smooth to slide on the wall bar.

In order to transfer the load from each actuator to the wall, a T-shaped steel bracket was fabricated from HSS3x2x¼ steel. An additional ½" plate was added to the vertical piece of the T-shaped bracket to bear against the ends of the double top plate, Photo 40. This was done to keep the load on the double top plates and not load the end stud. The T-shaped bracket was also necessary to allow the wall to rotate and the actuators to slide on corner of the wall. To eliminate adding additional stiffness to the wall, the bracket only extended to the second stud. The bracket was fastened to the top

Photo 37: Guide Rollers

plate with 2-¼ x 3" screws. The surface of the T-shaped bracket was smoothed with a belt sander to minimize friction on the T-bar.

The wall was restrained at the top to resist out of plane movement by adding two 2x4 strong-backs (two 2x4's fastened in an L-shape) with two rollers each. The strong-backs were fastened to the top of the wall with 2-¼ x 3" screws. The rollers were guided along an L5x5x¼ parallel to the wall and anchored to the portal frame columns as shown in Photo 37. The rollers were offset down 3" from the strong-backs to allow the rollers to be in contact with the guide as the wall rotated and moved upward. The strong-backs were skewed to the wall so that each roller is in contact with the guide. A 2x4 gauge block was placed between the top of the wall and the guide to locate the wall in the correct position (parallel to the guide) before fastening the strong-backs to the top of the wall.

Photo 38: Alignment of Vertical Actuator

Photo 39: Vertical Actuator Roller

Photo 40: Horizontal Actuator

A5 Instrumentation

The wall test specimen was instrumented as shown in Figure 23. A total of seven load cells were used and nine string potentiometers. The load cells measured both the actuator loading and the reactions. The string potentiometers captured the global displacement of the wall both vertically and horizontally by measuring the wall studs and plates. The global displacement of the sheathing was measured as well. Measurements at the two locations allow for the determination of the differential movement of the sheathing. A diagonal measurement of the wall was also made on the back side of the wall studs.

The equipment used for the tests is shown in Figure 23 and summarized in Table 41. A typical load cell is shown in Figure 24. A typical sting potentiometer is shown in Figure 25. The load cells and string potentiometers were all calibrated between September 24, 2010 and October 6, 2010. Each calibration had a text file that was imported into the data acquisition software. The calibrations of the string potentiometers were nonlinear.

A total of 17 channels were connected for the data acquisition, but only 16 were used; items 3-18 in Figure 23. The data acquisition equipment, Photo 41, was then connected to a desktop CPU, Photo 42, for processing and recording.

All of the string potentiometers, except the diagonal one, were connected to rigid fixtures. The two string potentiometers used to measure vertical displacement of the OSB sheathing were connected to a gate that could swing out of the way for the wall exchange. The string potentiometers were connected to the wall specimen with wood

screws that were installed in the same location for each wall, Photo 43. This allowed for quick set up of each wall.

Table 41: Test Equipment

Function	Model
Displacement Measurements- • Micro-Epsilon String Potentiometers	WDS-500-P60-SR-U WDS-7500-P60-SR-U WDS-1500-P60-SR-U
Load Actuator • Hydraulic Piston • 20” Stroke Maximum • 25,000 lb Load Maximum	
Load Cells • Interface Load Cells • Eccentric Load Compensated • Tension and Compression Capacity • Performance to 0.02% Error	1210 AF-10K-B & 1220 DRB-25K
Data Acquisition • Up to 1,000,000/# of Measuring Devices Hz	

Figure 24: Load Cell

Figure 25: String Potentiometer

A total of 17 channels were connected for the data acquisition, but only 16 were used; items 3-18 in Figure 23. The data acquisition equipment, Photo 41, was then connected to a desktop CPU, Photo 42, for processing and recording.

Photo 41: Data Acquisition

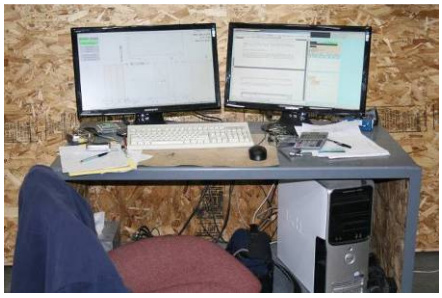

Photo 42: CPU For Recording Data

Photo 43: String Potentiometer Connection

A5.1 Test Equipment Software

Two separate software programs were used to conduct the test; one for the data acquisition and one for the actuator control. The data acquisition software used was Dasylab 10. This software had a wonderful interface that allowed pasting images of the test setup, created with AutoCAD, into its graphic view. Then, text boxes were created at each of the instruments that were linked to the instruments. This allowed real time views of the load and displacement that could quickly be identified on the graphic. Additionally, the load-deflection curve was plotted real time as well. The plot included

both the stud and the sheathing displacement. It was easy to see the peak load with this plot of the hysteresis curve. The peak load was also displayed on the screen along with the calculated unit shear in the wall panel. Figure 26 shows a view of the graphics

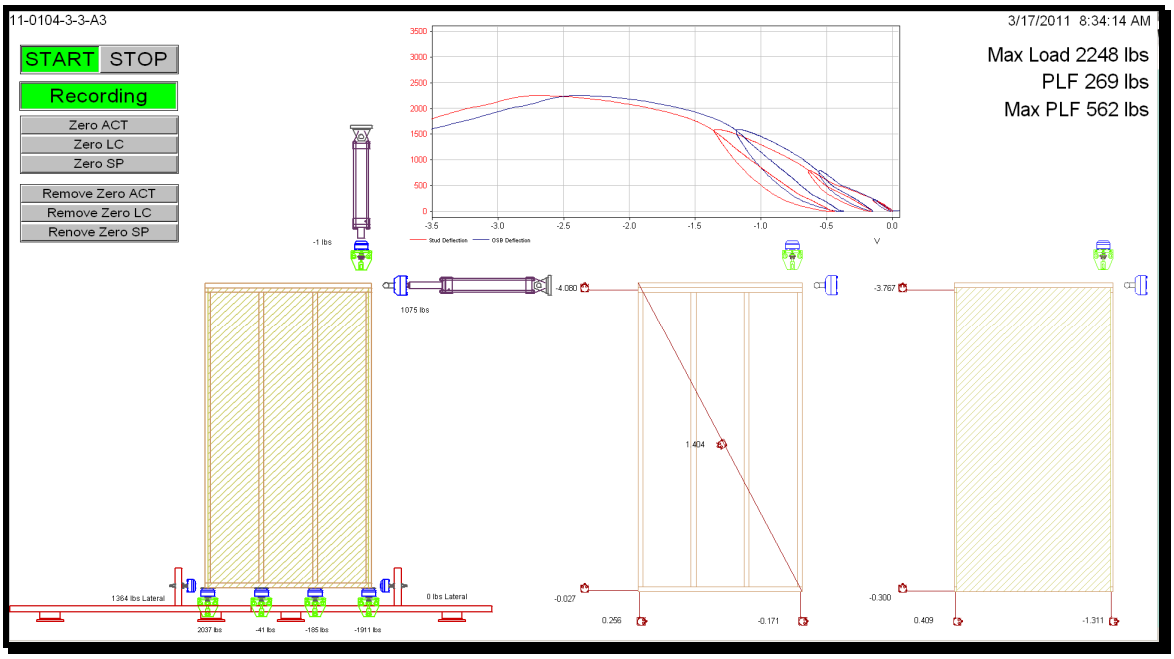

Figure 26: Data Acquisition Software Graphics Display

display from Dasylab. The actuator control software used was Adamation. This software controlled the actuators during the test as well as allowed manual control of the actuators during the test setup. The load protocol was entered into the software in a spreadsheet format, Figure 27. This allowed easy changes for the five different load test setups. The manual control allowed the user to retract the actuators when the test was complete and then bump them into the wall after the new wall was installed in the test assembly. The software also allows the user to set a maximum load that can be applied in manual mode for safety. This limit was set to 40 lb for this testing.

COMMAND ID	DURATION	PARAMETER 1	PARAMETER 2	PARAMETER 3	PARAMETER 4	PARAMETER 5	PARAMETER 6
7	30	0	0	0	0	0	0
4	42	240	0	0	0	0	0
8	300	0	0	0	0	0	0
4	21	1	0	0	0	0	0
8	300	0	0	0	0	0	0
4	140	800	0	0	0	0	0
8	60	0	0	0	0	0	0
4	70	1	0	0	0	0	0
8	300	0	0	0	0	0	0
4	280	1600	0	0	0	0	0
8	60	0	0	0	0	0	0
4	140	1	0	0	0	0	0
8	300	0	0	0	0	0	0
4	876	5000	0	0	0	0	0

Figure 27: Actuator Control Software Load Steps

A5.2 Test Procedure

A5.2.1 Test Sequence

The testing followed the alpha order indicated in Table 11. The purpose of this was to determine the hold down force from the Group A wall set and consider this as the full restraining force. The subsequent groups then used a fraction of this restraining force as indicated in Table 11.

A5.2.2 Test Loading

As described earlier, the five walls in Group A were restrained with a hold down. Each wall was placed in the test fixture tight against the lateral load cell at the base of the wall; the hold down bolt was installed through the hold down and into the load cell below; the top of the wall was supported with the two roller guides; the T-bar was connected to the top of the wall; the other two bottom load cells were aligned with the

Graph 36: Wall Group A Loading

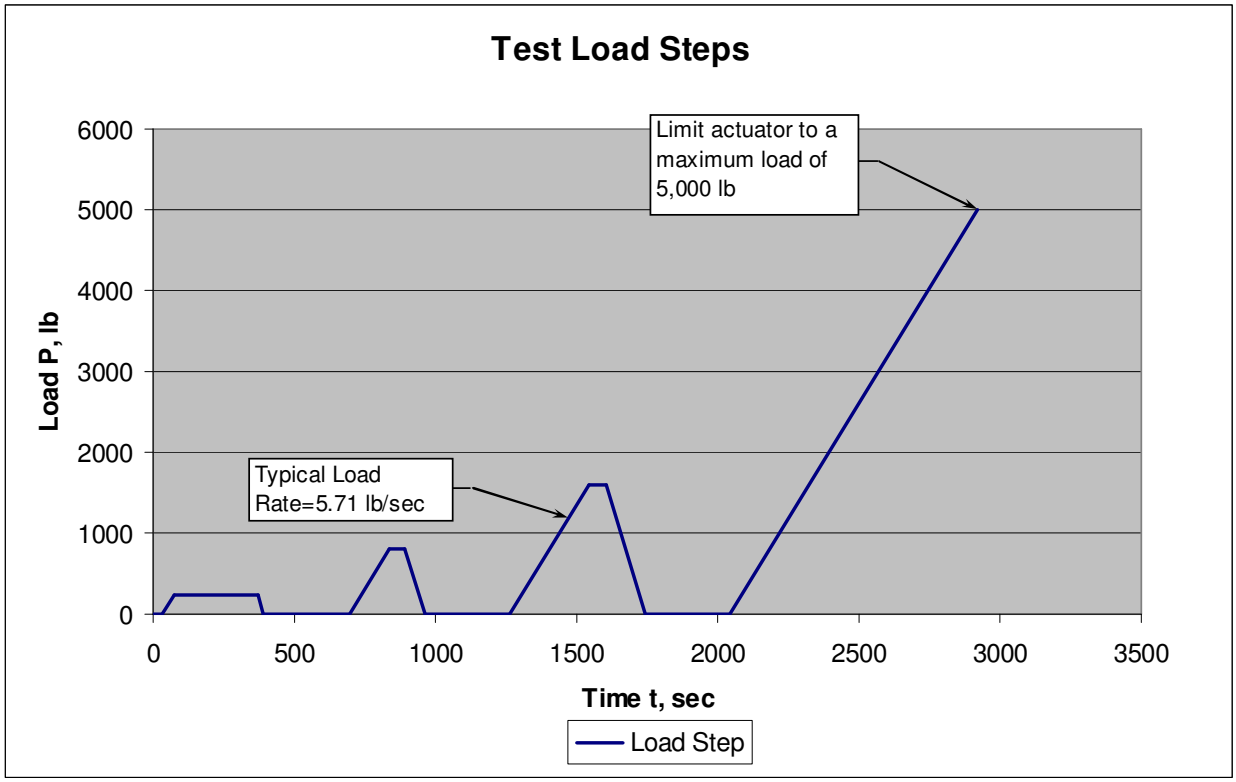

two interior studs; all string potentiometers were connected to the wall; and the horizontal actuator was placed up against the T-bar with a nearly zero force.

The loading for the wall specimen was based on ASTM E564. The load was applied in load steps as indicated in Graph 36. This illustrates the load steps that were entered into the actuator control software as shown in Figure 27. Load step one is the preload which was 10% of the estimated ultimate load and was applied for 5 minutes. Load steps two and three were at 1/3 and 2/3 the estimated ultimate load respectfully and are applied for 1 minute. Load step four was the final load step to determine the ultimate capacity. The load rate for each of the load steps was the same and was determined from the estimated ultimate load applied over a period of seven minutes. ASTM E564 requires the load to be applied in no less than five minutes. As shown in Graph 36 each of the first three load steps were unloaded at twice the loading rate.

The actuator was load controlled instead of deflection controlled. This was used because the actuator control software can either provide load control or displacement control. For two actuators, the control type must be the same. In other words, the vertical actuator could not be load controlled while the horizontal actuator was displacement controlled. Since the vertical actuator had to be load controlled, the horizontal actuator also was load controlled. The tests were typically manually stopped since the limit load was always well above the anticipated ultimate load.

The data for the tests was recorded by the data acquisition equipment. This recorded the load cell and string potentiometer data. The rate at which the data was recorded was two readings every second or 2 Hz.

Subsequent tests using ¼, ½, and ¾ of full restraint, and no restraint were conducted as Groups B, C, D and E respectively. The restraining forces for the partially restrained tests was provided by the vertical load actuator placed above the end of the wall with a load cell between the actuator and the wall to obtain the actual applied restraining force as shown in Figure 23. As noted earlier the unrestrained wall had one $^{5}/_{8}$" diameter anchor bolt 12" from the tension end and no load from the actuator above.

A5.2.3 Test Procedure

Once the test specimen was set and ready, the load cells and string potentiometers were zeroed on the data acquisition software and the software was set to record to a previously named text file in a project folder. Each filename and folder was unique for each test. The filename for each wall was of the same format so that it could be processed with Matlab software afterward. The load test was then started from the actuator control software.

Once the test began, the specimen was monitored for stability and performance and the data acquisition software display, Figure 26, was monitored for expected behavior. The data acquisition software display made it easy to see that the load cells and string potentiometers were working and that the readings were making sense based on the load input and displacement.

The project folder on the computer was checked regularly to make sure that the data text file was being written by the data acquisition software. During the test, notes and screenshots from the data acquisition software display were added to a unique word processing file for each wall specimen. The file used the same format so that it was easy to analyze the data afterward.

A5.2.4 Test Data

The test results were in the form of an ASCII text file. The file records the date and time of each reading. The readings were of the sixteen channels shown as items 3-18 in Figure 23. As noted earlier, the instrumentation readings were taken at a rate of 2 Hz. In addition to the data acquisition, photos of the wall after failure were also taken. The photos aided in recording the failure modes of the particular walls. In addition to the photos, video of the bottom plate on the tension side was taken on seven of the partially restrained and unrestrained wall specimens.

A6 Specific Gravity Test

The specific gravity of the studs, plates, and wall sheathing was determined with a specific gravity test in accordance with ASTM 2395. Upon completion of the tests, the wall specimens were dismantled and oversized specific gravity test specimens were cut from each individual piece, identified with a marker for the wall specimen and the location of the member in the wall specimen. The samples were immediately sealed in plastic bags, Photo 44 for transportation from the SBC Research Institute to the test lab.

Photo 44: Specific Gravity Samples from Wall Specimens

The samples were then cut to uniform sizes with square edges for volume measurements. The samples for the 2x4's were cut to 1 in. lengths (parallel to grain) and the wall sheathing was cut to 3 by 6 in. pieces. Each piece was identified as described above, measured, and weighed, Photo 45. The size measurements were made with a dial caliper with a precision of 1/1000 in. The weight of each sample was made with an AccuLab Pocket Pro 150-B digital scale with an accuracy of 0.1 g. The samples were all resealed in their plastic bags until they were oven-dried.

Photo 45: Scale and Calipers

All of the samples were oven-dried at Testing Engineers and Consultants lab for 48 hours in a Blue M electric oven at 103°. The temperature was checked twice daily with a Cen-Tech infrared thermometer. The weights of random samples were checked at 24 hours, 44 hours, and finally 48 hours to determine that they had reached constant weight.

Photo 46: Oven-Drying

Upon completion of drying, all samples were weighed immediately upon removal from the oven. Using the volume measurements, initial weight, and final weight, the moisture content and specific gravity were determined for each sample.

A6.1 Results of Specific Gravity Test

The results from the specific gravity tests were used to determine the probability distribution of the specific gravity. For each different material, the studs, the plates, and the OSB sheathing, the result data was grouped in bins as shown in Graph 37.

Using a Chi-Square test, the likely probability distribution was determined. An example of this is shown in Table 42.

The number of degrees of freedom for the Chi-Square test is $f = 10\text{-}3 = 7$. With a significance level $\alpha = 5\%$, $c_{.95,7} = 14.1$ (Ang & Tang 1975). Both distributions are valid, but since 8.88 is less than 14.1 and since lognormal always yields a positive value, lognormal is the preferred distribution.

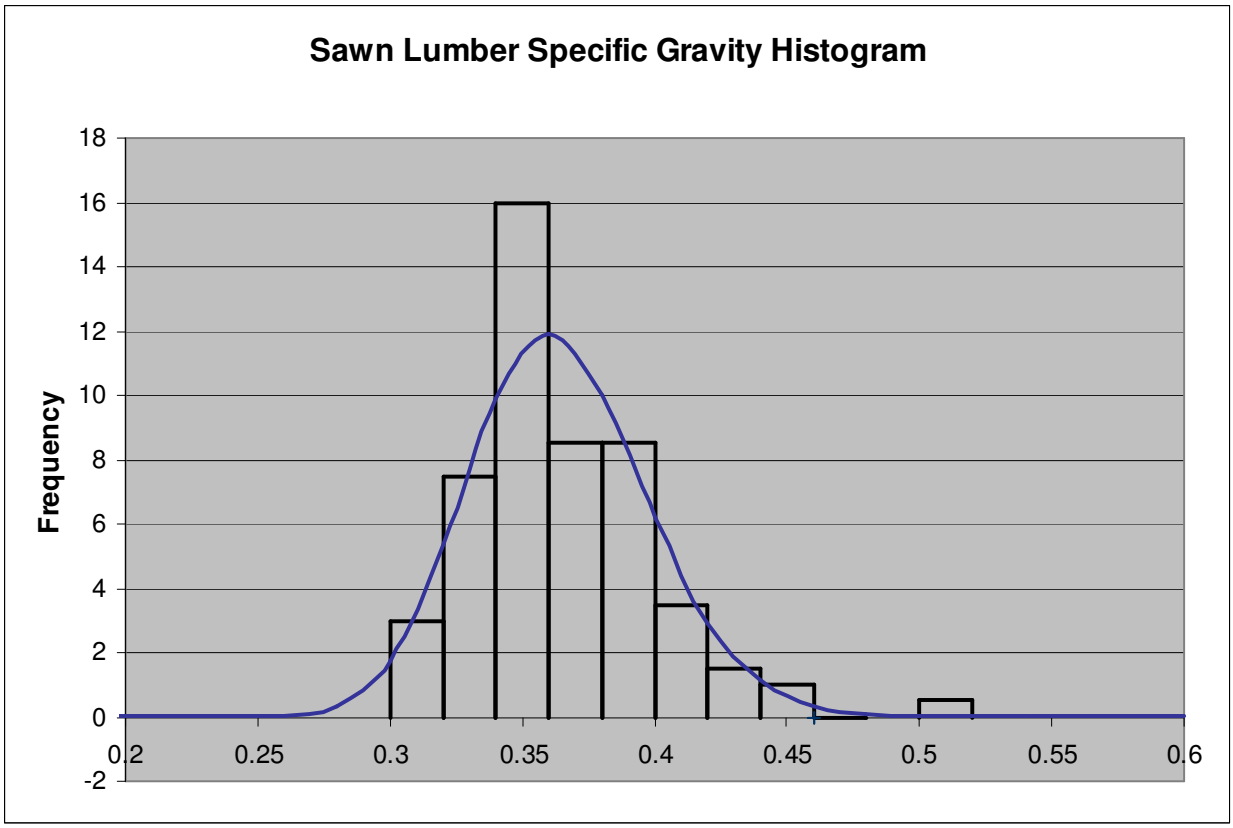

Graph 37: Distribution of the Specific Gravity for SPF-S Studs

Table 42: Chi-Square Test for Specific Gravity Probability Distribution for Studs

Chi-Square Test for Relative Goodness-of-fit

Interval	Observed frequency n_i	Theoretical frequency e_i		$(n_i-e_i)^2/e_i$	
		Normal	Lognormal	Normal	Lognormal
<0.3	0	2.9	2.0	2.89	2.04
0.3-0.32	6	6.7	6.8	0.07	0.09
0.33-0.34	15	14.1	15.4	0.06	0.01
0.34-0.36	32	21.2	22.4	5.44	4.08
0.36-0.38	17	22.9	22.4	1.51	1.31
0.38-0.40	17	17.6	16.2	0.02	0.04
0.40-0.42	7	9.6	8.9	0.72	0.41
0.42-0.44	3	3.8	3.9	0.15	0.19
0.44-0.46	2	1.0	1.4	0.86	0.30
>0.46	1	0.2	0.5	2.39	0.41
Σ	100	100.0	100.0	14.10	8.88

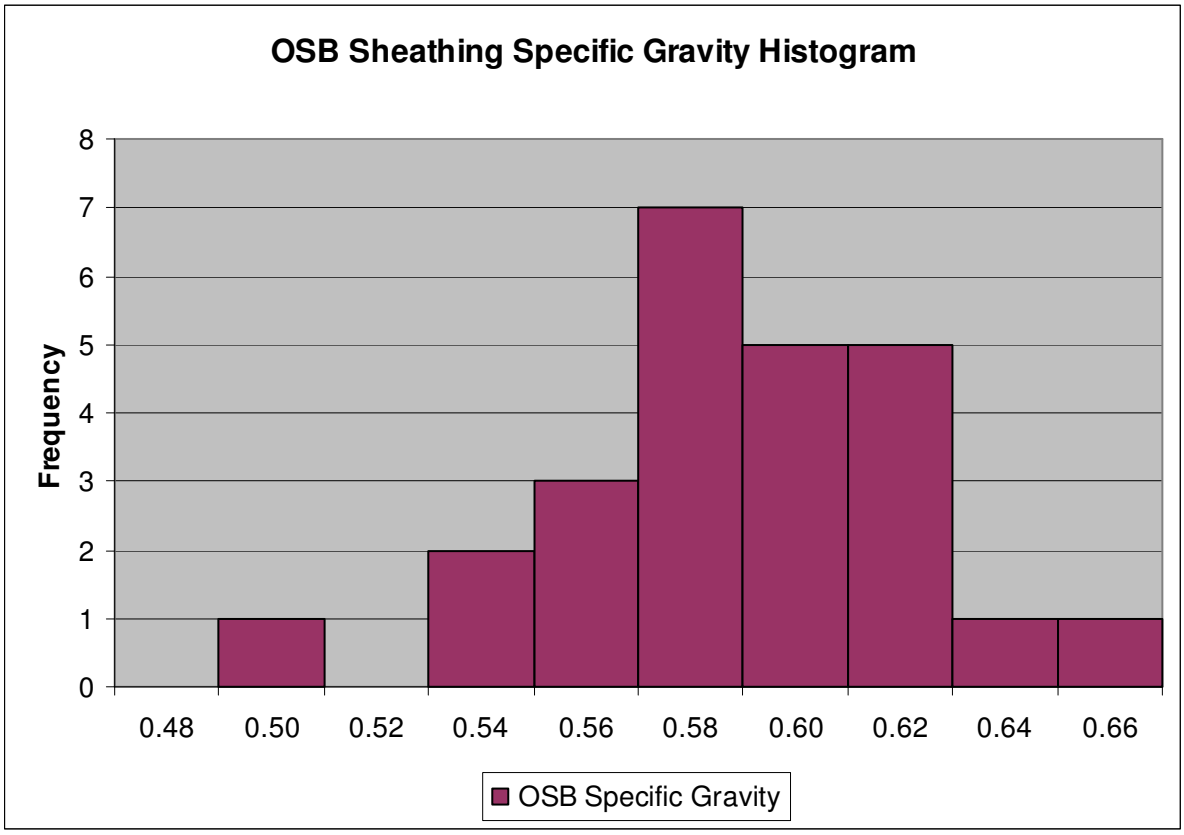

Graph 38: Distribution of the Specific Gravity for OSB Sheathing

The specific gravity of the materials for the five sets of walls are shown in the following tables .

Table 43: Specific Gravity of Members in Wall Group A

Set "A" with Holdown

Member	Wall				
	A1	A2	A3	A4	A5
	G	G	G	G	G
1	0.33	0.34	0.35	0.38	0.45
2	0.33	0.35	0.40	0.34	0.32
3	0.31	0.37	0.36	0.31	0.37
4	0.39	0.36	0.35	0.42	0.35
BP	0.36	0.40	0.42	0.36	0.40
TP	0.37	0.39	0.42	0.36	0.39
TP.2	0.37	0.39	0.47	0.37	0.39
OSB					
G	0.56	0.50	0.57	0.62	0.60
t, in	0.510	0.506	0.513	0.495	0.498

Table 44: Specific Gravity of Members in Wall Group B

Set "B" with 1/4 Restraint

Member	Wall				
	B1	B2	B3	B4	B5
	G	G	G	G	G
1	0.33	0.35	0.36	0.34	0.34
2	0.35	0.39	0.35	0.36	0.34
3	0.45	0.40	0.38	0.36	0.34
4	0.40	0.32	0.40	0.35	0.38
BP	0.38	0.43	0.39	0.43	0.37
TP	0.38	0.41	0.39	0.43	0.36
TP.2	0.37	0.43	0.39	0.43	0.38
OSB					
G	0.59	0.54	0.53	0.57	0.59
t, in	0.510	0.489	0.543	0.501	0.512

Table 45: Specific Gravity of Members in Wall Group C

Set "C" with 1/2 Restraint

Member	Wall				
	C1	C2	C3	C4	C5
	G	G	G	G	G
1	0.40	0.34	0.39	0.33	0.37
2	0.32	0.38	0.33	0.39	0.39
3	0.32	0.36	0.34	0.34	0.34
4	0.38	0.39	0.38	0.37	0.41
BP	0.43	0.41	0.44	0.40	0.39
TP	0.45	0.40	0.40	0.36	0.37
TP.2	0.43	0.40	0.48	0.37	0.36
OSB					
G	0.62	0.60	0.61	0.58	0.58
t, in	0.503	0.507	0.503	0.503	0.515

Table 46: Specific Gravity of Members in Wall Group D

Set "D" with 3/4 Restraint

Member	Wall				
	C1	C2	C3	C4	C5
	G	G	G	G	G
1	0.34	0.34	0.34	0.35	0.37
2	0.38	0.37	0.41	0.35	0.35
3	0.44	0.40	0.39	0.35	0.41
4	0.40	0.36	0.37	0.36	0.43
BP	0.48	0.37	0.36	0.39	0.43
TP	0.33	0.37	0.38	0.36	0.38
TP.2	0.39	0.39	0.34	0.40	0.33
OSB					
G	0.63	0.61	0.56	0.57	0.57
t, in	0.499	0.470	0.514	0.544	0.508

Table 47: Specific Gravity of Members in Wall Group E

Set "E" with no Restraint

Member	Wall				
	E1	E2	E3	E4	E5
	G	G	G	G	G
1	0.32	0.36	0.42	0.34	0.37
2	0.40	0.34	0.36	0.41	0.37
3	0.36	0.34	0.44	0.42	0.52
4	0.37	0.39	0.34	0.38	0.38
BP	0.42	0.41	0.45	0.40	0.41
TP	0.43	0.44	0.46	0.40	0.41
TP.2	0.44	0.41	0.34	0.41	0.41
OSB					
G	0.57	0.64	0.60	0.61	0.55
t, in	0.547	0.531	0.515	0.527	0.516

APPENDIX B

SBCRI ACCREDITATION CERTIFICATE

CERTIFICATE OF ACCREDITATION

ANSI-ASQ National Accreditation Board/ACLASS
500 Montgomery Street, Suite 625, Alexandria, VA 22314, 877-344-3044

This is to certify that

Structural Building Components
Research Institute (SBCRI)
6300 Enterprise Lane
Madison, WI 53719

has been assessed by ACLASS
and meets the requirements of international standard

ISO/IEC 17025:2005

while demonstrating technical competence in the field(s) of

TESTING

Refer to the accompanying Scope(s) of Accreditation for information regarding the types of tests to which this accreditation applies.

AT-1373
Certificate Number

ACLASS Approval
Certificate Valid: 02/05/2009-02/05/2011
Version No. 001

This laboratory is accredited in accordance with the recognized International Standard ISO/IEC 17025:2005. This accreditation demonstrates technical competence for a defined scope and the operation of a laboratory quality management system (*refer to joint ISO-ILAC-IAF Communiqué dated January 2009*).

ANSI-ASQ National Accreditation Board/ACLASS

SCOPE OF ACCREDITATION TO ISO/IEC 17025:2005

Structural Building Components Research Institute (SBCRI)
6300 Enterprise Lane, Madison, WI 53719
Dan Hawk Phone: 608-274-4849

TESTING

Valid to: February 5, 2011 Certificate Number: AT - 1373

I. Construction Materials / Mechanical

ITEMS, MATERIALS OR PRODUCTS TESTED	SPECIFIC TESTS OR PROPERTIES MEASURED	SPECIFICATION, STANDARD METHOD OR TECHNIQUE USED	*DETECTION LIMIT/ RANGE/ EQUIPMENT
Building Systems	Compression, Deflections, Tension, & Flexure	ASTM E72, E73, E455, E564, E2127	Load Cells, Actuators, String Potentiometers
Building Elements	Compression, Deflections, Tension, & Flexure	ASTM D4761, ASTM E8	Load Cells, Actuators, String Potentiometers

Notes:
1. ** = As Applicable*
2. *This scope is part of and must be included with the Certificate of Accreditation No. AT- 1373*

Vice President

500 Montgomery St. Suite 625 | Alexandria, VA 22314 | 703-836-0025 | www.aclasscorp.com

APPENDIX C

STRING POTENTIOMETER AND LOAD CELL SPECIFICATIONS

18

wireSENSOR
Digital series P60 / P96

Best seller - most economic model
Very robust sensor housing
Easy and flexible mounting

Universal digital sensors for industrial applications

The digital series P60 and P96 are for general purpose use. Numerous options enable a suitable sensor to be selected for almost any application. Mounting grooves on four sides of the housing facilitate quick and flexible mounting. The series has an attractive price/performance ratio based on state of the art technology. Various types of signal outputs and an optimized size make this series suitable for a wide range of applications, also in harsh environments.

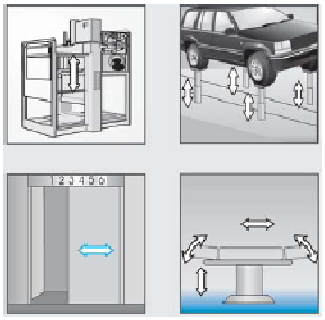

Model P60-HTL/TTL

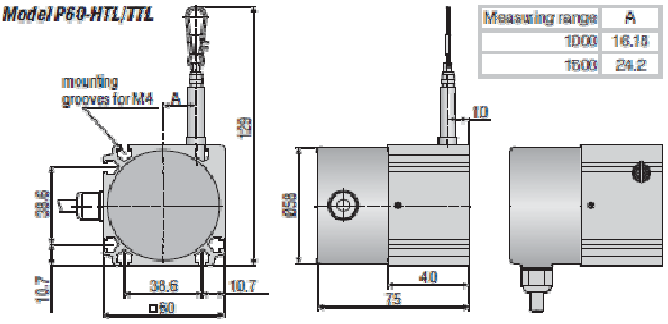

Measuring range	A
1000	16.15
1500	24.2

Model P96-HTL/TTL

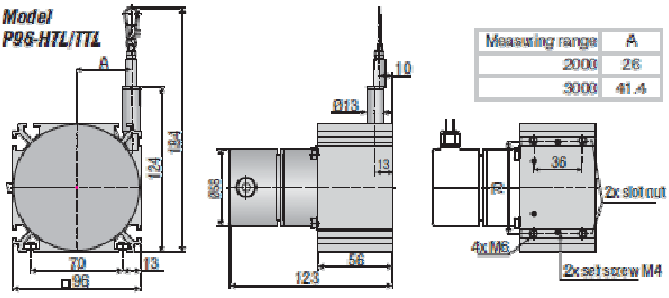

Measuring range	A
2000	26
3000	41.4

Model P96-SSI

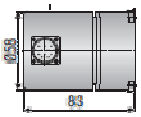

Model P96-CO/PB

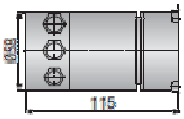

Dimensions in mm, not to scale. Please ask for detailed reference drawings.

Model		WDS-1000-P60	WDS-1500-P60	WDS-3000-P96
Output		HTL, TTL		HTL, TTL, SSI, PB, CO
Measuring range		1000mm	1500mm	3000mm
Linearity	±0.02 % FSO	±0.2mm	±0.3mm	±0.6mm
Resolution	HTL, TTL	0.067mm (15 pulse/mm)	0.1mm (10 pulse/mm)	0.087mm (11.53 pulse/mm)
Resolution	SSI, PR, CO	-	-	0.002mm
Sensor element		incremental encoder		incremental-/absolute-encoder
Temperature range		-20... +90 °C		
Material	housing	aluminum		
	draw wire	coated polyamid stainless steel (ø0.45mm)		ø 0.8mm
Sensor mortage		mounting grooves in the housing		slot nuts
Wire mounting		wire clip		
Wire acceleration		10g	15g	7g
Wire retraction force (min)		3 N	3.3 N	3.3 N
Wire extension force (max)		7.5 N	8.5 N	9 N
Protection class	DIN EN 60529	IP 65 (only if connected)		
Vibration	IEC 68-2-6	20g, 20Hz...2kHz		
Mechanical shock	IEC 68-2-27	50g, 10ms		
Electrical connection	output HTL, TTL	integral cable, radial, 1m long		
	output SSI	connector, radial, 12-pin		
	output PB, CO	bus cover		
Weight		appr. 1kg		appr. 1.7kg

FSO = Full Scale Output

Specifications for digital outputs on page 22 and continuing

Article description

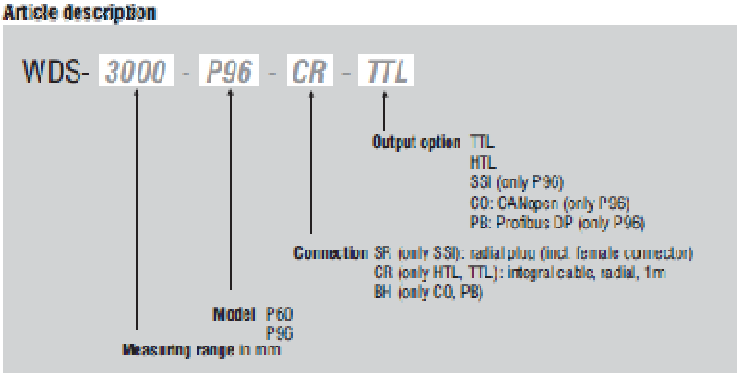

The Leader in Force Measurement **interface**

Model 1100 Ultra Precision Load Cell (U.S. & Metric)

Why the Interface model 1100 Ultra Precision Load Cell is the best in class:

- Proprietary Interface temperature compensated strain gages
- Performance to .02%
- High output – to 4 mV/V
- Eccentric load compensated
- Low deflection
- .0008%/°F (.0015%/°C) temp. effect on output
- Shunt calibration
- High precision base included
- Barometric compensation
- Tension and compression

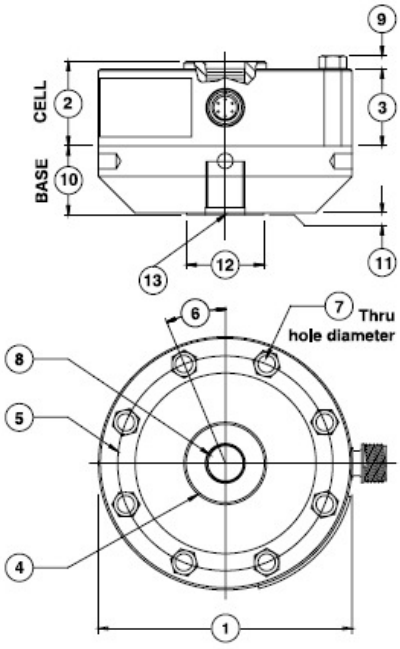

DIMENSIONS

See Drawing	MODEL 1110 CAPACITY U.S. (lbf) 300, 500, 1K,2K,3K, 5K, 10K	1110 Metric (kN) 1.5, 2.5 5, 10, 25, 50	1120 U.S. (lbf) 25K, 50K	1120 Metric (kN) 100, 250	1132 U.S. (lbf) 100K	1132 Metric (kN) 450	1140 U.S. (lbf) 200K	1140 Metric (kN) 900
	inch	mm	inch	mm	inch	mm	inch	mm
①	4.13	104.8	6.06	153.9	8.00	203.2	11.0	279.0
②	1.38	34.9	1.75	44.5	2.50	63.5	3.50	88.9
③	1.25	31.7	1.63	41.4	2.25	57.2	3.00	76.2
④	1.34	34.0	2.65	67.3	3.76	95.2	4.81	122.2
⑤	3.50	88.9	5.13	130.3	6.50	165.1	9.00	228.6
⑥	22.5°	22.5°	15.0°	15.0°	11.25°	11.25°	11.25°	11.25°
⑦	0.28	7.10	0.41	10.4	0.53	13.5	0.65	16.5
⑧	5/8-18 UNF-3B	M-16 X 2-4H	1 1/4-12 UNF-3B	M33 X 2-4H	1 3/4-12 UNF-3B	M42 X 2-4H	2 3/4-8 UNF-3B	M72 X 2-4H
	1.12 in deep	28.4 mm deep	1.40 in deep	35.6 mm deep	2.15 in deep	54.6 mm deep	3.25 in deep	82.6mm deep
⑨	0.20	5.10	0.30	7.60	0.40	10.2	0.50	12.7
⑩	1.13	28.6	1.75	44.5	2.00	50.8	3.00	76.2
⑪	0.03	0.80	0.03	0.80	0.03	0.80	0.03	0.80
⑫	1.25	31.8	2.25	57.2	3.00	76.2	4.50	114.3
⑬	5/8-18 UNF-3B	M-16 X 2-4H	1 1/4-12 UNF-3B	M33 X 2-4H	1 3/4-12 UNF-3B	M42 X 2-4H	2 3/4-8 UNF-3B	M72 X 2-4H
	.87 in deep	22.1 mm deep	1.40 in deep	35.6 mm deep	1.75 in deep	44.5 mm deep	2.75 in deep	69.8 mm deep

INTERFACE • 7401 E. Butherus Drive, Scottsdale, AZ 85260 • PHONE: (480) 948-5555 • FAX: (480) 948-1924
www.interfaceforce.com • Email: gen@interfaceforce.com • **ORDER TOLL-FREE 1-800-947-5598**

1100UP_12_13
12/05

SPECIFICATIONS

PARAMETERS	MODEL 1110	1110	1120	1132	1140
	CAPACITY				
U.S. Models (lbf)	300,500,1K,2K,3K	5K, 10K	25K, 50K	100K	200K
Metric Models (kN)	1.5, 2.5, 5, 10	25, 50	100, 250	450	900
ACCURACY – (MAX ERROR)					
Static Error Band–% FS	±0.02	±0.03	±0.04	±0.05	±0.06
Nonlinearity–% FS	±0.03	±0.04	±0.04	±0.05	±0.06
Hysteresis–% FS	±0.02	±0.04	±0.05	±0.05	±0.06
Nonrepeatability–% RO	±0.01	±0.01	±0.01	±0.01	±0.01
Creep, in 20 min–%	±0.025	±0.025	±0.025	±0.025	±0.025
Side Load Sensitivity–%	±0.1	±0.1	±0.1	±0.1	±0.1
Eccentric Load Sensitivity–%/in	±0.1	±0.1	±0.1	±0.1	±0.1
TEMPERATURE					
Compensated Range–°F	15 to 115	15 to 115	15 to 115	15 to 115	15 to 115
Compensated Range–°C	-10 to 45	-10 to 45	-10 to 45	-10 to 45	-10 to 45
Operating Range–°F	-65 to 200	-65 to 200	-65 to 200	-65 to 200	-65 to 200
Operating Range–°C	-55 to 90	-55 to 90	-55 to 90	-55 to 90	-55 to 90
Effect on Zero–%RO/°F – MAX	±0.0004	±0.0004	±0.0004	±0.0004	±0.0004
Effect on Zero–%RO/°C – MAX	±0.0007	±0.0007	±0.0007	±0.0007	±0.0007
Effect on Output–%/°F – MAX	±0.0008	±0.0008	±0.0008	±0.0008	±0.0008
Effect on Output–%/°C – MAX	±0.0015	±0.0015	±0.0015	±0.0015	±0.0015
ELECTRICAL					
Rated Output–mV/V (Nominal)	2.0	4.0	4.0	4.0	4.0
Excitation Voltage–VDC MAX	20	20	20	20	20
Bridge Resistance–Ohm (Nominal)	350	350	350	350	350
Zero Balance–% RO	±1.0	±1.0	±1.0	±1.0	±1.0
Insulation Resistance–Megohm	5000	5000	5000	5000	5000
MECHANICAL					
Safe Overload–% CAP	±150	±150	±150	±150	±150
Deflection @ RO–inch	0.002	0.004	0.004	0.006	0.012
Deflection @ RO–mm	0.05	0.10	0.10	0.15	0.20
Base Part Number (Ref) (Metric)	B101 (m)	B102 (m)	B103 (m)	B112 (m)	B105 (m)
Natural Frequency–kHz	2.7, 3.5, 4.9, 7.0, 8.5	4.7, 6.6	4.6, 5.0	4.0	3.5
Weight–lb	3.3	7.3	21.5	52	146
Weight–kg	1.5	3.3	9.8	24	66
Connector	PC04E-10-6P	PC04E-10-6P	PC04E-10-6P	PC04E-10-6P	PC04E-10-6P
Calibration	T & C	T & C	T & C	T & C	T & C

OPTIONS

Compression Overload Protection
Integral 10 ft Cable
Bayonet Connector
Multiple Bridge
Standardized Output
Connector Protection
Transducer Electronic Data Sheet (TEDS)

ACCESSORIES

Mating Connector
Instrumentation
Loading Hardware

Consult factory for more technical information

STANDARD CONFIGURATIONS

10 ft Integral Cable (11xxAJ-nn)
<or> PC04E-10-6P Connector (11xxAF-nn)
<or> PT02E-10-6P Bayonet Connector (11xxACK-nn)

INTERFACE • 7401 E. Butherus Drive, Scottsdale, AZ 85260 • PHONE: (480) 948-5555 • FAX: (480) 948-1924
www.interfaceforce.com • Email: gen@interfaceforce.com • ORDER TOLL-FREE 1-800-947-5598

1100UP_12_13
12/05

APPENDIX D

FOSM RELIABILITY OF SDPWS

APA Wall Reliability

For 15/32" WSP, 8d common nails at 6/12, and Douglas Fir framing,

APA Target Design Value, $V_{target} := 260$

From SDPWS, safety factor=2, and 40% increase for wind,

$$V_{SDPWS} := V_{target} \cdot 2 \cdot 1.4 \qquad V_{SDPWS} = 728$$

The mean wind load for ASD is then equal to,

$$a_1 := 0.8 \qquad \gamma_W := 1.0 \qquad \phi_W := 0.5$$

$$V_W := a_1 \cdot \phi_W \cdot V_{SDPWS}$$

$$\mu_S := V_W \qquad \mu_S = 291.2$$

The standard deviation for the wind load is,

$$\Omega_W := 0.35$$

$$\sigma_S := \Omega_W \cdot V_W \qquad \sigma_S = 101.92$$

R=LOGN(913,112)

$\mu_R := 913$ $\sigma_R := 112$ (From APA Report 154)

S=GUMB(291.2,101.92)

$\mu_S := 291.2$ $\sigma_S := 101.92$ (Calculated above)

For R,

$$\Omega_R := \frac{\sigma_R}{\mu_R} \qquad \zeta_R := \Omega_R \qquad \Omega_R = 0.123$$

$$\lambda_R := \ln(\mu_R) - \frac{1}{2} \cdot \zeta_R^{\,2} \qquad \lambda_R = 6.809$$

For S,

$$\alpha := \frac{\pi}{\sqrt{6}} \cdot \frac{1}{\sigma_S} \qquad \alpha = 0.0126$$

$$\mu_{SG} := \mu_S - \frac{0.577}{\alpha} \qquad \mu_{SG} = 245.348$$

G = R − S

$$R' := \frac{R - \mu_R}{\sigma_R} \qquad R := \sigma_R \cdot R' + \mu_R$$

$$S' := \frac{S - \mu_S}{\sigma_S} \qquad S := \sigma_S \cdot S' + \mu_S$$

$$G := \sigma_R \cdot R' + \mu_R - \sigma_S \cdot S' - \mu_S$$

$$\frac{d}{dR'}\left(\sigma_R \cdot R' + \mu_R - \sigma_S \cdot S' - \mu_S\right) = \quad \sigma_R$$

$$\frac{d}{dS'}\left(\sigma_R \cdot R' + \mu_R - \sigma_S \cdot S' - \mu_S\right) = \quad -\sigma_S$$

Convert to Normal,

$$r_1 := \mu_R$$

$$\sigma_{RN} := r_1 \cdot \zeta_R \qquad \sigma_{RN} = 112$$

$$\mu_{RN} := r_1 \cdot \left(1 - \ln(r_1) + \lambda_R\right) \qquad \mu_{RN} = 906.13$$

$$s_1 := \mu_S$$

$$F_S(s) := \exp\left[-\exp\left[-\alpha \cdot \left(s - \mu_{SG}\right)\right]\right] \qquad F_S(s_1) = 0.57$$

$$f_S(s) := \alpha \cdot \exp\left[-\alpha \cdot \left(s - \mu_{SG}\right) - \exp\left[-\alpha \cdot \left(s - \mu_{SG}\right)\right]\right] \qquad f_S(s_1) = 4.03 \times 10^{-3}$$

$$\sigma_{SN} := \frac{\mathrm{dnorm}\left(\mathrm{qnorm}\left(F_S(s_1), 0, 1\right), 0, 1\right)}{f_S(s_1)} \qquad \sigma_{SN} = 97.445$$

$$\mu_{SN} := s_1 - \sigma_{SN} \cdot \mathrm{qnorm}\left(F_S(s_1), 0, 1\right) \qquad \mu_{SN} = 273.937$$

$$\frac{d}{dR'}G := \sigma_{RN} \qquad \frac{d}{dS'}G := -\sigma_{SN}$$

$$\alpha_{r1} := \frac{\sigma_{RN}}{\sqrt{\sigma_{RN}^{\ 2} + \left(-\sigma_{SN}\right)^2}} \qquad \alpha_{r1} = 0.754$$

$$\alpha_{s1} := \frac{-\sigma_{SN}}{\sqrt{\sigma_{RN}^{2} + (-\sigma_{SN})^{2}}} \qquad \alpha_{s1} = -0.656$$

$$\mu_{RN} - \alpha_{r1} \cdot \beta_1 \cdot \sigma_{RN} = r_2$$

$$\mu_{SN} - \alpha_{s1} \cdot \beta_1 \cdot \sigma_{SN} = s_2$$

$$\beta_1 := \frac{\mu_{SN} - \mu_{RN}}{\alpha_{s1} \cdot \sigma_{SN} - \alpha_{r1} \cdot \sigma_{RN}} \qquad \beta_1 = 4.258$$

$$r_2 := \mu_{RN} - \alpha_{r1} \cdot \beta_1 \cdot \sigma_{RN} \qquad r_2 = 546.312$$

$$s_2 := \mu_{SN} - \alpha_{s1} \cdot \beta_1 \cdot \sigma_{SN} \qquad s_2 = 546.312$$

Second Iteration-

Convert to Normal,

$$\sigma_{RN} := r_2 \cdot \zeta_R \qquad \sigma_{RN} = 67.017$$

$$\mu_{RN} := r_2 \cdot (1 - \ln(r_2) + \lambda_R) \qquad \mu_{RN} = 822.757$$

$$F_S(s) := \exp\left[-\exp\left[-\alpha \cdot (s - \mu_{SG})\right]\right] \qquad F_S(s_2) = 0.978$$

$$f_S(s) := \alpha \cdot \exp\left[-\alpha \cdot (s - \mu_{SG}) - \exp\left[-\alpha \cdot (s - \mu_{SG})\right]\right] \qquad f_S(s_2) = 2.787 \times 10^{-4}$$

$$\sigma_{SN} := \frac{\mathrm{dnorm}(\mathrm{qnorm}(F_S(s_2), 0, 1), 0, 1)}{f_S(s_2)} \qquad \sigma_{SN} = 191.206$$

$$\mu_{SN} := s_2 - \sigma_{SN} \cdot \mathrm{qnorm}(F_S(s_2), 0, 1) \qquad \mu_{SN} = 162.658$$

$$\frac{d}{dR'} G := \sigma_{RN} \qquad \frac{d}{dS'} G := -\sigma_{SN}$$

$$\alpha_{r2} := \frac{\sigma_{RN}}{\sqrt{\sigma_{RN}^{2} + (-\sigma_{SN})^{2}}} \qquad \alpha_{r2} = 0.331$$

$$\alpha_{s2} := \frac{-\sigma_{SN}}{\sqrt{\sigma_{RN}^{\ 2} + (-\sigma_{SN})^2}} \qquad \alpha_{s2} = -0.944$$

$$\mu_{RN} - \alpha_{r2} \cdot \beta_2 \cdot \sigma_{RN} = r_2$$

$$\mu_{SN} - \alpha_{s2} \cdot \beta_2 \cdot \sigma_{SN} = s_2$$

$$\beta_2 := \frac{\mu_{SN} - \mu_{RN}}{\alpha_{s2} \cdot \sigma_{SN} - \alpha_{r2} \cdot \sigma_{RN}} \qquad \beta_2 = 3.258$$

$$r_3 := \mu_{RN} - \alpha_{r2} \cdot \beta_2 \cdot \sigma_{RN} \qquad r_3 = 750.537$$

$$s_3 := \mu_{SN} - \alpha_{s2} \cdot \beta_2 \cdot \sigma_{SN} \qquad s_3 = 750.537$$

Third Iteration-

Convert to Normal,

$$\sigma_{RN} := r_3 \cdot \zeta_R \qquad \sigma_{RN} = 92.07$$

$$\mu_{RN} := r_3 \cdot (1 - \ln(r_3) + \lambda_R) \qquad \mu_{RN} = 891.955$$

$$F_S(s) := \exp\left[-\exp\left[-\alpha \cdot (s - \mu_{SG})\right]\right] \qquad F_S(s_3) = 0.998$$

$$f_S(s) := \alpha \cdot \exp\left[-\alpha \cdot (s - \mu_{SG}) - \exp\left[-\alpha \cdot (s - \mu_{SG})\right]\right] \qquad f_S(s_3) = 2.178 \times 10^{-5}$$

$$\sigma_{SN} := \frac{\mathrm{dnorm}(\mathrm{qnorm}(F_S(s_3), 0, 1), 0, 1)}{f_S(s_3)} \qquad \sigma_{SN} = 255.449$$

$$\mu_{SN} := s_3 - \sigma_{SN} \cdot \mathrm{qnorm}(F_S(s_3), 0, 1) \qquad \mu_{SN} = 3.826$$

$$\frac{d}{dR'} G := \sigma_{RN} \qquad \frac{d}{dS'} G := -\sigma_{SN}$$

$$\alpha_{r3} := \frac{\sigma_{RN}}{\sqrt{\sigma_{RN}^{\ 2} + (-\sigma_{SN})^2}} \qquad \alpha_{r3} = 0.339$$

$$\alpha_{s3} := \frac{-\sigma_{SN}}{\sqrt{\sigma_{RN}^{2} + (-\sigma_{SN})^{2}}} \qquad \alpha_{s3} = -0.941$$

$$\mu_{RN} - \alpha_{r3} \cdot \beta_2 \cdot \sigma_{RN} = r_3$$

$$\mu_{SN} - \alpha_{s3} \cdot \beta_2 \cdot \sigma_{SN} = s_3$$

$$\beta_3 := \frac{\mu_{SN} - \mu_{RN}}{\alpha_{s3} \cdot \sigma_{SN} - \alpha_{r3} \cdot \sigma_{RN}} \qquad \beta_3 = 3.271$$

$$r_4 := \mu_{RN} - \alpha_{r3} \cdot \beta_3 \cdot \sigma_{RN} \qquad r_4 = 789.846$$

$$s_4 := \mu_{SN} - \alpha_{s3} \cdot \beta_3 \cdot \sigma_{SN} \qquad s_4 = 789.846$$

Fourth Iteration

Convert to Normal,

$$\sigma_{RN} := r_4 \cdot \zeta_R \qquad \sigma_{RN} = 96.892$$

$$\mu_{RN} := r_4 \cdot (1 - \ln(r_4) + \lambda_R) \qquad \mu_{RN} = 898.35$$

$$F_S(s) := \exp\left[-\exp\left[-\alpha \cdot (s - \mu_{SG})\right]\right] \qquad F_S(s_4) = 0.999$$

$$f_S(s) := \alpha \cdot \exp\left[-\alpha \cdot (s - \mu_{SG}) - \exp\left[-\alpha \cdot (s - \mu_{SG})\right]\right] \qquad f_S(s_4) = 1.329 \times 10^{-5}$$

$$\sigma_{SN} := \frac{\mathrm{dnorm}(\mathrm{qnorm}(F_S(s_4), 0, 1), 0, 1)}{f_S(s_4)} \qquad \sigma_{SN} = 266.493$$

$$\mu_{SN} := s_4 - \sigma_{SN} \cdot \mathrm{qnorm}(F_S(s_4), 0, 1) \qquad \mu_{SN} = -29.29$$

$$\frac{d}{dR'} G := \sigma_{RN} \qquad \frac{d}{dS'} G := -\sigma_{SN}$$

$$\alpha_{r4} := \frac{\sigma_{RN}}{\sqrt{\sigma_{RN}^{2} + (-\sigma_{SN})^{2}}} \qquad \alpha_{r4} = 0.342$$

$$\alpha_{s4} := \frac{-\sigma_{SN}}{\sqrt{\sigma_{RN}^{\ 2} + \left(-\sigma_{SN}\right)^2}} \qquad \alpha_{s4} = -0.94$$

$$\mu_{RN} - \alpha_{r4} \cdot \beta_4 \cdot \sigma_{RN} = r_4$$

$$\mu_{SN} - \alpha_{s4} \cdot \beta_4 \cdot \sigma_{SN} = s_4$$

$$\beta_4 := \frac{\mu_{SN} - \mu_{RN}}{\alpha_{s4} \cdot \sigma_{SN} - \alpha_{r4} \cdot \sigma_{RN}} \qquad \boxed{\beta_4 = 3.271}$$

$$r_5 := \mu_{RN} - \alpha_{r4} \cdot \beta_4 \cdot \sigma_{RN} \qquad \boxed{r_5 = 790.04}$$

$$s_5 := \mu_{SN} - \alpha_{s4} \cdot \beta_4 \cdot \sigma_{SN} \qquad \boxed{s_5 = 790.04}$$

APPENDIX E

FOSM RELIABILITY OF WALL

Unrestrained Wall E Reliability

For 15/32" WSP, 8d common nails at 6/12, and Spruce-Pine-Fir framing,

Wall 'E' average ultimate unit shear capacity, $V_E := 162$

The mean wind load for ASD is then equal to,

$a_1 := 0.8 \qquad \gamma_W := 1.0 \qquad \phi_W := 0.5$

$V_W := a_1 \cdot \phi_W \cdot V_E$

$\mu_S := V_W \qquad \mu_S = 64.8$

The standard deviation for the wind load is,

$\Omega_W := 0.35$

$\sigma_S := \Omega_W \cdot V_W \qquad \sigma_S = 22.68$

R=LOGN(162,23.49)

$\mu_R := 162$

$\sigma_R := 0.145\mu_R \qquad \sigma_R = 23.49$

S=GUMB(64.8,22.68)

$\mu_S := \frac{\mu_R \cdot 0.8}{2}$ (Bias factor = 0.8) $\qquad \mu_S = 64.8$

$\sigma_S := 0.35 \cdot \mu_S \qquad \sigma_S = 22.68$

For R,

$\Omega_R := \frac{\sigma_R}{\mu_R} \qquad \zeta_R := \Omega_R \qquad \Omega_R = 0.145$

$\lambda_R := \ln(\mu_R) - \frac{1}{2} \cdot \zeta_R^{\,2} \qquad \lambda_R = 5.077$

For S,

$\alpha := \frac{\pi}{\sqrt{6}} \cdot \frac{1}{\sigma_S} \qquad \alpha = 0.0565$

$\mu_{SG} := \mu_S - \frac{0.577}{\alpha} \qquad \mu_{SG} = 54.597$

$G = R - S$

$$R' := \frac{R - \mu_R}{\sigma_R} \qquad R := \sigma_R \cdot R' + \mu_R$$

$$S' := \frac{S - \mu_S}{\sigma_S} \qquad S := \sigma_S \cdot S' + \mu_S$$

$$G := \sigma_R \cdot R' + \mu_R - \sigma_S \cdot S' - \mu_S$$

$$\frac{d}{dR'}\left(\sigma_R \cdot R' + \mu_R - \sigma_S \cdot S' - \mu_S\right) = \quad \sigma_R$$

$$\frac{d}{dS'}\left(\sigma_R \cdot R' + \mu_R - \sigma_S \cdot S' - \mu_S\right) = \quad -\sigma_S$$

Convert to Normal,

$$r_1 := \mu_R$$

$$\sigma_{RN} := r_1 \cdot \zeta_R \qquad \sigma_{RN} = 23.49$$

$$\mu_{RN} := r_1 \cdot \left(1 - \ln\left(r_1\right) + \lambda_R\right) \qquad \mu_{RN} = 160.297$$

$$s_1 := \mu_S$$

$$F_S(s) := \exp\left[-\exp\left[-\alpha \cdot \left(s - \mu_{SG}\right)\right]\right] \qquad F_S\left(s_1\right) = 0.57$$

$$f_S(s) := \alpha \cdot \exp\left[-\alpha \cdot \left(s - \mu_{SG}\right) - \exp\left[-\alpha \cdot \left(s - \mu_{SG}\right)\right]\right] \qquad f_S\left(s_1\right) = 0.018$$

$$\sigma_{SN} := \frac{\mathrm{dnorm}\left(\mathrm{qnorm}\left(F_S\left(s_1\right), 0, 1\right), 0, 1\right)}{f_S\left(s_1\right)} \qquad \sigma_{SN} = 21.684$$

$$\mu_{SN} := s_1 - \sigma_{SN} \cdot \mathrm{qnorm}\left(F_S\left(s_1\right), 0, 1\right) \qquad \mu_{SN} = 60.959$$

$$\frac{d}{dR'}G := \sigma_{RN} \qquad \frac{d}{dS'}G := -\sigma_{SN}$$

$$\alpha_{r1} := \frac{\sigma_{RN}}{\sqrt{{\sigma_{RN}}^2 + \left(-\sigma_{SN}\right)^2}} \qquad \alpha_{r1} = 0.735$$

$$\alpha_{s1} := \frac{-\sigma_{SN}}{\sqrt{\sigma_{RN}^{2} + (-\sigma_{SN})^{2}}} \qquad \alpha_{s1} = -0.678$$

$$\mu_{RN} - \alpha_{r1} \cdot \beta_1 \cdot \sigma_{RN} = r_2$$

$$\mu_{SN} - \alpha_{s1} \cdot \beta_1 \cdot \sigma_{SN} = s_2$$

$$\beta_1 := \frac{\mu_{SN} - \mu_{RN}}{\alpha_{s1} \cdot \sigma_{SN} - \alpha_{r1} \cdot \sigma_{RN}} \qquad \beta_1 = 3.107$$

$$r_2 := \mu_{RN} - \alpha_{r1} \cdot \beta_1 \cdot \sigma_{RN} \qquad r_2 = 106.663$$

$$s_2 := \mu_{SN} - \alpha_{s1} \cdot \beta_1 \cdot \sigma_{SN} \qquad s_2 = 106.663$$

Second Iteration-

Convert to Normal,

$$\sigma_{RN} := r_2 \cdot \zeta_R \qquad \sigma_{RN} = 15.466$$

$$\mu_{RN} := r_2 \cdot (1 - \ln(r_2) + \lambda_R) \qquad \mu_{RN} = 150.119$$

$$F_S(s) := \exp\left[-\exp\left[-\alpha \cdot (s - \mu_{SG})\right]\right] \qquad F_S(s_2) = 0.949$$

$$f_S(s) := \alpha \cdot \exp\left[-\alpha \cdot (s - \mu_{SG}) - \exp\left[-\alpha \cdot (s - \mu_{SG})\right]\right] \qquad f_S(s_2) = 2.824 \times 10^{-3}$$

$$\sigma_{SN} := \frac{\mathrm{dnorm}(\mathrm{qnorm}(F_S(s_2), 0, 1), 0, 1)}{f_S(s_2)} \qquad \sigma_{SN} = 37.262$$

$$\mu_{SN} := s_2 - \sigma_{SN} \cdot \mathrm{qnorm}(F_S(s_2), 0, 1) \qquad \mu_{SN} = 45.829$$

$$\frac{d}{dR'}G := \sigma_{RN} \qquad \frac{d}{dS'}G := -\sigma_{SN}$$

$$\alpha_{r2} := \frac{\sigma_{RN}}{\sqrt{\sigma_{RN}^{2} + (-\sigma_{SN})^{2}}} \qquad \alpha_{r2} = 0.383$$

$$\alpha_{s2} := \frac{-\sigma_{SN}}{\sqrt{\sigma_{RN}^{2} + (-\sigma_{SN})^{2}}} \qquad \alpha_{s2} = -0.924$$

$$\mu_{RN} - \alpha_{r2} \cdot \beta_2 \cdot \sigma_{RN} = r_2$$

$$\mu_{SN} - \alpha_{s2} \cdot \beta_2 \cdot \sigma_{SN} = s_2$$

$$\beta_2 := \frac{\mu_{SN} - \mu_{RN}}{\alpha_{s2} \cdot \sigma_{SN} - \alpha_{r2} \cdot \sigma_{RN}} \qquad \beta_2 = 2.585$$

$$r_3 := \mu_{RN} - \alpha_{r2} \cdot \beta_2 \cdot \sigma_{RN} \qquad r_3 = 134.792$$

$$s_3 := \mu_{SN} - \alpha_{s2} \cdot \beta_2 \cdot \sigma_{SN} \qquad s_3 = 134.792$$

Third Iteration-

Convert to Normal,

$$\sigma_{RN} := r_3 \cdot \zeta_R \qquad \sigma_{RN} = 19.545$$

$$\mu_{RN} := r_3 \cdot (1 - \ln(r_3) + \lambda_R) \qquad \mu_{RN} = 158.158$$

$$F_S(s) := \exp\left[-\exp\left[-\alpha \cdot (s - \mu_{SG})\right]\right] \qquad F_S(s_3) = 0.989$$

$$f_S(s) := \alpha \cdot \exp\left[-\alpha \cdot (s - \mu_{SG}) - \exp\left[-\alpha \cdot (s - \mu_{SG})\right]\right] \qquad f_S(s_3) = 6.001 \times 10^{-4}$$

$$\sigma_{SN} := \frac{\text{dnorm}(\text{qnorm}(F_S(s_3), 0, 1), 0, 1)}{f_S(s_3)} \qquad \sigma_{SN} = 46.992$$

$$\mu_{SN} := s_3 - \sigma_{SN} \cdot \text{qnorm}(F_S(s_3), 0, 1) \qquad \mu_{SN} = 26.618$$

$$\frac{d}{dR'}G := \sigma_{RN} \qquad \frac{d}{dS'}G := -\sigma_{SN}$$

$$\alpha_{r3} := \frac{\sigma_{RN}}{\sqrt{\sigma_{RN}^{2} + (-\sigma_{SN})^{2}}} \qquad \alpha_{r3} = 0.384$$

$$\alpha_{s3} := \frac{-\sigma_{SN}}{\sqrt{\sigma_{RN}^{\ 2} + \left(-\sigma_{SN}\right)^2}} \qquad \alpha_{s3} = -0.923$$

$$\mu_{RN} - \alpha_{r3} \cdot \beta_3 \cdot \sigma_{RN} = r_3$$

$$\mu_{SN} - \alpha_{s3} \cdot \beta_3 \cdot \sigma_{SN} = s_3$$

$$\beta_3 := \frac{\mu_{SN} - \mu_{RN}}{\alpha_{s3} \cdot \sigma_{SN} - \alpha_{r3} \cdot \sigma_{RN}} \qquad \beta_3 = 2.585$$

$$r_4 := \mu_{RN} - \alpha_{r3} \cdot \beta_3 \cdot \sigma_{RN} \qquad r_4 = 138.76$$

$$s_4 := \mu_{SN} - \alpha_{s3} \cdot \beta_3 \cdot \sigma_{SN} \qquad s_4 = 138.76$$

Fourth Iteration-

Convert to Normal,

$$\sigma_{RN} := r_4 \cdot \zeta_R \qquad \sigma_{RN} = 20.12$$

$$\mu_{RN} := r_4 \cdot \left(1 - \ln\left(r_4\right) + \lambda_R\right) \qquad \mu_{RN} = 158.788$$

$$F_S(s) := \exp\left[-\exp\left[-\alpha \cdot \left(s - \mu_{SG}\right)\right]\right] \qquad F_S\left(s_4\right) = 0.991$$

$$f_S(s) := \alpha \cdot \exp\left[-\alpha \cdot \left(s - \mu_{SG}\right) - \exp\left[-\alpha \cdot \left(s - \mu_{SG}\right)\right]\right] \qquad f_S\left(s_4\right) = 4.805 \times 10^{-4}$$

$$\sigma_{SN} := \frac{\mathrm{dnorm}\left(\mathrm{qnorm}\left(F_S\left(s_4\right), 0, 1\right), 0, 1\right)}{f_S\left(s_4\right)} \qquad \sigma_{SN} = 48.279$$

$$\mu_{SN} := s_4 - \sigma_{SN} \cdot \mathrm{qnorm}\left(F_S\left(s_4\right), 0, 1\right) \qquad \mu_{SN} = 23.603$$

$$\frac{d}{dR'}G := \sigma_{RN} \qquad \frac{d}{dS'}G := -\sigma_{SN}$$

$$\alpha_{r4} := \frac{\sigma_{RN}}{\sqrt{\sigma_{RN}^{\ 2} + \left(-\sigma_{SN}\right)^2}} \qquad \alpha_{r4} = 0.385$$

$$\alpha_{s4} := \frac{-\sigma_{SN}}{\sqrt{\sigma_{RN}^{\ 2} + \left(-\sigma_{SN}\right)^2}} \qquad \alpha_{s4} = -0.923$$

$$\mu_{RN} - \alpha_{r4} \cdot \beta_4 \cdot \sigma_{RN} = r_4$$

$$\mu_{SN} - \alpha_{s4} \cdot \beta_4 \cdot \sigma_{SN} = s_4$$

$$\beta_4 := \frac{\mu_{SN} - \mu_{RN}}{\alpha_{s4} \cdot \sigma_{SN} - \alpha_{r4} \cdot \sigma_{RN}} \qquad \beta_4 = 2.585$$

$$r_5 := \mu_{RN} - \alpha_{r4} \cdot \beta_4 \cdot \sigma_{RN} \qquad r_5 = 138.784$$

$$s_5 := \mu_{SN} - \alpha_{s4} \cdot \beta_4 \cdot \sigma_{SN} \qquad s_5 = 138.784$$

APPENDIX F

MONTE CARLO SIMULATION

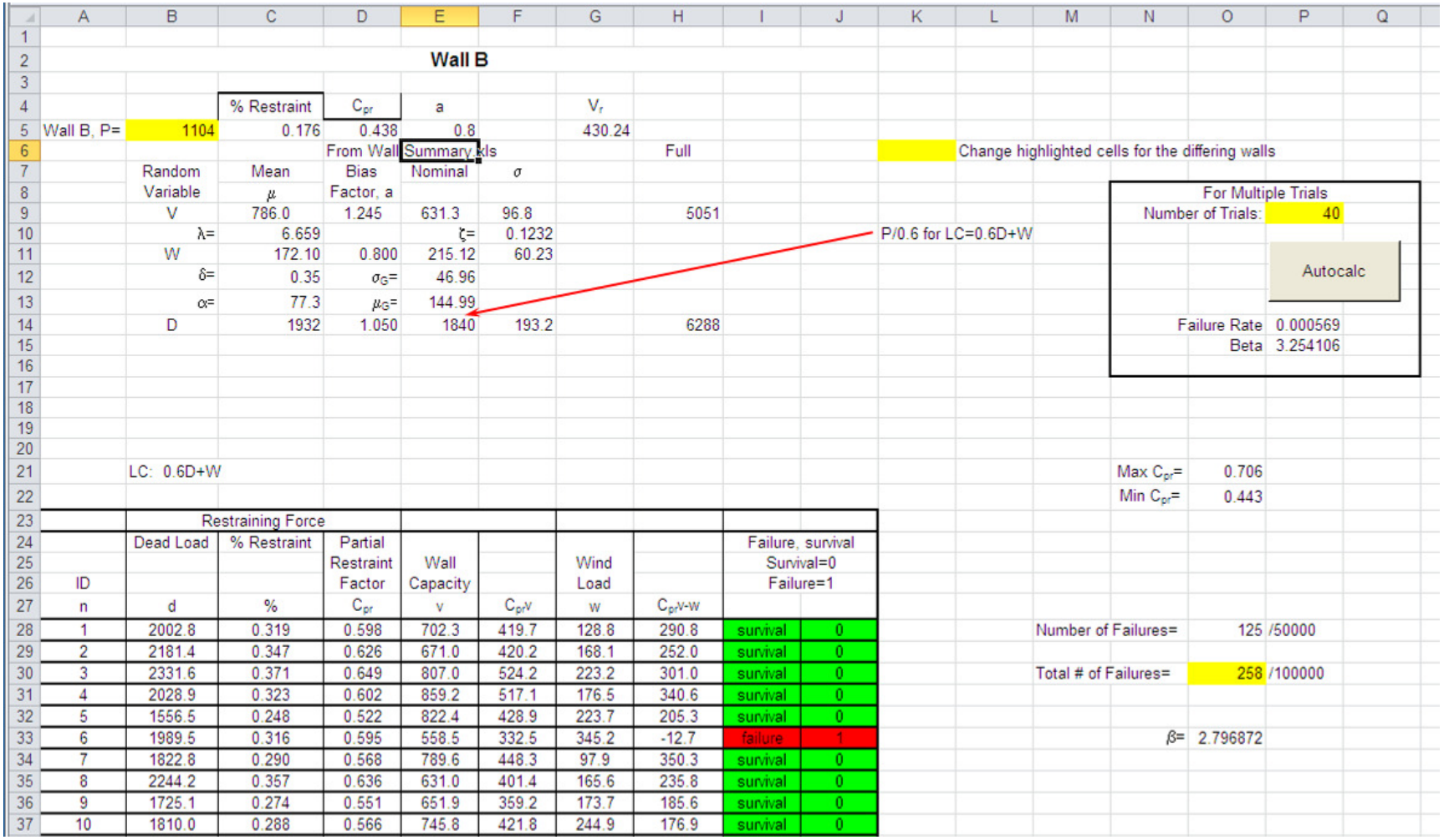

Wall B

	% Restraint	C_{pr}	a		V_r
Wall B, P= 1104	0.176	0.438	0.8		430.24

From Wall Summary.xls — Full

Change highlighted cells for the differing walls

Random Variable	Mean μ	Bias Factor, a	Nominal	σ		
V	786.0	1.245	631.3	96.8		5051
λ=	6.659		ζ=	0.1232		
W	172.10	0.800	215.12	60.23		
δ=	0.35	σ_G=	46.96			
α=	77.3	μ_G=	144.99			
D	1932	1.050	1840	193.2		6288

P/0.6 for LC=0.6D+W

For Multiple Trials
Number of Trials: 40
Autocalc
Failure Rate 0.000569
Beta 3.254106

LC: 0.6D+W

Max C_{pr}= 0.706
Min C_{pr}= 0.443

	Restraining Force								
	Dead Load	% Restraint	Partial Restraint Factor	Wall Capacity		Wind Load		Failure, survival Survival=0 Failure=1	
ID			C_{pr}						
n	d	%		v	$C_{pr}V$	w	$C_{pr}V$-w		
1	2002.8	0.319	0.598	702.3	419.7	128.8	290.8	survival	0
2	2181.4	0.347	0.626	671.0	420.2	168.1	252.0	survival	0
3	2331.6	0.371	0.649	807.0	524.2	223.2	301.0	survival	0
4	2028.9	0.323	0.602	859.2	517.1	176.5	340.6	survival	0
5	1556.5	0.248	0.522	822.4	428.9	223.7	205.3	survival	0
6	1989.5	0.316	0.595	558.5	332.5	345.2	-12.7	failure	1
7	1822.8	0.290	0.568	789.6	448.3	97.9	350.3	survival	0
8	2244.2	0.357	0.636	631.0	401.4	165.6	235.8	survival	0
9	1725.1	0.274	0.551	651.9	359.2	173.7	185.6	survival	0
10	1810.0	0.288	0.566	745.8	421.8	244.9	176.9	survival	0

Number of Failures= 125 /50000

Total # of Failures= 258 /100000

β= 2.796872

APPENDIX G

EXAMPLE CALCULATIONS OF UNIT SHEAR

This appendix illustrates the use of the proposed partial restraint factor. Also, a comparison of both ASD and LRFD methods are provided as examples and comparison.

Examples of Proposed Design Method-

Consider a wall partially restrained with a dead load. The following design information is provided. What is the wall unit shear capacity?

Given:

P=2,000 lb
H=8'
L=4'
SPF-S Framing Members, G=0.36
$^{15}/_{32}$" OSB Sheathing
8d Common nails with 6:12 nail pattern
½" Anchor bolt 12" from leading edge

ASD-

Solution-

From SDPWS (2005), Table A.4.3A,

$$V_n = 730 \times (1 - (0.5 - 0.36)) = 628 \text{ plf}$$

Load Combination 1: D+W

$$C_p = \frac{2000}{628 \times 8} = 0.398$$

$$C_{pr} = -0.509(0.398^2) + 1.309(0.398) + 0.199 = 0.639$$

$$V'_n = \frac{628(0.639)}{2} = 201 \text{ plf}$$

Load Combination 2: 0.6D+W

$$C_p = \frac{0.6(2000)}{628 \times 8} = 0.239$$

$$C_{pr} = (10.642 + 0.163(0.239)^{-7.925})^{-0.097} + 0.207 = 0.604$$

$$V'_n = \frac{628(0.604)}{2} = 190 \text{ plf} \leftarrow \text{Governs}$$

ASD Unit Shear Capacity is 190 plf

LRFD-

Solution-

From SDPWS (2005), Table A.4.3A,

$$V_n = 730 \times (1 - (0.5 - 0.36)) = 628 \text{ plf}$$

Load Combination 1: 1.2D+1.6W

$$C_p = \frac{1.2(2000)}{628 \times 8} = 0.478$$

$$C_{pr} = -0.498(0.478^2) + 1.294(0.477) + 0.203 = 0.708$$

$$\phi V'_n = 0.8(628)(0.708) = 355 \text{ plf}$$

$$V = \frac{\phi V'_n}{\gamma} = \frac{0.355}{1.6} = 222 \text{ plf}$$

Load Combination 2: 0.9D+1.6W

$$C_p = \frac{0.9(2000)}{628 \times 8} = 0.358$$

$$C_{pr} = -0.498(0.358^2) + 1.294(0.358) + 0.203 = 0.603$$

$$\phi V'_n = 0.8(628)(0.603) = 303 \text{ plf}$$

$$V = \frac{\phi V'_n}{\gamma_W} = \frac{303}{1.6} = 190 \text{ plf} \leftarrow \text{Governs (Same as ASD)}$$

LRFD Unit Shear Capacity is 190 plf (unfactored)

REFERENCES

ABAQUS Analysis User's Manual V6.10. 2010. Dassault Systems. Providence, RI.

American Forest & Paper Association (AF&PA). 1991. National Design Specification for Wood Construction Commentary. AF&PA, Washington, DC.

American Forest & Paper Association (AF&PA). 2005. Special Design Provisions for Wind and Seismic (ANSI/AF&PA SDPWS-2005). AF&PA, Washington, DC.

American Forest & Paper Association (AF&PA). 2005. National Design Specification for Wood Construction (ANSI/AF&PA NDS-2005). AF&PA, Washington, DC.

American Forest & Paper Association (AF&PA). 1999. General Dowel Equations for Calculating Lateral Connection Values (Technical Report 12). AF&PA, Washington, DC.

American Plywood Association (APA), 2004. Panel Design Specification (Form No. D510). APA, Tacoma, Washington.

American Plywood Association (APA), 2007. Engineered Wood Construction Guide (Form No. E30U). APA, Tacoma, Washington.

American Plywood Association (APA), 2004. Wood Structural Panel Shear Walls (Research Report 154). APA, Tacoma, Washington.

American Plywood Association (APA), 2007. Wood Structural Panel Shear Wall Deflection Formula (TT-053). APA, Tacoma, Washington.

American Society of Civil Engineers (ASCE). 2005. Minimum Design Loads for Buildings and Other Structures, ASCE 7-05. ASCE, Reston, VA.

Barringer. 2007. Problem of The Month – March 2001 – Heat Exchanger IRIS Wall Thickness and Gumbel Smallest Distributions. http://www.barringer1.com/mar01prb.htm.

American Society for Testing and Materials (ASTM). 2000. "Standard Practice for Static Load Test for Shear Resistance of Framed Walls for Buildings". ASTM E564-00. Philadelphia, PA

American Society for Testing and Materials (ASTM). 2005. "Standard Test Methods of Conducting Strength Tests of Panels for Building Construction". ASTM E72-05. Philadelphia, PA

American Society for Testing and Materials (ASTM). 2006. "Standard Practice for Establishing Clear Wood Strength Values". ASTM D 2555-06. Philadelphia, PA

American Society for Testing and Materials (ASTM). 2002, "Standard Test Methods for Specific Gravity of Wood and Wood-Based Materials," ASTM D2395-02. Philadelphia, PA.

Cassidy, D. 2002. "Development and Structural Testing of FRP Reinforced OSB Panels for Disaster Resistant Construction." Masters Thesis. The University of Maine. Orono, ME.

Crandell, J.H. 2007. "The story behind the *IRC* wall bracing provisions." Wood Design Focus, 17(2) (Summer). Forest Products Society, Madison, WI.

Crandell, J.H. and Martin, Z. 2009. "The story behind the 2009 *IRC* wall bracing provisions (Part 2: New wind bracing requirements)." Wood Design Focus, 19(1) (Spring). Forest Products Society, Madison, WI.

Crandell, J.H. and Kochkin, V. 2003. "Common engineering issues in conventional construction." Wood Design Focus, 13(3) (Fall). Forest Products Society, Madison, WI.

Dolan, J.D. and Foshci, R.O. 1991. "Structural Analysis Model for Static and Dynamic Loads on Timber Shear Walls." *J. Struct. Eng.*, American Society of Civil Engineers, 117(1), 851-861.

Dolan, J.D. and Madsen, B. 1992. "Monotonic and Cyclic Tests of Timber Shear Walls." *Canadian Journal of Civil Engineering*, 19(1), 97-104.

Dolan, J.D. and Heine, C. 1997. "Sequential phased displacement tests of wood-framed shear walls with corners." Report No. TE-1997-003. Brooks Forest Products Research Center, VPI&SU, Blacksburg, VA.

Dolan, J.D., Gutshall, S.T., and McClain, T.E. 1995. "Monotonic and Cyclic Tests to Determine Short-Term Load Duration Performance of Nail and Bolt Connections." Report No. TE-1994-001. Brooks Forest Products Research Center, VPI&SU, Blacksburg, VA.

Ellingwood, B.R., Galambos, T.V., MacGregor, J.G., and Cornell, C.A. 1980. "Development of a probability based load criterion for American National Standard A58." *Special Publication SP577*, U.S. Department of Commerce – National Bureau of Standards, Washington, DC.

Ellingwood, B.R. 1999. "A comparison of general design and load requirements in building codes in Canada, Mexico, and the United States." *Eng. J.* AISC, Second Quarter, 67-80.

FSC. RB148 “Improved wind bracing analysis.” http://www.foamsheathing.org/bracing analysis.php.

Folz, B., and Filiatrault, A. 2000. “CASHEW – Version 1.0, A Computer Program for Cyclic Analysis of Wood Shear Walls.” *Report No. SSRP – 2000/10,* Structural Systems Research Project, Department of Structural Engineering, University of California, San Diego, La Jolla, California.

Folz, B., and Filiatrault, A. 2001. “Cyclic Analysis of Wood Shear Walls.” *J. Struct. Eng.*, American Society of Civil Engineers, 127(4), 433-441.

HUD. 2001. Review of Structural Materials and Methods for Home Building in the United States: 1900 to 2000. U.S. Department of Housing and Urban Development, Washington, DC. (publication available through www.huduser.org).

International Code Council (ICC). 2009. International Residential Code. ICC, Falls Church, VA.

JCSS. 2001. Probabilistic Model Code (Parts I and II). Joint Committee of Structural Safety. http://www.jcss.ethz.ch/publications/publications_pmc.html.

Judd, J. 2005. “Analytical Modeling of Wood-Frame Shear Walls and Diaphragms.” Master’s Thesis. Brigham Young University. Provo, UT.

Mack, J.J. 1966. “The strength and stiffness of nailed joints under short duration loading.” *Technical Paper No. 40, CSIRO Division of Forest Products*. Commonwealth Scientific and Industrial Research Organization. Melbourne, Australia.

Mack, J.J. 1977. "The load-displacement curve for nailed joints." *Journal of the Institute of Wood Science*. Institute of Wood Science, 7(6), 34-36.

Ni, C and Karacabeyli, E. 2000. "Effect of overturning restraint on performance of shear walls." Proceedings of the World Conference of Timber Engineering, 2000.

NIST/SEMATECH. 2010 e-Handbook of Statistical Methods. http://www.itl.nist.gov/div898/handbook/.

NIST. 2004. Performance Standard for Wood-Based Structural Use Panels, DOC PS2-04. United States Department of Commerce, National Institute of Standards and Technology, Gaithersburg, MD.

Seaders, P. 2004. "Performance of Partially and Fully Anchored Wood Frame Shear Walls Under Monotonic, Cyclic & Earthquake Loads." Masters Thesis. Oregon State University. Corvallis, OR.

Structural Building Components Research Institute (SBCRI), 2010. "IRC Wall Panel Testing." http://www.sbcri.info/common/kb/techIRCnotes.php.

Structural Building Components Research Institute (SBCRI), 2010. "2009 International Residential Code (IRC) Braced Wall Panel Design Value Comparative Equivalency Testing – Braced Wall Panel Design Values." SBCA, Madison, Wisconsin.

van de Lindt, J.W., and Walz, M.A. 2003. "Development and Application of Wood Shear Wall Reliability Model." *J. Struct. Eng.*, American Society of Civil Engineers, 129(3), 405-413.

van de Lindt, J.W. 2004. "Evolution of wood shear wall testing, modeling, and reliability analysis: Bibliography." *Pract. Period. Struct. Des. Const.,* 9(1), 44-53.

van de Lindt, J.W., and Rosowsky, D.V. 2005. "Strength-based reliability of wood shearwalls subject to wind load." *J. Struct. Eng.*, American Society of Civil Engineers, 131(2), 359-363.

Waltz, N and Hamburger, R. 2008. "New Rules for Evaluating Seismic Performance of Prefabricated Shear Panels." *Structure Magazine*, August, 2008.

WBDG. 2010. Wind Safety of the Building Envelope. http://www.wbdg.org/resources/env_wind.php?r=dd_fireprotecteng.

Zunzun.com

ABSTRACT

RELIABILITY AND EFFECT OF PARTIALLY RESTRAINED WOOD SHEAR WALLS

by

JOHN J. GRUBER

May 2012

Advisor: Dr. Gongkang Fu

Major: Civil Engineering

Degree: Doctor or Philosophy

The prescriptive design of the most widely used residential building code in the United States, the IRC, allows the use of partially restrained wood shear walls to resist wind and seismic loads. Wind load is the most common controlling lateral design load for these structures. In contrast, the complimenting building code, the IBC, requires either a restraining dead load or a mechanical hold down device to resist overturning. To prescribe a safe structure, it is important to know the effect of partial restraint on the overturning resistance of wood shear walls constructed in accordance with the IRC and equally important whether the partially restrained wood shear walls provide the same level of reliability as fully restrained wood shear walls for wind load. This is the focus of this research.

Twenty five Monotonic tests were conducted of 4’ x 8’ wood shear walls with five varying restraining methods (wall types). There were five sets of five wall types. One of the sets had only an anchor bolt, three sets had different dead loads with one anchor bolt, and one set had a mechanical hold down. The results of the test program were used to determine the partial restraint effect, create a nonlinear finite element model,

and to determine the statistical data required to perform a Monte Carlo simulation of the wall behavior.

The Monte Carlo simulation result was used to calibrate a nonlinear partial restraint factor to a target reliability index of 3.25. The calibration was performed for both ASD and LRFD load combinations as required by the IBC. The research concludes with a closed-form solution, including the calibrated nonlinear partial restraint factor developed, to determine the unit shear capacity of a partially restrained or fully restrained (with dead load or mechanical hold down) wood shear wall constructed in accordance with the IRC by utilizing the fully restrained nominal unit shear values of AF&PA's *Special Design Provisions for Wind and Seismic*.

AUTOBIOGRAPHICAL STATEMENT

John J. Gruber

Mr. Gruber was born in Grosse Pointe, Michigan on May 21, 1965. He received his B.S. degree in Construction Engineering in 1991 from Lawrence Technological University, Southfield, MI. Upon graduation from LTU, he became employed as a structural consulting engineer at Sheppard Engineering in Troy, MI. In 2001, he and three partners, purchased Sheppard Engineering from the owner and he has been a partner and President of Sheppard Engineering since the purchase. He is a licensed professional engineer in four states and a licensed structural engineering in Illinois. He has also instructed both undergraduate and graduate courses at Wayne State University as an adjunct professor since 2009.

Mr. Gruber resumed his college studies in 2003 at the Civil and Environmental Engineering Department at Wayne State University where he completed his M.S. degree in Civil Engineering in 2006. He continued studying towards his doctoral degree since that time.

Mr. Gruber is a past and current member of the ANSI/TPI 1 project committee as well as the ANSI/TPI 3 project committee and is a member of the SBCA Engineering & Technology Committee. He as authored and presented the following publication:

Gruber, John J. "Permanent Bracing of Metal Plate Connected Wood Trusses," 9th World Conference of Timber Engineering. 2006. Portland, OR, USA.